

Université du Québec
Institut national de la recherche scientifique
Énergie, Matériaux et Télécommunications

Smart Localization in Underground Mines using Fingerprinting and ANNs: Strategies and Applications

A dissertation submitted in partial fulfillment of the requirements for the degree of
Doctor of Philosophy

By

Shehadi Dayekh

Evaluation Jury

Research Director

Prof. Sofiène Affes

INRS-Énergie, Matériaux et Télécommunications

Research Co-director

Prof. Nahi Kandil

UQAT, Prof. associé a à l'INRS-EMT

Research Co-director

Prof. Chahé Nerguizian

École Polytechnique, Prof. associé a à l'INRS-EMT

Internal Examiner

Dr. Charles Despins

Prompt Inc., Prof. associé à l'INRS-EMT

External Examiner

Prof. Paul Fortier

Université Laval

External Examiner

Dr. Basile Agba

IREQ Hydro-Québec, Prof. associé à l'ETS

To my dear Mom and Dad.

Résumé

Les mines souterraines sont connues pour l'adversité de leurs milieux de propagation sans fil; une adversité qui pose de très grands défis au déploiement des systèmes de communication sans fil. Bien que l'exploitation minière soit florissante, les mines d'or souterraines sont toujours critiquées pour leurs mesures de sécurité désuètes. Notre mission dans les mines souterraines provient de la nécessité d'un système de localisation fiable qui réussit à localiser avec précision les mineurs et leur équipement dans les entrailles de la Terre.

Après avoir étudié les raisons de l'échec des techniques de localisation traditionnelles dans les mines souterraines, nous recommandons une technique efficace qui utilise les réseaux de neurones artificiels (RNA) et les empreintes digitales extraites de la réponse impulsionnelle du canal (RIC). L'essence de ce travail réside dans sa capacité à repousser les limites de performance des techniques de positionnement basées sur les RNA en intégrant les concepts de diversité de transmetteur (T_x) et récepteur (R_x) spatiale et/ou temporelle dans les empreintes digitales avant d'estimer la position d'un émetteur dans le confinement des tunnels souterrains. En faisant cela, nous établissons les principes de localisation coopérative dans le domaine des RNA en utilisant les empreintes digitales concaténées qui sont extraites de plus d'un point d'accès, à plusieurs instances temporelles, en utilisant des systèmes d'antenne simples ou doubles. En conséquence, de nouvelles techniques d'empreintes, qui exploitent les diversités spatiales et/ou temporelles des signatures rassemblées, sont introduites pour la première fois avec des erreurs de positionnement remarquables de moins de

50 cm dans 90 % des cas.

Les nouvelles techniques de positionnement basées sur les empreintes digitales sont par la suite optimisées pour utiliser moins d'échantillons dans le but d'identifier un compromis de précision qui minimise la complexité et le coût d'acquisition d'empreintes digitales. Avec moins de la moitié des échantillons, nous démontrons que les RNA, s'ils sont bien conçus, peuvent interpoler et estimer précisément (spatialement et/ou temporellement) les empreintes digitales qui n'ont pas été vues par les RNA dans le processus d'entraînement.

Les réalisations présentées dans cette recherche montrent que la localisation basée sur la RIC peut atteindre jusqu'à 75 % de gains en précision en exploitant la diversité spatiale et/ou temporelle en présence de systèmes d'antennes doubles, tout en réduisant le coût de la collecte d'échantillons de moitié.

Abstract

Underground gold mines are known for their disruptive indoor channels that challenge the deployment of wireless communication systems by severely distorting their wireless transmitted signals. Although mining is among the most booming industries, yet underground gold mines are still criticized for their outdated safety and security measures. Our mission in underground mines stems from the profound need of a reliable localization system that succeeds to accurately localize miners and their equipment in one of earth's most dangerous entrails. After studying the reasons behind the failure of traditional localization techniques in underground mines, we recommend an effective localization technique that uses Artificial Neural Networks (ANNs) and fingerprints extracted from the channel's impulse response (CIR). The essence of this work lies in its ability to push the performance limits of ANN-based positioning techniques by integrating the concepts of T_x and R_x spatial and/or temporal diversities in fingerprints prior to estimating a transmitter's position in the confinement of underground tunnels. By doing so, we lay down the guidelines of cooperative localization in the realm of ANNs using concatenated fingerprints which are extracted from more than one access point, at multiple time instances, using single or dual antenna systems. As a result, new fingerprinting techniques, that exploit spatial and/or temporal diversities of the collected signatures, are introduced for the first time with outstanding positioning errors of less than 50 cm 90% of the time. The novel fingerprint positioning techniques are then optimized to use less data measurements in an effort to tradeoff pinpoint accuracy for lower complexity and fingerprint-acquisition cost.

By using less than half of the measurement campaign's data, we prove that ANNs, if well designed, may interpolate and precisely estimate spatially and/or temporally diverse fingerprints taken from measurement gaps not seen by ANNs in the training process. The new realizations of this research show that CIR-based localization may attain up to 75% accuracy gains when exploiting spatial and/or temporal diversities in the presence of dual antenna systems while, at the same time, cutting down the measurement campaign's cost in less than half.

Smart Localization in Underground Mines using Fingerprinting and ANNs: Strategies and Applications

Sommaire Récapitulatif

Cette partie contient les chapitres [A](#), [B](#), [C](#), [D](#) et [E](#) qui sont la traduction française des chapitres [1](#), [3](#), [4](#), [5](#) et [6](#) respectivement.

Chapitre A

Introduction

Cette thèse introduit de nouvelles techniques de positionnement basées sur les empreintes qui sont conçues pour les zones souterraines et confinées telles que les mines d'or. Dans le cadre de mon doctorat à l'*Institut National de la Recherche Scientifique-Energie Matériaux et Télécommunications* (INRS-EMT) et en collaboration avec le *Laboratoire de Recherche Télébec en Communications Souterraines* (LRTCS), je présente et analyse les constatations et les résultats des techniques de positionnement basées sur les empreintes dans les mines souterraines. Dans la suite de cette thèse, la portée des travaux est définie en soulignant la problématique de recherche, les objectifs et les méthodologies appliquées.

A.1 Problématique de recherche

La localisation des mineurs et/ou leurs équipements dans les mines souterraines est un besoin essentiel qui garantit les mesures de sécurité de base dans l'un des environnements de travail les plus dangereux. Cependant, les techniques de localisation modernes qui garantissent la précision dans les canaux extérieurs peuvent échouer si elles sont implémentées dans des milieux intérieurs instables tels que les

mines. Jusqu'à présent, de nombreuses recherches au LRTCS ont révélé l'efficacité des techniques de positionnement intérieures entraînées par l'intelligence artificielle que nous considérons, dans notre étude, comme de bonnes candidates pour la localisation souterraine. Toutefois, il y a encore un défi à relever par l'absence d'adaptation de ces techniques à des systèmes de communication modernes et sophistiqués qui utilisent plus d'un point d'accès en coopération et exploitent la présence d'antennes à entrée(s) unique/multiples et sorties multiples (SIMO / MIMO). La valeur de cette recherche provient de sa capacité à introduire des méthodes d'empreintes coopératives qui exploitent les diversités spatiales et/ou temporelles en la présence d'antennes émettrices simples et/ou doubles comme dans le cas des dispositifs MIMO de communication modernes. En conséquence, toutes les techniques de localisation qui s'appuient sur une seule antenne d'empreintes peuvent utiliser notre approche innovante pour faire usage de la diversité espace-temps, ce qui garantit une plus grande précision, robustesse et réduction des coûts d'acquisition des empreintes.

A.2 Objectifs

L'objectif principal de cette recherche est d'étudier les techniques de localisation souterraine basées sur les empreintes sans fil dans le domaine de la diversité temporelle et/ou spatiale d'une part, et en présence de plus d'une antenne émettrice et réceptrice d'autre part. Ainsi, non seulement nous améliorons les précisions du positionnement et les résultats de précision, mais nous introduisons aussi de nouvelles méthodes basées sur les empreintes qui peuvent être adaptées pour les systèmes de localisation souterrains. Un autre objectif de cette recherche est de réduire le coût des campagnes d'acquisition des empreintes, qui constitue la source principale de critique. En concevant des techniques à base d'empreintes qui assurent des précisions ponctuelles pour moins de données de mesure hors ligne, nous réussissons à réduire le

coût à moins de la moitié, tout en maintenant des résultats de positionnement précis en utilisant nos nouvelles méthodologies d’empreintes sophistiquées.

A.3 Méthodologie

La méthode employée utilise de 480 points de mesure des données recueillies dans une mine souterraine à 2.4 GHz, en présence d’une seule antenne de réception, à partir desquelles les réponses impulsionnelles du canal (RIC) sont extraites. En utilisant les empreintes extraites à partir des RIC et des Réseaux de Neurones Artificiels (RNA), la localisation est ensuite adaptée en tant que paradigme pour localiser la position de l’émetteur. De nouvelles empreintes sont ensuite formées en exploitant les diversités espace et/ou temps. Il convient de souligner que les résultats de la localisation sont basés sur la distance de séparation entre l’émetteur et le récepteur le long de l’axe x seulement, en négligeant les petites variations le long de l’axe y qui sont de moindre valeur dans les tunnels étroits des mines d’or souterraines.

Après discussion de la technique de localisation de base en présence d’un seul récepteur, nous simulons, en utilisant les mêmes mesures, la présence d’une autre antenne de réception pour étudier l’effet de l’utilisation de la diversité spatiale des empreintes collectées. En ayant deux récepteurs collectant les signaux transmis, deux empreintes sont extraites de chaque récepteur pour former une empreinte digitale spatiale R_x pour chaque position donnée. Les résultats de l’exploitation de la diversité spatiale R_x surpassent la présence d’un seul récepteur et contribuent à clarifier l’ambiguïté de la position de l’émetteur dans la présence des jonctions. La diversité spatiale R_x seule ne peut pas être améliorée sans l’ajout de points d’accès supplémentaires ce qui n’est pas possible dans le confinement des mines à filons étroits.

Cependant, une autre dimension de recherche va au-delà de la diversité spatiale pour inclure les empreintes de type mémoire exploitant la diversité de temps. L’étude

de l'utilisation des empreintes temporelles est réalisée par la production de toutes les empreintes des chemins possibles qui conduisent à une position spécifique, pour une profondeur de mémoire donnée, à l'intérieur des tunnels. Une empreinte digitale de chemin est une concaténation de toutes les sous-empreintes extraites le long d'un chemin spécifique qui conduit à la position finale à estimer. Les RNA sont ensuite formés sur tous les chemins possibles pour un niveau de mémoire donné et utilisés pour estimer les données qui ne sont pas vues dans les phases d'apprentissage. Il est observé que les seuils de performances sont améliorés en exploitant la diversité temporelle avec une augmentation de la complexité de la formation.

Afin d'améliorer davantage les performances des techniques de positionnement basées sur les empreintes, une étude a été menée afin d'évaluer la performance de la localisation en présence de capacités de mémoire et la collaboration entre deux récepteurs. Lorsque les chaînes des sous-empreintes temporelles recueillies du premier récepteur sont combinées avec d'autres sous-empreintes au deuxième récepteur, des empreintes spatio-temporelles sont obtenues. En conséquence, l'utilisation de la diversité espace-temps surpasse les performances des approches précédentes en termes d'exactitude, de précision et de complexité.

Un autre axe de recherche étudie la possibilité d'exploiter la présence d'antennes doubles à l'émetteur, pour des fins de localisation, comme dans le cas de l'équipement utilisateur (UE) moderne MIMO. Par la concaténation de deux sous-empreintes du côté de l'émetteur séparées par un espacement d'antenne donné, nous formons un type d'empreintes SIMO si une seule antenne de réception est présente et des empreintes de type MIMO en présence de deux antennes de réception. Les empreintes de type MIMO/SIMO sont étudiées sur un espacement antenne de 1 m suivant l'axe des x , de 0,5 m et 1 m suivant l'axe des y .

Après la réalisation de très hautes précisions qui ont dépassé les attentes, une

recherche pour une performance optimisée commence dans un effort pour réduire la surcharge de coût des campagnes d'acquisition des empreintes. Chaque technique de localisation a été mise sous le test de l'utilisation de moins de mesures de données, pour l'apprentissage des RNA, en réduisant la résolution de la grille à un sixième de sa taille originale. Les RNA ont été mis au défi pour localiser dans les lacunes de mesure qui ne sont pas visibles dans les phases d'apprentissage, tout en essayant de maintenir une précision de positionnement. Après la formation de plus de 14000 RNA, le nombre le plus adéquat de neurones qui correspond à chaque technique de localisation a été identifié sur la base de la résolution de la grille.

Comme prévu, les précisions de la localisation diminuent légèrement lorsque la résolution de la grille diminue, cependant, les techniques basées sur les empreintes nouvelles et sophistiquées, comme le positionnement basé sur le type MIMO d'empreintes, réussit à obtenir des résultats de positionnement précis même avec une résolution de grille inférieure.

A.4 Structure de la thèse

La thèse est écrite en utilisant le format article et elle est divisée en deux parties, chacune divisée en plusieurs chapitres.

Dans la première partie, chapitre 2 (dans la version anglaise) présente les principes de localisation et les recherches les plus récentes effectuées dans les techniques de localisation intérieure. Au chapitre B, les nouveaux résultats de ce travail sont brièvement discutés, y compris les nouvelles techniques de positionnement basées sur les empreintes qui exploitent les diversités spatiales et temporelles. En plus, la section B.5 p. xxii du même chapitre illustre les méthodes utilisées pour optimiser le système de localisation en abaissant son coût d'acquisition des empreintes. Les résultats de performance sont ensuite discutés au chapitre C. Les résultats sont suivis d'une conclusion

au chapitre [D](#), avant de révéler les futurs thèmes de recherche qui sont recommandés comme une continuité de ce travail au chapitre [E](#).

Dans la deuxième partie, nous incluons les publications et les manuscrits qui légitiment ce travail et montrent l'importance de ses résultats. Chaque chapitre, étant un article de conférence ou de journal, porte une nouvelle technique d'empreintes. Une description complète de ce travail est résumée dans le journal inclus au chapitre [12](#).

Chapitre B

Localisation intelligente dans les mines souterraines à l'aide des empreintes et les RNA

Dans ce chapitre, nous examinerons les résultats de la recherche en profondeur en montrant leurs méthodes fonctionnelles et les techniques basées sur les empreintes. Ce chapitre constitue les principales réalisations de ce travail qui ont été publiées en parties puis résumées dans un manuscrit de journal qui peut également être consulté au chapitre [12](#).

Comme étude préliminaire, il est recommandé de réviser l'efficacité de la localisation basée sur les empreintes utilisant les RNA dans [\[31\]](#), qui a également été examinée avant dans la section [2.3](#) p. [16](#). Dans un premier temps, nous examinons la méthodologie adaptée pour la localisation coopérative, en présence de plus d'un récepteur dans la section [B.1](#) p. [xiii](#) qui contribue à la réalisation de l'article joint au chapitre [7](#). La localisation utilisant la diversité temporelle est alors expliquée dans la section [B.2](#) p. [xv](#) et ses résultats peuvent être consultés également dans la publication

mentionnée au chapitre 8. De même, la section B.3 p. xviii explique les concepts de la localisation exploitant la diversité spatio-temporelle qui contribuent au travail publié au chapitre 9.

L'innovation des empreintes de type SIMO/MIMO, qui sont examinées dans la section B.4 p. xx et au chapitre 11, présente les techniques qui peuvent être utilisées pour enrichir les techniques basées sur les empreintes avec la présence d'antennes Tx doubles. Enfin, les techniques d'optimisation et de réduction de coût sont traitées dans la section B.5 p. xxii et à travers les publications des chapitres 10, 11 et 12.

B.1 La localisation en exploitant la diversité spatiale R_x

La localisation dans les mines souterraines à l'aide de plus d'un point d'accès a été la première étape vers un système coopératif qui utilise plus d'une sous-empreinte digitale avant d'estimer la position d'un émetteur. Non seulement la collaboration entre les points d'accès augmente la précision du positionnement, mais elle élimine également l'ambiguïté sur la définition de la direction de la transmission dans les cas où des jonctions sont présentes dans les galeries et tunnels souterrains. La localisation exploitant la diversité spatiale R_x est le premier chapitre de réalisations et est décrite en détail dans la publication présenté au chapitre 7 et dans la section 12.3.1 p. 144.

Avant l'innovation des empreintes collaboratives, une seule empreinte digitale a été utilisée par un seul récepteur pour extraire la distance à un émetteur sans connaître le sens exact de la transmission. L'objectif de ce chapitre est d'incorporer plus d'une empreinte digitale (c'est-à-dire, qui sera appelée sous-empreinte digitale) à partir des récepteurs spatialement éloignés avant d'estimer la position finale de la transmission.

Compte tenu de la topologie étroite spéciale des tunnels souterrains, deux récepteurs seraient suffisants pour couvrir chaque tunnel, comme indiqué sur la figure 7.2. Les mêmes mesures qui ont été prises à partir du premier récepteur R_1 dans [31] sont utilisées dans le sens opposé afin de simuler la présence d'un autre récepteur R_2 comme indiqué sur la figure 3.1.

Exploitant la diversité spatiale R_x de deux récepteurs R_1 et R_2 , dans la région de couverture commune, se traduit par deux ensembles d'empreintes $S^{R_1} = \{f_1, f_2, f_3, \dots, f_m\}$ et $S^{R_2} = \{f'_1, f'_2, f'_3, \dots, f'_m\}$, respectivement. L'ensemble de sortie des RNA $D = \{d_1, d_2, d_3, \dots, d_m\}$ représente les distances à l'un des récepteurs qui est pris par défaut pour être la distance de R_1 à l'émetteur. Il convient également de noter que de multiples scénarios sont analysés à des distances de séparation du récepteur de 60 m, 80 m et 100 m, en supposant que les signaux se désintègrent après 64 m tel que rapporté dans [31] et remarqué dans les mesures collectées. Après avoir recueilli les ensembles de mesure pour chaque scénario, on peut penser à deux façons pour estimer la position d'un émetteur en utilisant les RNA.

La première conception, illustrée dans la figure 7.4, permet à chaque récepteur de localiser séparément en utilisant son propre RNA avec sept paramètres d'entrée correspondant à chaque empreinte respective ou signal reçu. En connaissant à *priori* la carte du tunnel et la position de chaque récepteur, on peut faire la moyenne des deux distances et estimer la position finale de chaque récepteur. Le deuxième type est fournit de meilleurs résultats de l'estimation et est appelé "technique de localisation coopérative" et utilise les sous-empreintes recueillies des deux récepteurs et les concatène pour former des empreintes spatialement diverses, qui sont le double de la taille de l'empreinte digitale originale. En d'autres termes, la concaténation de deux ensembles, S^{R_1} et S^{R_2} résulte en un ensemble d'empreintes représenté par:

$$S = \{F_1, F_2, F_3, \dots, F_m\} = \{(f_1, f'_1), (f_2, f'_2), (f_3, f'_3), \dots, (f_m, f'_m)\}. \quad (\text{B.1})$$

Comme le montre la figure 7.5, la diversité spatiale R_x est exploitée en utilisant un seul RNA formé avec les empreintes de longueurs de chaîne plus élevées. Les résultats de la localisation en utilisant la diversité spatiale R_x sont présentés pour les empreintes d'apprentissage dans les figures 7.6, 7.7 et 7.8, tandis que les résultats des tests sont présentés dans les figures 7.9, 7.10 et 7.11, à des distances de séparation du récepteur de 60 m, 80 m et 100 m, respectivement. L'estimation finale obtenue des précisions pour les techniques d'empreintes spatialement diverses R_x , après optimisation de leurs RNA pour un coût faible d'acquisition des empreintes comme discuté plus tard dans la section B.5 p. xxii, sont résumées dans le tableau C.1 à 77 cm et 90 cm pour 90% des données d'apprentissage et de test, respectivement.

B.2 Localisation en exploitant la diversité temporelle

La localisation utilisant la diversité spatiale R_x a été efficace dans les régions qui sont couvertes par plus d'un seul point d'accès. D'une part, il manque à la solution une technique efficace qui puisse garantir la même précision lors de la perte de couverture du deuxième récepteur R_2 . D'autre part, l'augmentation de la précision dans le cadre de la diversité spatiale nécessite seulement l'ajout de plus d'un point d'accès, ce qui n'est ni faisable ni pratique dans les tunnels étroits et confinés.

La recherche pour une technique complémentaire basée sur les empreintes, qui fait usage de la mobilité limitée des mineurs sous terre, a conduit à la formulation de la localisation basée sur les empreintes exploitant la diversité temporelle. La localisation exploitant la diversité temporelle est le second chapitre des réalisations et elle est expliquée en détail dans la publication présente au chapitre 8 et dans les procédures de la section 12.3.2 p. 147.

Ce travail présente une technique basée sur les empreintes qui enregistre les signatures (c'est-à-dire, ensembles de 7 paramètres) jusqu'à un certain niveau l de mémoire. Par exemple, une empreinte digitale spatialement diverse R_x a la même longueur d'empreinte digitale qu'une empreinte digitale temporelle extraite avec le niveau mémoire $l = 2$. Toutefois, celle-ci est obtenue à l'aide d'un seul récepteur en présence de la capacité d'enregistrement de la mémoire qui a incorporé la sous-empreinte digitale précédente du mineur, au moment t_{-1} et l'a concaténée à une autre sous-empreinte digitale au moment t_0 . En d'autres termes, une empreinte digitale temporelle

$$f_i^j = \left(f_{i_{t_0}}, f_{i_{t_{-1}}}, f_{i_{t_{-2}}}, \dots, f_{i_{t_{-(l-1)}}} \right). \quad (\text{B.2})$$

est la concaténation des sous-empreintes mesurées dans des intervalles de temps courts en déplaçant vers une destination à être estimée à X . l étant le nombre de sous-empreintes concaténées ou ce que nous appelons le niveau de la mémoire, on définit la longueur d'une empreinte digitale temporelle L_f où:

$$L_f = 7l. \quad (\text{B.3})$$

La localisation exploitant uniquement la diversité temporelle, en présence d'un récepteur, est étudiée pour $l = 1, 2, 3, 4$ et 5 (c'est-à-dire, RNA (1,0), RNA (2,0), RNA (3,0), RNA (4,0) et RNA (5,0)), après quoi aucun gain significatif n'est observé.

Pour illustrer davantage l'extraction des empreintes temporelles à travers un exemple à $l = 2$, considérons la figure 8.5. Pour une position à t_0 , cinq chemin-empreintes peuvent être extraits, dans la phase hors ligne, et ils représentent des chaînes d'empreintes qui combinent une signature de la position précédente extraite du CIR à t_{-1} comme indiqué dans le tableau 8.1. Un autre exemple pour $l = 3$ est illustré en détail dans figure 12.7 où un mineur peut avoir jusqu'à 25 chemins-

empreintes temporellement diverses pour une seule position. Le nombre de chemin-empreintes j_{max} qui peut être obtenu pour une position donnée est limité par le nombre supérieur de chemin-empreintes N_{fp} :

$$j_{max} \leq N_{fp} = 5^{(l-1)}. \quad (\text{B.4})$$

Tous les chemin-empreintes possibles sont recueillis pour toutes les positions d'intérêt tout en respectant les limites des tunnels confinés. L'ensemble total des empreintes temporelles est désigné par $S = \{S_1, \dots, S_i, \dots, S_m\}$ et il correspond à toutes les distances $D = \{d_1, \dots, d_i, \dots, d_m\}$. La puissance de cette technique réside dans sa capacité à augmenter de façon exponentielle le nombre de chemin-empreintes dans l'ensemble d'apprentissage, en utilisant uniquement un seul récepteur, sans avoir besoin de mesures supplémentaires. Toutefois, cela se fait au prix d'une augmentation du nombre d'entrées et le nombre de neurones pour les RNA d'apprentissage.

Les résultats de la localisation en utilisant la diversité temporelle sont présentés pour les empreintes d'apprentissage dans les figures 8.9 et 8.10 pour les empreintes d'apprentissage et de test, respectivement. Les précisions définitives d'estimation rapportées pour toutes les techniques basées sur les empreintes temporellement diverses ont montré des gains de haute précision avec seulement 50 cm d'erreurs d'estimation pour 90% des empreintes à $l = 4$ et $l = 5$. Un aperçu complet des résultats peut être consulté à la section 8.4.2 p. 75 et dans les tableaux C.1 ou 9.1.

B.3 Localisation exploitant la diversité spatio - temporelle

En comparant des empreintes R_x spatialement et temporellement diverses, on peut conclure que les deux sont uniques dans leur mise en œuvre. Les premières exploitent la diversité spatiale des empreintes recueillies à partir de deux récepteurs distincts alors que les dernières utilisent des mesures d'empreintes dans des intervalles de temps courts. Cela a conduit à la réalisation que la combinaison des deux concepts ensemble dans une technique basée sur les empreintes spatio-temporelles stimulerait les précisions de la localisation et ajouterait plus de robustesse au système de localisation. En effet, augmenter la précision à une valeur extrême peut ne pas être nécessaire pour le positionnement des mineurs en souterrain, mais on aura en échange une moindre complexité et un moindre coût, comme discuté ci-après dans la section B.5 p. xxii. La localisation exploitant la diversité spatio-temporelle est le troisième chapitre de réalisations des résultats très précis et satisfaisants ont été présentés dans la publication du chapitre 9 et dans les procédures de la section 12.3.3 p. 151.

La localisation à mémoire assistée exploitant la diversité spatio-temporelle est le résultat de la collaboration de deux récepteurs quand au moins l'un d'eux introduit de la mémoire (par exemple, produisant des chemin-empreintes) [5]. Les niveaux de mémoire des récepteurs R_1 et R_2 sont désignés par l_1 et l_2 , respectivement. Les empreintes sont extraites pour différents niveaux de mémoire et analysées complètement dans la section 9.3 p. 91. Un ensemble S_i d'empreintes spatio-temporelles, pour une distance d_i donnée, est une concaténation de deux sous-ensembles d'empreintes $S_i^{R_1}$ et $S_i^{R_2}$ recueillies par les récepteurs R_1 et R_2 , respectivement, où: $S_i^{R_1} = \{F_i^{R_1,1}, F_i^{R_1,2}, F_i^{R_1,3}, \dots, F_i^{R_1,j_{max}}\}$ and $S_i^{R_2} = \{F_i^{R_2,1}, F_i^{R_2,2}, F_i^{R_2,3}, \dots, F_i^{R_2,j_{max}}\}$. Le résultat est un ensemble d'empreintes

spatio-temporelles, qui est concaténé, et définit pour l_1 et l_2 comme suit:

$$S_i = \left\{ (F_i^{R_{1,1}}, F_i^{R_{2,1}}), (F_i^{R_{1,2}}, F_i^{R_{2,2}}), (F_i^{R_{1,3}}, F_i^{R_{2,3}}), \dots, (F_i^{R_{1,j_{max}}}, F_i^{R_{2,j_{max}}}) \right\}.$$

Un exemple peut être tiré lors de la localisation d'un émetteur à une distance d_i et à un instant t_0 avec des niveaux de mémoire ($l_1 = 2, l_2 = 1$), qui conclut une empreinte digitale spatio-temporelle $F_i = (F_i^{R_1}, F_i^{R_2})$ où

$$F_i^{R_1} = (f_{i_{t_0}}^{R_1}, f_{i_{t_{-1}}}^{R_1}), \quad (\text{B.5})$$

$$F_i^{R_2} = (f_{i_{t_0}}^{R_2}). \quad (\text{B.6})$$

Pour ($l_1 = 2, l_2 = 1$), R_2 extrait une empreinte digitale $F_i^{R_2}$ de longueur 7 (c'est-à-dire, une empreinte sans mémoire) tandis que $F_i^{R_1}$, collectée à partir de R_1 , est la concaténation de deux sous-ensembles d'empreintes enregistrées à partir de deux instants t_0 et t_{-1} (c'est-à-dire, empreinte digitale à mémoire assistée de longueur 14). En conséquence, une empreinte spatio-temporelle $F_i = (F_i^{R_1}, F_i^{R_2})$ peut être utilisée dans une technique basée sur les empreintes qui combine trois CIRs (à savoir, 21 paramètres) pour chaque position à l'intérieur de la topologie quasi-curveiligne des mines étroites. Le nombre d'entrées N_{inputs} , définit la conception du RNA et est identifié par la longueur de l'empreinte spatio-temporelle qui dépend à la fois de l_1 et l_2 où:

$$N_{inputs} = 7(l_1 + l_2). \quad (\text{B.7})$$

Le test des empreintes spatio-temporelles se fait en deux étapes. Dans un premier temps, R_2 est maintenu à un niveau de mémoire $l_2 = 1$ (c'est-à-dire sans mémoire),

tandis que le niveau de la mémoire de R_1 varie (par exemple, $l_2 = 2, 3$). Puis, dans la deuxième étape, les deux niveaux de mémoire sont augmentés simultanément. Les résultats de la localisation utilisant la diversité spatio-temporelle sont présentés pour l'apprentissage et le test des empreintes aux figures 9.6 et 9.7, respectivement. Il a été prouvé, dans la section 9.4 p. 93, que les approches basées sur la mémoire assistée coopérative qui combinent les diversités spatiales et temporelles pour les empreintes sont plus performantes que les techniques solitaires même lorsque la longueur des empreintes est la même comme les cas du RNA (3,0) (c'est-à-dire, en exploitant la diversité temporelle seulement) et le RNA (2,1) (c'est-à-dire, en exploitant la diversité spatio-temporelle). Les résultats de toutes les techniques spatio-temporelles étudiées peuvent être consultés dans le tableau 9.1, tandis que ceux résultant des RNA optimisés pour un coût faible d'acquisition des empreintes digitales, discutés plus tard dans la section B.5 p. xxii, sont résumées dans le tableau C.1.

B.4 Localisation exploitant la diversité spatiale R_x et T_x

La localisation exploitant des empreintes basées sur des systèmes d'antennes doubles, présents dans les systèmes de communication entrée unique/multiple sortie multiple (SIMO/MIMO), est le quatrième chapitre de réalisations et pousse les limites de performance de la localisation basée sur la RIC. En utilisant les concepts de deux antennes présentes dans les systèmes de communications SIMO/MIMO, une nouvelle technique de localisation basée sur les empreintes est introduite pour combiner des sous-empreintes extraites des antennes émettrices doubles (T_x) et recueillies sur une ou plusieurs antennes de réception (R_x). Le résultat est un ensemble d'empreintes spatialement diverses sur les antennes T_x et R_x , qui estime avec précision la distance

à l'émetteur. Le fondement de ce travail est présenté dans la publication du chapitre 11 et dans les procédures de section 12.3.4 p. 153.

Dans ce qui suit, nous établissons les bases d'une nouvelle technique établie par des empreintes de type SIMO et MIMO extraites de deux antennes émettrices (c'est-à-dire, T_{x1} et T_{x2}) en présence d'une antenne de réception (c'est-à-dire, R_{x1}) et deux antennes de réception (c'est à dire, R_{x1} et R_{x2}) respectivement. La diversité spatiale est exploitée deux fois au niveau du récepteur et de l'émetteur, où l'espacement des antennes est $\delta^{T_x} = 1$ m le long de l'axe des x ou $\delta^{T_x} = 0.5$ m le long de l'axe des y du tunnel. D'un point de vue de mise en œuvre, les antennes peuvent être placées sur la machinerie lourde ou construites dans les costumes des mineurs sur les épaules.

Les empreintes de type SIMO (c'est-à-dire, les empreintes recueillies à R_1 à partir des deux antennes T_x) exploitent la diversité spatiale T_x du côté de l'émetteur en présence d'un seul récepteur sans la nécessité de la mémoire (cf. section 12 p. 133). Une empreinte digitale de type SIMO est représentée comme suit:

$$F_i^{SIMO} = (f_i^{T_{x1}}, f_i^{T_{x2}}), \quad (\text{B.8})$$

où $f_i^{T_{x1}}$ et $f_i^{T_{x2}}$ sont les empreintes recueillies par R_{x1} , à une position i , pour T_{x1} et T_{x2} , respectivement. D'autre part, les empreintes de type MIMO, qui exploitent à la fois les diversités spatiales T_x et R_x , sont simulées en considérant deux antennes de réception R_{x1} et R_{x2} , étant celles de R_1 et R_2 , respectivement. Une empreinte digitale de type MIMO peut être exprimée comme suit:

$$F_i^{MIMO} = \{(f_i^{T_{x1}}, f_i^{T_{x2}}), (f_{i'}^{T_{x1}}, f_{i'}^{T_{x2}})\}. \quad (\text{B.9})$$

$f_i^{T_{x1}}$ et $f_i^{T_{x2}}$ représentent les empreintes recueillies par R_{x1} , tandis que $f_{i'}^{T_{x1}}$ and $f_{i'}^{T_{x2}}$, sont les empreintes recueillies par R_{x2} , à une position $i' = D - i$, pour T_{x1} et T_{x2} ,

respectivement. L'estimation finale est la distance, le long de l'axe x , séparant R_1 et le point médian de T_{x1} et T_{x2} . au chapitre 11, la localisation utilisant à la fois les diversités spatiales R_x et T_x est étudiée à $\delta_x^{T_x} = 1$ m le long de l'axe des x et à $\delta_y^{T_x} = 1$ ou 0.5 m le long de l'axe des y du tunnel.

Les résultats de performance de l'exploitation des diversités spatiales T_x et R_x , représentées sur la figure 11.8 et résumées dans le tableau C.1, dépassent ceux de toutes les techniques développées basées sur les empreintes, discutées ci-dessus, en termes de précision et d'exactitude. Leurs précisions tombent en dessous de 40 cm pour 90% des données de test. En plus de cela, en exploitant la présence de systèmes d'antennes doubles dans l'apprentissage des empreintes, la robustesse du système de localisation augmente et les RNA, s'ils sont bien conçus, interpoleront avec des précisions plus élevées même en présence d'écarts de mesure comme abordé plus tard dans la section B.5 p. xxii.

B.5 Techniques d'optimisation et de réduction des coûts

Dans la littérature, la plupart des techniques basées sur les empreintes sont critiquées en raison de leur besoin de campagnes de mesures coûteuses pour la construction de la base de données d'apprentissage des RNA. Réduire la quantité de mesures de données, d'autre part, peut risquer le processus de généralisation que les RNA nécessitent pour interpoler et estimer dans les écarts de mesure invisibles tout au long du processus d'apprentissage. Une conclusion tirée après une tentative réussie, à la fin du chapitre 10, pour récolter les avantages de la diversité, en échange d'un plus faible coût d'acquisition des empreintes. Cependant, une étude plus poussée a été réalisée pour défier toutes nos techniques de localisation développées qui utilisent les

diversités spatiales, temporelles et spatio-temporelles en présence d'antennes de transmission simples ou doubles, et mettre leurs RNA respectifs à l'épreuve de l'utilisation de moins de mesures de données en cachant progressivement jusqu'à un sixième des points de mesure de la grille. Les neurones obtenus, nécessaires pour chaque technique et qui ont été produits après des simulations étendues des RNA, constituent l'argument décisif de ce travail et ils sont entièrement décrits dans la publication du chapitre 11 et dans les procédures de la section 12.5 p. 159.

Les techniques de localisation ont été discutées à une taille de pas d'échantillonnage $S_x = 1$ m qui représente la taille du pas entre n'importe quels deux points de mesure consécutifs hors ligne le long de l'axe x du tunnel. Cela signifie que les RNA ont été formés en utilisant un taux d'échantillonnage hors ligne S_r de 1 ensemble-empreinte digitale par mètre sans lacunes cohérentes dans la résolution de la grille. Dans ce qui suit, on augmente S_x , à 2 m, 3 m et jusqu'à 6 m (c'est-à-dire, réduire S_r pour un ensemble-empreinte digitale par S_x), résultant en une fraction de la grille d'origine en deux, trois et jusqu'à 6 sous-grilles, respectivement, en comptant pour la position initiale de l'émetteur sur la grille.

Le défi de la diminution extrême du nombre d'empreintes vient de la capacité d'alterner les conceptions des RNA en cherchant le nombre optimal de neurones nécessaires pour chaque ensemble d'empreintes. Un très grand nombre de neurones se traduirait par une convergence profonde et des précisions *over fitting* qui riposteraient et entraîneraient des erreurs d'estimation très élevées lors de la localisation dans des écarts de mesure ou dans des sous-grilles omises dans le processus d'apprentissage des RNA. De même, peu de neurones peut amener le système à perdre beaucoup de sa performance en essayant de généraliser le domaine de solution. Pour cette raison précise, une simulation approfondie a été effectuée et plus de 14000 RNA ont été

formés, chacun avec un nombre de neurones n_n , variant entre 1 et N_n , tels que:

$$1 < n_n < N_n = 2N_i + 1, \quad (\text{B.10})$$

où N_i est le nombre d'entrées du RNA qui dépend de la technique de localisation utilisée et des niveaux de mémoire. Un RNA successeur pour chaque technique est celui qui obtient la meilleure performance, en termes de précision, lorsqu'il est testé sur sa sous-grille formée et sur 25% de toutes les sous-grilles restantes à un certain S_x . Le nombre de neurones sélectionnés par chaque technique de localisation est représenté sur la figure 12.10 et il peut être utilisé comme une référence pour de futures études.

Étonnamment, les résultats de performance montrent des enregistrements très précis, même lorsque les RNA sont formés en utilisant un sixième des empreintes de la grille permettant aux empreintes de type MIMO de surpasser le reste des techniques de localisation en termes de robustesse envers la résolution de la grille. A $S_x = 6$ m, la localisation utilisant les diversités spatiales T_x et R_x atteint des résultats similaires à la référence d'origine dans [31] à $S_x = 1$ m. Les autres résultats d'optimisation des coûts pour toutes les techniques spatiales, temporelles et spatio-temporelles basées sur les empreintes sont présentées dans la publication du chapitre 11 et dans les procédures de la section 12.5.1 p. 160 en particulier dans les figures 12.13 et 12.14.

Chapitre C

Analyse des données et résultats

La fonction de densité cumulative (FDC) est utilisée tout au long de la dissertation pour montrer et comparer les erreurs d'estimation de toutes les techniques de localisation développées en mettant l'accent sur leurs précisions de positionnements en mètres par rapport à la précision (c'est-à-dire, le pourcentage des empreintes traitées). La granularité des erreurs d'estimation est complètement montrée sur les figures [12.8](#), [12.9](#), [12.13](#), [12.14](#) et dans le tableau [C.1](#), puis les résultats de performance sont analysés ensemble dans les sections [12.4](#) p. [154](#) et [12.5.2](#) p. [162](#). Dans ce qui suit, les techniques de positionnement basées sur les empreintes développées, qui constituent les résultats de ce travail, sont comparées et analysées sur la base des facteurs importants tels que l'exactitude, la précision, la complexité, la robustesse et le coût.

C.1 Exactitude et précision

La précision est l'une des plus importantes métriques de performance de n'importe quel système de positionnement. Dans certaines applications telles que les systèmes de positionnement militaire, la précision est le facteur le plus important et il ne peut

Table C.1 – Précisions à résolution multiple

Technique ANN	Précision de positionnement					
	1 m	2 m	3 m	4 m	5 m	6 m
ANN(1,0)	1.42 m	1.44 m	1.81 m	2.04 m	2.12 m	2.83 m
ANN, 2Tx1Rx $\delta_y^{Tx} = 0.5$ m	1.10 m	1.43 m	1.73 m	1.81 m	2.26 m	2.58 m
ANN, 2Tx1Rx $\delta_y^{Tx} = 1$ m	0.85 m	1.36 m	1.53 m	1.66 m	1.94 m	1.97 m
ANN(2,0)	1.15 m	1.35 m	1.58 m	1.92 m	1.97 m	2.07 m
ANN(3,0)	0.53 m	1.36 m	1.58 m	1.78 m	1.94 m	2.02 m
ANN(4,0)	0.48 m	1.30 m	1.46 m	1.72 m	1.91 m	1.93 m
ANN, 2Tx1Rx $\delta_x^{Tx} = 1$ m	1.05 m	1.23 m	1.33 m	1.51 m	1.61 m	2.07 m
ANN(1,1)	0.91 m	1.07 m	1.15 m	1.28 m	1.39 m	1.45 m
ANN, 2Tx2Rx $\delta_y^{Tx} = 1$ m	0.64 m	0.84 m	1.07 m	1.14 m	1.35 m	1.51 m
ANN(2,2)	0.49 m	0.95 m	1.07 m	1.22 m	1.26 m	1.41 m
ANN, 2Tx2Rx $\delta_x^{Tx} = 1$ m	0.43 m	0.93 m	1.10 m	1.14 m	1.19 m	1.32 m
ANN, 2Tx2Rx $\delta_y^{Tx} = 0.5$ m	0.38 m	0.83 m	0.98 m	1.12 m	1.20 m	1.28 m

pas être échangé contre la complexité et le coût, alors que dans les systèmes de positionnement commercial, un compromis entre la précision et le coût peut avoir lieu pour maintenir le prix dans la rationalité économique. D'autre part, le facteur de précision détermine si une précision donnée est rapportée fréquemment dans de multiples mesures. Pour ces raisons, nous avons choisi de comparer toutes les techniques de localisation en utilisant un percentile de 90% obtenus à partir des FDC de chaque technique de localisation.

Dans notre problème de localisation, toutes les techniques de localisation abordées peuvent être considérées précises car leurs erreurs de positionnement tombent en dessous de 1.5 mètre. Toutefois, pour les besoins du raisonnement, la technique la plus précise de toutes est celle qui introduit les empreintes de type MIMO poussant les limites de la précision à 38 cm pour 90% des données de test à $S_x = 1$ m. Une précision similaire a été rapportée pour le positionnement basé sur des empreintes spatio-temporelles avec RNA (2,2) avec des erreurs d'estimation aussi basses que 49 cm pour le même niveau de précision qui sont aussi proches des résultats de performance des empreintes temporellement diverses avec RNA (3,0) et RNA (4,0).

C.2 Complexité

La complexité du système de positionnement implique des facteurs tels que le temps de calcul, la mémoire, la conception matérielle et logicielle, la consommation d'énergie et l'implémentation. En tenant compte du temps de traitement du système, les techniques de localisation basées sur les empreintes peuvent être comparées sur la base du nombre de neurones utilisés par les RNA à la fois à l'entrée et dans les couches cachées. L'apprentissage des RNA avec des empreintes de grandes longueurs de chaîne est beaucoup plus lent que l'apprentissage des RNA avec quelques neurones d'entrée. Cela rendrait une technique de mémoire assistée avec un RNA (3,0) et une précision de 53 cm plus attractive qu'un RNA (4,0) qui rapporte une meilleure précision de 48 cm, car celui-ci utilise 7 neurones d'entrée en plus. On peut aussi comparer le nombre de neurones cachés des deux techniques comme montré sur la figure 12.10 pour trouver qu'elles commencent toutes les deux avec 40 neurones à $S_x = 1$ m.

D'autre part, d'un point de vue implémentation, l'ajout de mémoire aux points d'accès peut augmenter la complexité de la conception du système. Si la complexité est la principale préoccupation, le positionnement basé sur des empreintes utilisant les diversités spatiales T_x et R_x peut revenir à une complexité moindre que celle de la localisation basée sur la mémoire, en termes d'acquisition des empreintes et les techniques de reconnaissance de chemin.

C.3 Robustesse

La robustesse est la capacité de maintenir le système en stabilité une fois que les informations reçues sont corrompues ou inconnues. Pour cette raison, ce travail a étudié l'effet d'avoir moins de mesures de données dans le processus d'apprentissage

des RNA de toutes les techniques. Il est montré à $S_x = 6$ m que les techniques de positionnement basées sur les empreintes temporellement diverses n'ont pas réussi à maintenir leurs résultats de haute précision à $S_x = 1$ m, ce qui est dû au fait qu'à un S_x supérieur, les sous-empreintes extraites des positions antérieures portent moins d'informations sur la position actuelle de l'émetteur. On peut observer que les empreintes spatio-temporelles et celles de type MIMO ont maintenu leurs tendances de précision, même si un sixième des mesures étaient absentes du processus d'apprentissage.

C.4 Coût

Le coût d'un système de localisation dépend de la complexité de ses conceptions matérielles et logicielles; il dépend également du facteur d'intégration et de temps. Toutes les techniques de localisation basées sur les empreintes doivent subir des campagnes de mesure qui ajoutent des coûts supplémentaires à la facture d'implémentation. Plus les économies qu'une technique de localisation peut apporter sont meilleures, plus elle devient attractive aux investisseurs et aux propriétaires d'entreprises. Le coût de déploiement est minimum lors de l'utilisation des empreintes qui n'introduisent pas de mémoire et n'utilisent pas des appareils MIMO compatibles avec des antennes doubles, mais à ce faible coût des erreurs plus élevées et une faible robustesse pour la résolution d'échantillonnage apparaissent. Cependant, il est prouvé ici que les campagnes de mesure peuvent être réduites à moins de la moitié quand des techniques basées sur les empreintes spatio-temporelles ou de type MIMO réussissent à maintenir des résultats de haute performance.

Chapitre D

Conclusion

Pour conclure, si les diversités spatiales, temporelles ou spatio-temporelles sont bien appliquées dans les algorithmes de localisation basés sur les empreintes, le système de localisation gagnerait une haute précision et des précisions de positionnement ponctuelles. L'utilisation des empreintes de l'antenne double, d'autre part, est recommandée pour les appareils à capacité MIMO et est prouvée pour augmenter la performance du système. D'autre part, la réduction de la résolution d'échantillonnage des mesures hors ligne nécessite une conception minutieuse des RNA qui réussissent à localiser les lacunes de mesure invisibles dans le processus d'apprentissage. Enfin, l'échange de la précision ponctuelle pour une complexité et un coût plus faible est étudié pour des fins d'implantation dans un effort pour réduire le temps nécessaire pour les campagnes d'acquisition des empreintes.

Chapitre E

Recherche future

Les études futures analyseront la performance de toutes les techniques de localisation basées sur les empreintes dans différentes bandes de fréquences, telle que la bande des ondes millimétriques (c'est-à-dire, la bande de 60 GHz). Les applications de localisation à 60 GHz peuvent être utiles dans les domaines de la robotique, les réseaux de capteurs et les communications machine-vers-machine.

Puisque le système de localisation basé sur les RNA est centralisé (c'est-à-dire, la connaissance de l'emplacement est du côté du récepteur), un autre domaine de recherche serait d'analyser la capacité de diffusion des poids et des biais du RNA et permettre aux utilisateurs de s'auto-localiser dans les environs d'une couverture réseau sans fil.

Enfin, dans un meilleur effort pour optimiser le système de localisation, une étude peut être réalisée pour recommander le nombre optimal de paramètres dans chaque empreinte digitale basée sur la RIC selon que la localisation exploite la diversité spatiale, temporelle ou spatio-temporelle.

Acknowledgments

First I would like to express my deep gratitude to my director, professor Sofiène Affes, for his intellectual vision and guidance throughout my whole Ph.D. studies. I am grateful for all his cooperation and enthusiasm that led to the success of this work. I also hold my co-director, professor Nahi Kandil, in high regards for his continuous support in every step along the path of my research. I would also like to acknowledge the contribution of my co-director, professor Chahé Nerguizian, in providing the data measurements upon which our study is based.

I thank the board of directors and executive staff in the *Institut National de la Recherche Scientifique-Énergie Matériaux et Télécommunications* (INRS-EMT) for accepting me as part of their family and for giving me a great opportunity to contribute to global telecommunications research.

I dedicate this work to my family who never stopped backing me up until the final step of this long, yet prosperous journey.

Table of Contents

Résumé	i
Abstract	iii
Sommaire Récapitulatif	v
A Introduction	vi
A.1 Problématique de recherche	vi
A.2 Objectifs	vii
A.3 Méthodologie	viii
A.4 Structure de la thèse	x
B Localisation intelligente dans les mines souterraines à l'aide des empreintes et les RNA	xii
B.1 La localisation en exploitant la diversité spatiale R_x	xiii
B.2 Localisation en exploitant la diversité temporelle	xv
B.3 Localisation exploitant la diversité spatio-temporelle	xviii
B.4 Localisation exploitant la diversité spatiale R_x et T_x	xx
B.5 Techniques d'optimisation et de réduction des coûts	xxii
C Analyse des données et résultats	xxv
C.1 Exactitude et précision	xxv

C.2	Complexité	xxvii
C.3	Robustesse	xxvii
C.4	Coût	xxviii
D	Conclusion	xxix
E	Recherche future	xxx
	Acknowledgments	xxxii
	Table of Contents	xxxii
	List of Figures	xxxix
	List of Tables	xliv
	List of Acronyms	xliv
	List of Symbols	xlvi
I	Part 1 - Synopsis	2
1	Introduction to the Thesis	3
1.1	Research Problems	3
1.2	Objectives	4
1.3	Methodology	5
1.4	Structure of the Thesis	7
2	Literature review	8
2.1	Localization using Triangulation Techniques	9
2.1.1	Localization using RSS	9

2.1.2	Localization using ToA	11
2.1.3	Localization using TDoA	13
2.1.4	Localization using AoA	14
2.2	Fingerprint-Based Localization	15
2.3	Background of Localization in Underground Mines	16
2.3.1	Original Fingerprinting Technique	17
2.3.2	Basic Artificial Neural Network Architecture	20
3	Smart Localization in Underground Mines using Fingerprinting and ANNs	23
3.1	Localization Exploiting R_x Spatial Diversity	24
3.2	Localization Exploiting Temporal Diversity	26
3.3	Localization Exploiting Spatio-Temporal Diversity	28
3.4	Localization Exploiting R_x and T_x Spatial Diversity	31
3.5	Optimization and Cost Reduction Techniques	32
4	Data Analysis and Findings	35
4.1	Accuracy and Precision	35
4.2	Complexity	36
4.3	Robustness	37
4.4	Cost	38
5	Conclusion	39
6	Future Research	40

II	Part 2 - Articles	42
7	Cooperative Localization in Mines Using Fingerprinting and Neural Networks	43
7.1	Introduction	45
7.2	Localization Using Fingerprinting and Neural Networks	46
7.2.1	Fingerprinting technique	46
7.2.2	Artificial neural network	49
7.3	Localization Using One Receiver	50
7.4	Cooperative Localization Using Two Receivers or More	52
7.4.1	Localization based on separate neural networks	53
7.4.2	Localization based on one neural network	53
7.5	Results of Different Techniques	55
7.6	Conclusion	60
8	Radio-Localization in Underground Narrow-Vein Mines Using Neural Networks with In-built Tracking and Time Diversity	61
8.1	Introduction	63
8.2	Localization using Fingerprinting and Neural Networks	65
8.2.1	Localization in the presence of one receiver	65
8.2.2	Cooperative localization using two references in space	67
8.3	Localization using Tracking in the Time Domain	68
8.3.1	Concept of time domain diversity with tracking	69
8.3.2	ANN structure with time-domain diversity using tracking	72
8.4	Evaluation Results	73
8.4.1	Results of cooperative localization in the spatial domain	74
8.4.2	Results of localization using tracking in the time domain	75

8.5	System Design: Complexity vs. Accuracy	77
8.6	Conclusion	78
9	Cooperative Geo-location in Underground Mines: A Novel Fingerprint Positioning Technique Exploiting Spatio-Temporal Diversity	80
9.1	Introduction	82
9.2	Localization in Mines Using CIR-based Fingerprinting and ANNs . .	84
9.2.1	Cooperative memoryless localization using spatial diversity . .	87
9.2.2	Solitary memory-assisted localization using temporal diversity	88
9.3	Cooperative Memory-Assisted Localization Exploiting Spatio-Temporal Diversities	91
9.4	Performance Results	93
9.5	Conclusion	97
10	Smart Spatio-Temporal Fingerprinting for Cooperative ANN-based Wireless Localization in Underground Narrow-Vein Mines	98
10.1	Introduction	100
10.2	Measurement Campaign for CIR-BASED Fingerprinting	102
10.3	Overview of ANN-Based Localization Techniques using Fingerprinting	103
10.3.1	Original technique	103
10.3.2	Exploiting spatial diversity	104
10.3.3	Exploiting temporal diversity	105
10.3.4	Exploiting spatio-temporal diversity	108
10.3.5	Overview of performance results	109
10.4	Impact of Spatial Sampling Grid Resolution	110
10.5	Conclusion	113

11 Cost-Effective Localization in Underground Mines Using New SIMO/MIMO-Like Fingerprints and Artificial Neural Networks	114
11.1 Introduction	116
11.2 Localization in Underground Mines Using CIR-based Fingerprinting .	118
11.2.1 ANNs and CIR-based fingerprint positioning	118
11.2.2 Exploiting R_x spatial, temporal and space-time diversities . .	120
11.3 Exploiting T_x and R_x Spatial Diversities:	
SIMO/MIMO-type Fingerprint Positioning	123
11.4 Complexity and Cost Reduction	125
11.5 Performance Results	126
11.5.1 Results of SIMO/MIMO-type fingerprinting using T_x and R_x spatial diversities	128
11.5.2 Results of low fingerprint-acquisition rate on accuracy	129
11.6 Conclusion	131
12 Neural-Networks and Fingerprint-Based Localization in Underground Mines with Novel Use of Collaboration and Space-Time Diversity	133
12.1 Introduction	135
12.2 Related Work	138
12.2.1 Localization challenges in underground mines	138
12.2.2 Localization using wireless sensor networks	139
12.2.3 Localization using fingerprinting and ANNs	140
12.3 Cooperative Localization Using Spatial and Temporal Diversities . . .	143
12.3.1 Exploiting R_x -spatial diversity	144
12.3.2 Exploiting temporal diversity	147
12.3.3 Exploiting both R_x -spatial and temporal diversities	151

12.3.4	Exploiting both Tx and Rx spatial diversities	153
12.4	Experimental Results	154
12.4.1	Results of memoryless localization techniques using Rx spatial diversity	155
12.4.2	Results of solo memory-assisted localization techniques	156
12.4.3	Results of cooperative memory-assisted localization using spatio- temporal diversity	157
12.4.4	Results of MISO/MIMO-type fingerprinting using Tx and Rx spatial diversities	158
12.5	Reaping Diversity Benefits to Simplify Measurement Campaigns	159
12.5.1	Designing ANNs at higher S_x : Interpolation versus accuracy	160
12.5.2	Experimental results	162
12.6	Conclusion	167
	Bibliography	169
	A Copyright Permission Letter	175

List of Figures

2.1	Localization using triangulation.	11
2.2	Localization based on ToA.	12
2.3	Localization based on TDoA.	14
2.4	Localization based on AoA.	15
2.5	ANN's structure.	21
3.1	Fingerprinting in the presence of two receivers.	25
7.1	Map of the tunnel.	48
7.2	Localization using one fixed receiver. The CIR is extracted at different distances to the transmitter with 1 meter step size.	51
7.3	Localization using two signatures of two receivers in the area where two signals intersect.	53
7.4	Localization based on two separate estimations.	54
7.5	Neural network based on multiple signatures.	54
7.6	CDF plots of the position estimation errors at a receivers' separation distance $D=60\text{m}$ using several localization techniques.	56
7.7	CDF plots of the position estimation errors at a receivers' separation distance $D=80\text{m}$ using several localization techniques.	56
7.8	CDF plots of the position estimation errors at a receivers' separation distance $D=100\text{m}$ using several localization techniques.	57

7.9	CDF plots of the position estimation errors at a receivers' separation distance $D=60\text{m}$ using several localization techniques.	58
7.10	CDF plots of the position estimation errors at a receivers' separation distance $D=80\text{m}$ using several localization techniques.	59
7.11	CDF plots of the position estimation errors at a receivers' separation distance $D=100\text{m}$ using several localization techniques.	59
8.1	Map of the tunnel.	65
8.2	Localization using one fixed receiver.	66
8.3	Localization using two signatures of two receivers.	67
8.4	Neural network based on multiple signatures.	68
8.5	Possibilities of previous positions for $l = 2$	71
8.6	Possibilities of previous positions for $l = 3$	72
8.7	CDF plots of the position estimation errors for the training data at a receivers' separation distance $D = 80$ m using several localization techniques.	74
8.8	CDF plots of the position estimation errors for the testing data at a receivers' separation distance $D = 80$ m using several localization techniques.	75
8.9	CDF plots for the training data using tracking.	76
8.10	CDF plots for the testing data using tracking.	77
9.1	Map of the underground tunnels.	85
9.2	Solitary localization using one receiver.	86
9.3	Cooperative localization using two receivers.	87
9.4	Neural network based on multiple signatures.	88
9.5	Possibilities of previous positions for $l = 2$	89

9.6	CDF of the training data for different localization techniques at memory levels (l_1, l_2)	95
9.7	CDF of the testing data for different localization techniques at memory levels (l_1, l_2)	95
10.1	Map of the underground tunnels.	103
10.2	Solitary localization using one receiver.	104
10.3	Cooperative localization using two receivers.	105
10.4	ANN based on multiple signatures.	106
10.5	Possibilities of previous positions for $l = 2$	106
10.6	Solitary localization performance.	111
10.7	Cooperative localization performance.	112
11.1	Map of the tunnel.	118
11.2	The CIRs are extracted at different distances to the transmitter with 1-meter step-size along the x -axis.	119
11.3	Localization using two signatures of two receivers in the area where two signals intersect.	120
11.4	Neural network based on multiple signatures.	120
11.5	Possibilities of previous positions for $l = 3$	122
11.6	Optimum number of neurons for different ANNs.	126
11.7	Positioning errors from CDFs of testing data at 90% precision.	127
11.8	Positioning errors from CDFs of SIMO/MIMO-type testing data at 90% precision.	127
11.9	Localization performance at $S_x = 3$ m.	130
11.10	Localization performance at $S_x = 6$ m.	131
12.1	Map of the tunnel.	139

12.2	The CIRs are extracted at different distances to the transmitter with 1-meter step size along the x -axis.	142
12.3	Localization using two signatures of two receivers in the area where two signals intersect.	145
12.4	Localization based on two separate estimations.	146
12.5	Neural network based on multiple signatures.	147
12.6	Possibilities of previous positions for $l = 2$	149
12.7	Possibilities of previous positions for $l = 3$	150
12.8	CDF of the training data for different localization techniques at mem- ory levels (l_1, l_2)	155
12.9	CDF of the testing data for different localization techniques at memory levels (l_1, l_2)	156
12.10	Optimum number of neurons for different ANNs.	163
12.11	Localization performance at $S_x = 3$ m.	164
12.12	Localization performance at $S_x = 6$ m.	164
12.13	Positioning errors from CDFs of testing data at 90% precision.	165
12.14	Positioning errors from CDFs of MISO/MIMO-type testing data at 90% precision.	166

List of Tables

C.1	Précisions à résolution multiple	xxvi
4.1	Performance Results with Multiple Resolution	36
8.1	Fingerprints of each location for $l=2$	71
9.1	Estimation errors of different localization techniques	96
10.1	Estimation errors of different localization techniques with 90% precision.	110
10.2	Accuracy results at 90% precision for multiple spatial sampling grid resolutions	113
11.1	Performance Results with Multiple Resolution	129
12.1	Fingerprints of each location for $l = 2$	149
12.2	Performance results with multiple resolution	167

List of Acronyms

ANN	Artificial Neural Network
AOA	Angle Of Arrival
AP	Access Point
BP	Back Propagation
CIR	Channel Impulse Response
GPS	Global Positioning System
GRNN	Generalized Regression Neural Network
GSM	Global System for Mobile communication
IFT	Inverse Fourier Transform
LOS	Line Of Sight
MLP	MultiLayer Perceptron
MS	Mobile Station
NLOS	Non Line Of Sight
PDP	Power Delay Profile
PL	Path Loss
RF	Radio Frequency
RMS	Root Mean Square
RSS	Received Signal's Strength
TDOA	Time Difference Of Arrival
TOA	Time Of Arrival
UWB	Ultra Wide Band

WLAN Wireless Local Area Network

List of Symbols

A_k	Received signals' attenuation due to k^{th} transmitter
b	Bias of a neuron
BW_{meas}	Measurement bandwidth
c	Speed of light
d	Distance (Euclidian)
d_i	Distance from R_1 to a reference position i
d_p	Distance separating consecutive fingerprint measurement
D	Separation distance of two receivers
D	Set of distances ($d = 1$ to $d = d_i$)
e	Positioning error
f	Frequency
f_i	Fingerprint at position i
f_p	Path fingerprint (temporal fingerprint)
F^{SIMO}	SIMO-type fingerprint
F^{MIMO}	MIMO-type fingerprint
G_r	Antenna gain at the receiver
G_t	Antenna gain at the transmitter
$h(s, t, \tau)$	Channel impulse response (function of space, time and delay)
$ h(\tau) $	Channel impulse response's amplitude (function of delay)
$H(s, t, f)$	Channel impulse response (function of space, time and frequency)
$H(f)$	Function of the channel impulse response (function of frequency)
i	Position index
j	A given input's index

j_{max}	Maximum number of path fingerprints
k	Index of used inputs
K	Maximum number of given inputs (threshold)
l	Memory level (number of sub-fingerprints in one spatial, temporal or spatio-temporal fingerprint)
$L(s, t)$	Number of multipath components (function of space and time)
L	Number of multipath components
L_f	Length of a fingerprint (formed from one or more sub-fingerprints)
n	Signals' attenuation coefficient
$n(t)$	Noise
n_n	Optimum number of neurons
N_{inputs}	Number of ANN's inputs
N_{fp}	Number of path fingerprints
P	Total power of multipath components
P_r	Received power
P_t	Transmitted power
$P(\tau)$	Power delay profile
$P(\phi)$	Angular power profile
PL	Path loss
$r(t)$	Received signal
$s(t)$	Transmitted signal
s	Spatial position
S_r	Sampling rate
S_{R_1}	Fingerprint set at R_1
S_{R_2}	Fingerprint set at R_2
S_x	Sampling step-size (m)

t	Time
τ_s	Sampling time
V_t	Transmitter's speed
\mathbf{W}	ANNs' weights
x	x -axis coordinate
y	y -axis coordinate
δ_x^{Tx}	Antenna's separation on the x -axis
δ_y^{Ty}	Antenna's separation on the y -axis
$\alpha_i(t)$	Complex amplitude of the i^{th} multipath component
β	Phase propagation coefficient
$\delta(.)$	Dirac Impulse
ω_{kj}	Weight of k^{th} neuron for input j
ϕ_i	Phase of the i^{th} multipath component
τ_i	Propagation delay of the i^{th} multipath component
τ_m	Mean excess delay
τ_{rms}	RMS delay spread
τ_{max}	Maximum excess delay
σ_s^2	Signal power
σ_n^2	Noise Power

Part I

Smart Localization in Underground Mines using Fingerprinting and ANNs: Strategies and Applications

Synopsis

Chapter 1

Introduction to the Thesis

This dissertation contains novel fingerprint-positioning techniques that are designed for underground and confined areas such as gold mines. Being a Ph. D. candidate in the *Institut National de la Recherche Scientifique – Énergie Matériaux et Télécommunications* (INRS-EMT) and in collaboration with Telebec’s Underground Communications Research Laboratory (LRTCS), we bring forward and analyze the most recent findings and results of fingerprint-based positioning techniques in underground gold mines. In the following, the scope of work is defined highlighting the research problems, objectives and applied methodologies.

1.1 Research Problems

Localization of miners and/or their equipment in underground mines is an essential need that guarantees basic safety measures in one of Earth’s most dangerous work environments. However, modern localization techniques that perform accurately in outdoor channels may not succeed if implemented in unstable indoor mediums such as mines. So far, many research studies at LRTCS have revealed the effectiveness of indoor positioning techniques driven by artificial intelligence that we consider, in

our study, as good candidates for underground localization. One of the problems is the absence of adaptation of such techniques to modern sophisticated communication systems that use more than one access point cooperatively and exploit the presence of single/multiple-input and multiple-output (SIMO/MIMO) antenna capabilities. The value of this research comes from its ability to introduce cooperative fingerprinting methods that exploit spatial and/or temporal diversities in the presence of single and/or dual transmitter antennas such as in the case of modern, MIMO-capable communication devices. As a result, all localization techniques that rely on single-antenna fingerprinting may use our innovative approach to make use of space-time diversity, which guarantees more accuracy, robustness and fingerprint-acquisition cost reduction.

1.2 Objectives

The main objective of this research is to study underground wireless fingerprint localization techniques in the realm of temporal and/or spatial diversities on one hand, and in the presence of more than one transmitter and receiver antennas on the other. By doing so, not only do we enhance positioning accuracies and precision results, but we also introduce new fingerprinting methodologies that can be adapted for underground localization systems. Another objective of this research is to reduce the cost of fingerprint-acquisition campaigns, which is the main criticism. By designing fingerprinting-based techniques that tradeoff pinpoint accuracies for less offline measurement data, we succeed in cutting down the cost to less than half while maintaining accurate positioning results using our new, sophisticated fingerprinting methodologies.

1.3 Methodology

This work makes use of 480 data measurement points collected in an underground mine at 2.4 GHz, in the presence of one receiver antenna, from which the channel impulse responses (CIRs) are extracted. Localization using fingerprints extracted from CIRs and artificial neural networks (ANNs) is then adapted as a paradigm to localize the transmitter's position. New fingerprints are then formed when exploiting space and/or time diversities. For simplicity, underground tunnels are assumed to have a two-dimensional structure with the x -axis taken along the tunnel's length while the y -axis is along its width. It should be noted that localization results are based on the separation distance of the transmitter and receiver along the x -axis only, neglecting the small variations along the y -axis which is less valuable in the narrow tunnels of underground gold mines.

After discussing the basic localization technique in the presence of one receiver, we simulate, using the same measurements, the presence of another receiver antenna to study the effect of using the spatial diversity of the collected fingerprints. By having two receivers collecting the transmitted signals, two fingerprints are extracted from each receiver to form an R_x spatial fingerprint for each given position. The results of exploiting R_x spatial diversity outperform the presence of one receiver only and contribute in clarifying the ambiguity of the transmitter's position in the presence of junctions. R_x spatial diversity alone may not be enhanced without the addition of extra access points which is not feasible in the confinement of narrow-vein mines.

However, another dimension of research goes beyond spatial diversity to include memory-type fingerprints exploiting time diversity. The study of using temporal fingerprints is achieved by producing all possible path-fingerprints which lead to a specific position, for a given memory depth, inside the tunnels. A path fingerprint is a concatenation of all sub-fingerprints extracted along a specific way that leads

to the final position to be estimated. ANNs are then trained on all possible paths for a given memory level and used to estimate data not seen in the training phases. It is observed that performance thresholds are improved when exploiting temporal diversity with an increase in training complexity.

In order to further enhance the performance of fingerprint-positioning techniques, a study was conducted to evaluate the performance of localization in the presence of memory capabilities and collaboration between two receivers. When chains of temporal sub-fingerprints collected from the first receiver are combined path wise with another sub-fingerprints at the second receiver, spatio-temporal fingerprints are obtained. As a result, the use of space-time diversity outperforms the performance of previous approaches in terms of accuracy, precision and complexity.

Another axis of research investigates the capability of exploiting the presence of dual antennas at the transmitter, for localization purposes, as in the case of modern MIMO-capable user equipment (UE). By concatenating two sub-fingerprints at the transmitter's end separated by a given antenna spacing, we form SIMO-type fingerprints if one receiver antenna is present and MIMO-type fingerprints in the presence of two receiver antennas. SIMO/MIMO-type fingerprints are studied at antenna spacing of 1 m along the x -axis, 0.5 m and 1 m along the y -axis.

After achieving very high accuracies that exceeded expectations, a search for optimized performance starts in an effort to reduce the cost overhead of fingerprint acquisition campaigns. Each localization technique was put under the test of using less data measurements, for ANNs' training, by reducing the grid's resolution down to one sixth of its original size. ANNs were challenged to localize in measurement gaps that are not seen in the training phases while trying to maintain positioning accuracies. After training more than 14,000 ANNs, the most adequate number of neurons that fits each localization technique was identified based on the grid's resolution.

As expected, localization accuracies slightly drop as the grid's resolution decreases, however, the new and sophisticated fingerprinting techniques, such as MIMO-type fingerprint positioning, succeed to achieve accurate positioning results even at lower grid's resolution.

1.4 Structure of the Thesis

The thesis is written using the article format and it's divided into two parts, each divided into multiple chapters.

In the first part, chapter 2 sheds light on the principles of localization and the latest research done in indoor localization techniques. In chapter 3, the novel findings of this work are briefly discussed including the novel fingerprint-positioning techniques that exploit spatial and temporal diversities. In addition to that, section 3.5 p. 32 of the same chapter illustrates the methods used to further optimize the localization system by cutting down its fingerprint-acquisition cost. The performance results are then discussed in chapter 4. Results are followed by a conclusion in chapter 5, before revealing the future research topics that are recommended as a continuity of this work in chapter 6.

In part two, we include the publications and manuscripts that legitimize this work and show the importance of its findings. Each chapter, being a conference article or a journal paper, carries a new fingerprinting technique and is introduced to in the beginning of chapter 3. A complete summarized description of this work is wrapped up in the journal paper included in chapter 12.

Chapter 2

Literature review

Localization of people, vehicles and equipment is an essential need for the functionality of various applications in outdoor and indoor environments. In some outdoor scenarios, localization may be used for the positioning of emergency call origins, fraud users and for traffic management. Similarly, localization may be used for indoor applications such as the cases of home automation, tracking of fire-fighters/miners, intruder detection and patient monitoring.

In theory, several localization techniques may be used in order to estimate a transmitter's position. However, the importance of each technique may be measured in terms of its ability to extract, at the receiver's end, the main components of the received signals and estimate the distance separating the transmitter and receiver in a given channel. While wireless signals carry certain characteristics such as the power, frequency, time of arrival and multipath components, they are not often exploited together in localization techniques. In the following, we summarize various localization algorithms showing their effectiveness and performance after which we investigate indoor positioning in underground gold mines.

2.1 Localization using Triangulation Techniques

Triangulation algorithms, which are used in major localization applications, exploit at least three reference points or receivers in order to estimate the source of wireless transmission. Receivers collect the transmitted signals where one or more signals' parameters are extracted prior to estimating the distance that separates the transmitter from each of the reference points. Lateration techniques (i.e., localization using triangulation) are methods that extract the received signal's strength (RSS) or time of arrival (ToA) whereas the angulation techniques use the received signals' angle of arrival (AoA) for position estimation.

Localization using triangulation is based on collecting the wireless signals from three or more reference points before estimating the transmitter's position. While three reference points are used in order to estimate a two-dimensional location, four receivers are needed in order to estimate a three-dimensional point. In the following we discuss the lateration techniques that use the RSS or AoA alone in order to estimate a mobile's position.

2.1.1 Localization using RSS

The laws of physics state that electromagnetic signals traversing through open space or channels lose energy until they fade after a certain distance. In wireless communication systems, we make use of these laws to estimate the distance traveled by a wireless signal after analyzing its power at the receiver's end while a priori knowing the signals' frequency and antenna gains. In a Free Space Path Loss (FSPL) model, the received power of a transmitted signal is given by:

$$P_r = \frac{P_t G_t}{4\pi d^2} A = \frac{\lambda^2}{(4\pi d)^2} P_t G_t G_r. \quad (2.1)$$

where P_r is the received signal's strength measured in dB, P_t is the transmitted signal's strength, G_t and G_r are the receiver and transmitter antennas' gains, respectively. λ is the wavelength derived from the transmitted signal's central frequency and d is the distance separating the transmitter and the receiver. However, indoor channels are more complex because wireless transmitted signals undergo many reflections, refractions and attenuations on their way to the receiver. In the case of underground mines, humid rough surfaces and non line of sight (NLOS) scenarios challenge the capability of deriving an accurate path loss model. Estimating the distance traveled by a wireless signal follows a generic path loss model that can be written as follows:

$$P_{r-d}(dB) = P_t(dB) - P_{e-d}(dB) + G_t(dB) + G_r(dB). \quad (2.2)$$

where P_{r-d} is the received signal's strength at a distance d away from the transmitter, and P_t is the transmitted signal's strength. G_t and G_r are the gains of the antennas at the transmitter and at the receiver, respectively. P_{e-d} is the distance function and it is of the following form:

$$P_{e-d}(dB) = P_{e-d_0}(dB) + 10n \log(d/d_0) + X. \quad (2.3)$$

where P_{e-d_0} is the loss measured for a distance d_0 which is taken as 1 meter, n is the attenuation coefficient and X is a random variable depending on the nature of the channel. By combining both equations we conclude the following:

$$P_{r-d}(dB) = P_t(dB) - P_{e-d_0}(dB) - 10n \log(d/d_0) - X + G_t(dB) + G_r(dB). \quad (2.4)$$

In a 2D scenario, three receivers may estimate a transmitter's position by calculating three distances d_1 , d_2 and d_3 , using the RSS of each received signal, respectively.

In the example of figure 2.1, the nodes A, B and C estimate a transmitter's position in the intersection region of three circles, each of radius d_A , d_B and d_C , respectively.

The performance of RSS-based localization techniques depends on the accuracy

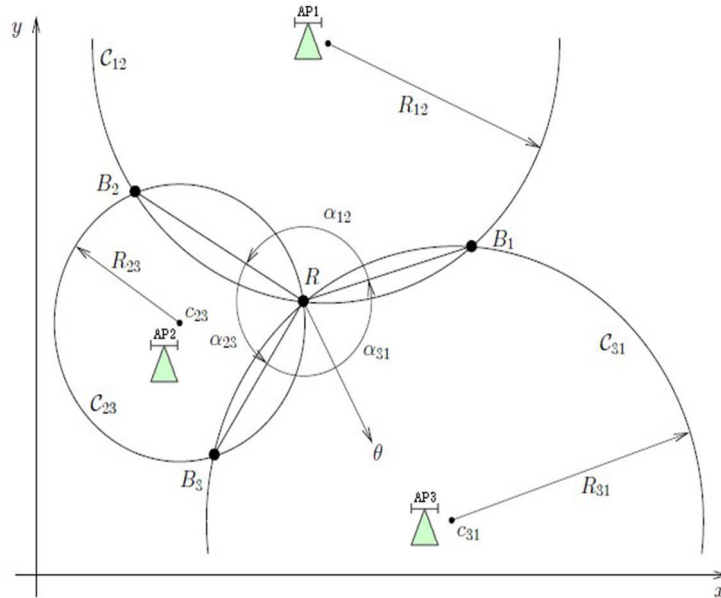


Figure 2.1 – Localization using triangulation.

of its path loss model. In many scenarios, such as indoor channels and underground mines, multipath components and small/large scale fading introduces distance estimation errors due to the fact that RSS measurements may vary for the same position especially in the presence of NLOS regions and interconnected tunnels. It is also noted in [16] that positioning using RSS-based techniques may result in wider intersecting circles that lead to lower accuracy and certainty about the transmitter's exact position.

2.1.2 Localization using ToA

Localization using Time of Arrival (ToA) is a technique that exploits the propagation time needed by wireless signals to reach a position to be estimated. Similar

to localization using RSS, ToA-based localization techniques use three measurement points, in a 2D scenario, to estimate the transmitter's position. However, unlike RSS-based techniques, localization using ToA requires time synchronization of the reference points or the exchange of timing information using protocols such as two-way ranging protocols [36], [19], [44]. A straightforward approach uses the geometric

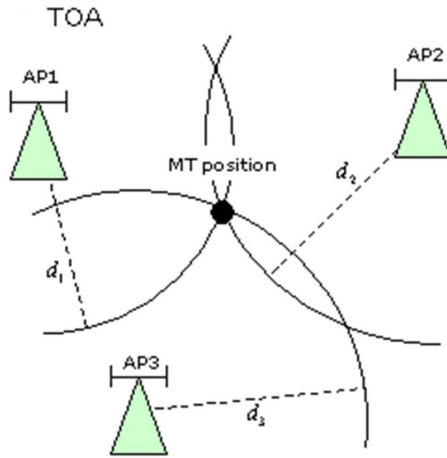


Figure 2.2 – Localization based on ToA.

method to calculate the distance from each receiver to the transmitter using the intersection region of three circles as presented earlier in RSS-based localization. Another approach may introduce a non-linear cost function that helps tune the accuracy results by adding a reliability factor to each of the nodes. Assuming that a transmitter, located at (x_0, y_0) , transmits at time t_0 , the n base stations located at (x_0, y_0) , (x_1, y_1) , \dots (x_n, y_n) receive that signal at times $t_1, t_2, \dots t_n$ and the cost function would be:

$$F(x) = \sum_{i=1}^n \alpha_i^2 f_i^2(x), \quad (2.5)$$

where α_i is the reliability of each node and can be chosen depending on each topology or measuring unit i , and $f_i(x)$ represents the delta between the straight-forward distance calculated at the speed of light c and the estimated position at (x_i, y_i) such

that:

$$f_i(x) = c(t_i - t) - \sqrt{(x_i - x)^2 + (y_i - y)^2}. \quad (2.6)$$

The location is then determined by minimizing the cost function $F(x)$. Two challenges face the deployment of TOA-based localization techniques in underground mines. The first relies on the ability to synchronize all nodes using a time-based protocol that can guarantee the estimation of high-resolution time delays. On the other hand, the presence of NLOS and quasi-curvilinear tunnels adds more delays to transmitted signals as a result of the numerous reflections that the signals encounter along their way to the receiver. In other words, the time that the signals need to reach a receiver does not necessarily represent the separation distance but it represents the trajectory taken after bouncing through the walls inside the tunnels. All the above adds ambiguity to the real position of the transmitter in indoor environments such as underground mines.

2.1.3 Localization using TDoA

Another time-based triangulation technique uses the time difference of arrival (TDoA) between the receivers in order to calculate the distance to a given transmitter. Assume a signal is received at a receiver i such that:

$$x_i(t) = s(t - d_i) + n_i(t), \quad (2.7)$$

where $s_i(t)$ is the transmitted signal, d_i and n_i are the delay and noise at receiver i , respectively. Similarly, the received signal can be written at another receiver j as:

$$x_j(t) = s(t - d_j) + n_j(t). \quad (2.8)$$

The cross-correlation function of the two signals is the integration of their lag product over a time period T :

$$\hat{R}_{x_i, x_j}(\tau) = \frac{1}{T} \int_0^T x_i(t)x_j(t - \tau)dt. \quad (2.9)$$

By maximizing \hat{R}_{x_i, x_j} , the TDoA t is obtained. Similarly, a third receiver is needed in order to come up with another TDOA t' forming two hyperbolas that intersect in the position to be estimated. The solution of the hyperbolic equation can be conducted through nonlinear regression and it can also be solved using the Taylor-series expansion as shown in [43].

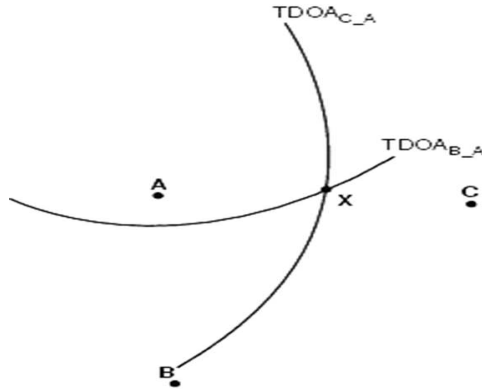


Figure 2.3 – Localization based on TDoA.

2.1.4 Localization using AoA

Localization based on the angle of arrival (AoA) requires antennas that can sense the received signals' direction in the presence of two or more receivers. This can be the case of directional antennas or arrays of antennas that are able to measure the angles of arrival of wireless signals. As shown in figure 2.4, two receivers located at positions A and B are able to spot a transmitter P in the intersection of two straight lines with angles θ_1 and θ_2 , respectively. The advantages of this technique rely in its

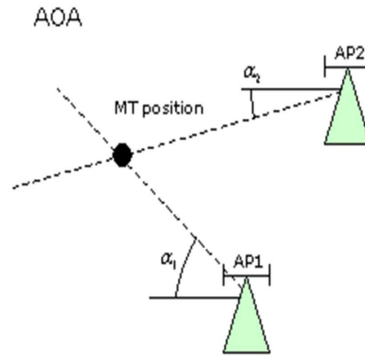


Figure 2.4 – Localization based on AoA.

ability to localize a transmitter without the need of time synchronization. However, AoA-based localization techniques are not suitable for indoor positioning because wireless signals undergo multiple reflections before reaching the receiver. Similarly, in underground mines, the confinement of narrow tunnels and the presence of NLOS scenarios challenge the functionality of this technique.

2.2 Fingerprint-Based Localization

Fingerprint positioning techniques are backed up by measurement campaigns conducted in the channel where localization may take place. First, the data is collected throughout the area of interest then it is stored in a database for offline analysis. Several matching algorithms may be used afterwards to compare the available data to the desired output, which is the distance to the transmitter in the localization problems. After the system forms a reliable estimation model, new fingerprints may be used to test its ability to generalize and estimate new positions in the measurement's grid.

In indoor localization, fingerprinting is often used due to the increased complexity in channel estimation. For instance, the random number of reflections that a signal encounters on its way to the receiver, at different measurement points in an indoor channel, severely affects the main wireless waves' characteristics such as the RSS,

ToA, etc ... For that reason, taking multiple measurements and introducing statistical, probabilistic or artificially intelligent matching algorithms becomes a better alternative to traditional fitting or model estimation techniques. Several matching algorithms are found in the literature and may be used in the field of scene analysis such as probabilistic methods, k -nearest-neighbor (kNN), artificial neural networks, support vector machine (SVM), and smallest M -vertex polygon (SMP). While some are used in different estimation problems, we shall discuss artificial neural networks and explain why we recommend them for localization problems in underground mines.

2.3 Background of Localization in Underground Mines

Localization in the presence of one receiver only was introduced in [31] as a novel approach to localization and it is explained in Part II especially in sections 7.3 p. 50 and 12.2 p. 138. In the following, we will review the localization technique in [31] that constitutes the groundwork of all developed spatial, temporal or spatio-temporal fingerprint-positioning techniques discussed later in chapter 3.

In underground mines, positioning personnel and their equipment is an essential need that guarantees basic security and safety protocols. However, localization in underground mines is challenged by the special narrow-vein nature of its interconnecting tunnels. For that reason, estimating a miner's position using traditional localization techniques discussed earlier in section 2.1 p. 9 may introduce major estimation errors and can mislead the localization system about the real position of a user inside its interconnected tunnels.

The challenges of underground positioning were discussed in multiple research

projects at Telebec’s Underground Communications Research Laboratory (LRTCS), a pioneering lab with research focus on underground communications (cf. surveys [16] and [46]). After many pioneering works on wireless channel characterization and modeling in underground mines at 2.4 GHz and 5.8 GHz bands [32], [2], then over Ultra-wideband (UWB) [34], and most recently using the mmWave [26], LRTCS succeeded in bringing forward an accurate positioning technique that combined the essential signals’ characteristics in underground mines and the power of ANNs to precisely localize in one of Earth’s most disruptive indoor channels.

2.3.1 Original Fingerprinting Technique

Fingerprint positioning is based on collecting information about wireless signals’ characteristics from measurement points, in the offline phase, then trying to match the presence or absence of certain parameters upon the reception of new signals in the online phase. In this work we illustrate the fundamentals of fingerprints extracted from CIRs in underground mines.

When a signal is wirelessly transmitted in the confinement of underground tunnels, it undergoes many reflections and refractions creating multipath components (i.e., multiple versions of the same signal with different variations/distortions of its original characteristics). In theory, the transfer function of the channel can be mathematically represented in the time and frequency domains as follows:

$$H(s, t, f) = \sum_{i=1}^{L(s,t)} \rho_i(s, t) \cdot e^{j\theta_i(s,t)} \cdot e^{-j2\pi f\tau_i(s,t)}. \quad (2.10)$$

$$h(s, t, \tau) = \sum_{i=1}^{L(s,t)} \rho_i(s, t) \cdot e^{j\theta_i(s,t)} \cdot \delta(\tau - \tau_i(s, t)). \quad (2.11)$$

where $\rho_i(s, t)$, $\tau_i(s, t)$ and $\theta_i(s, t)$ are random variables that represent the sequence amplitude, time of arrival and the phase of arrival, respectively. $L(s, t)$ is the total number of multipath components defined at time t and spatial position s . $\delta(\tau - \tau_i(s, t))$ represents the Dirac distribution and i stands for the index of the multipath component.

In the following we shall consider the channel to be time invariant, i.e. there is no spatial variations between the transmitter and receiver due to dynamic activity such as human or natural variations. Therefore, the simplified versions of both transfer functions may be represented as follows:

$$H(s, f) = \sum_{i=1}^{L(s)} \rho_i(s) \cdot e^{j\theta_i(s)} \cdot e^{-j2\pi f\tau_i(s)}. \quad (2.12)$$

$$h(s, \tau) = \sum_{i=1}^{L(s)} \rho_i(s) \cdot e^{j\theta_i(s)} \cdot \delta(\tau - \tau_i(s)). \quad (2.13)$$

where $\rho_i(s)$, $\tau_i(s)$ and $\theta_i(s)$ become a function of space only. Once a signal is received, the channel impulse response is extracted from which we obtain the time impulse response using Inverse Fast Fourier Transform (IFFT).

In 2006, real time measurements were taken from a gold mine named CANMET in Val d'Or. The measurements were recorded at a central frequency of 2.4 GHz and they were taken from the confinement of one tunnel shown in figure 7.1. The measurements led to the collection of 480 CIRs from which a novel fingerprinting technique was introduced for the first time in [31]. The fingerprinting technique makes use of seven parameters (discussed below) extracted from the CIR of a given position located at a distance d away from the transmitter. The parameters, stated in section 7.2 p. 46, which guarantee uniqueness to the transmitter's position as per [31] are:

- The mean excess delay ($\bar{\tau}$) that is the first moment of the power delay profile measured at the first detectable signal that arrives at the receiver and is related to the power of that profile. In other words it is related to the amplitudes of the multipath components, and is given by:

$$\bar{\tau} = \frac{\sum_k a_k^2 \tau_k}{\sum_k a_k^2}. \quad (2.14)$$

- The root mean square (τ_{rms}), that represents the square root of the second central moment of the power delay profile and it is given by:

$$\sigma = \sqrt{\bar{\tau}^2 - (\bar{\tau})^2}, \quad (2.15)$$

where:

$$\bar{\tau}^2 = \frac{\sum_k a_k^2 \tau_k^2}{\sum_k a_k^2}. \quad (2.16)$$

- The maximum excess delay (τ_{max}) which is the time at which the signal drops below X dB of the maximum power measured in the power delay profile. It can be seen as the time that a signal stays above a given threshold based on the highest received power in a profile. In the following, the value of 20 dB is taken as a threshold.
- The total power of the received signal (P) measured in dBm.
- The number of multipath components (N) which form the entire received signal measured at a 20 dB floor level.
- The power of the first arrival (P_1) which is the power of the first multipath component.
- The delay of the first path component (τ_1) and it is used along with P_1 in order

to distinguish between the LOS and NLOS scenarios.

2.3.2 Basic Artificial Neural Network Architecture

ANNs are computational models that are capable of defining complex mathematical relationships between a set of inputs and a set of outputs. Each ANN is made up of three important layers shown in figure 2.5. The input layer takes an input vector (set of signature from the received signals) whose length defines the number of input neurons to be used. Similarly, the output layer is made up of neurons that constitute the observed output (i.e., distance to the transmitter) of the introduced input vectors. In the middle lies the hidden layer that is made of a pre-defined number of neurons, which connect the input and output neurons together through weights and biases. The most important factor in ANNs' design is the ability to define the number of neurons needed in the hidden layer and the capability of training ANNs to make sense of the input and output layers by carefully adjusting the weights and biases.

ANNs that are capable of estimating non-linear regression functions are of two types. The first model is the Multi-Layer Perceptron (MLP), which represents the most prominent and well-researched class of ANNs in classification and implementation. The second type is the Radial Basis Function (RBF), which is also a multi-layer network but it performs in a significantly different way. To be more specific, the activation of a hidden layer is based on the dot product between the input and weight vectors in MLP-type ANNs. However, in RBF-type models, hidden units are activated based on the distance between the input and prototype vectors [17]. The use of feed-forward ANNs with back-propagation learning algorithms is proven to provide high positioning accuracy in [31] and is adapted for all developed localization techniques.

In CIR-based localization techniques, the input layer is made of one or more finger-

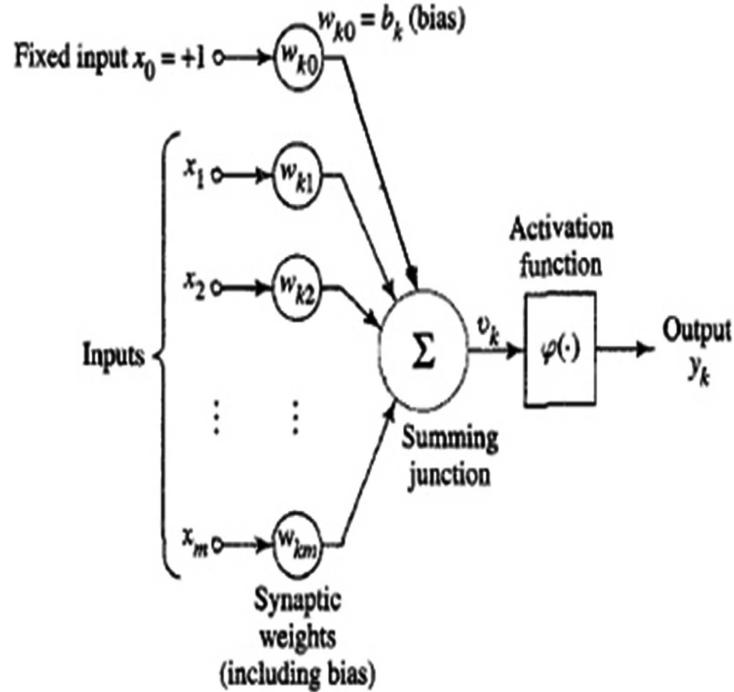


Figure 2.5 – ANN's structure.

prints extracted from the CIRs while the output layer is the distance d that separates the transmitter and the localizing unit. In the offline phase, ANNs are trained to adjust their weights and biases in order to match the signals' characteristics to the desired output. However, in order to make sure that ANNs are capable of generalizing the mathematical model and in an effort to avoid overfitting, ANNs are trained using part of the measurement campaign while leaving fingerprints for testing purposes. In the online phase that follows the training phase, ANNs would be ready to instantaneously estimate distances using new fingerprints extracted in real-time and fed to ANNs' input layer.

Localization in the presence of one receiver only [31] uses fingerprints extracted for each position in the tunnel, as shown in figures 7.1 and 7.2, along the x and y axes with 1 m and 0.5 m separation distances, respectively. The fingerprint set

$S = \{f_1, f_2, f_3, \dots, f_n\}$ is formed and successfully matched to the corresponding set of distances $D = \{d_1, d_2, d_3, \dots, d_n\}$ using an ANN. For simplicity throughout this work, the distance to the transmitter is considered along the x -axis only, neglecting the small variations along the y -axis which are less significant in the confinement of narrow tunnels. Also, since measurements vary for the same position in underground mines, the collection of more than one fingerprint for a given distance adds more robustness to the system's design (i.e., around four to six fingerprints along the y -axis correspond to the same output distance represented by the x position).

Chapter 3

Smart Localization in Underground Mines using Fingerprinting and ANNs

In this chapter we discuss the research's findings in depth showing their functional methods and fingerprinting techniques. This chapter constitutes the major accomplishments of this work which were published in parts and then summed in one journal manuscript which can also be reviewed in [chapter 12](#).

As a background study, it is recommended to revise the effectiveness of fingerprint-based localization using ANNs in [\[31\]](#), which was also reviewed before in [section 2.3 p. 16](#). At first, we examine the methodology adapted for cooperative localization in the presence of more than one receiver in [section 3.1 p. 24](#) which contributes to the fulfillment of the article given in [chapter 7](#). Localization using temporal diversity is then explained in [section 3.2 p. 3.2](#) and its findings may be reviewed also in the publication listed under [chapter 8](#). Similarly, [section 3.3 p. 28](#) explains the concepts of localization exploiting spatio-temporal diversity which contribute to the published

work in chapter 9.

The innovation of SIMO/MIMO-type fingerprints, which are examined in section 3.4 p. 31 and chapter 11, shows the techniques that can be used to enrich the fingerprinting techniques in the presence of dual T_x antennas. Finally, optimization and cost reduction techniques are discussed in section 3.5 p. 32 and through the publications of chapters 10, 11 and 12.

3.1 Localization Exploiting R_x Spatial Diversity

Localization in underground mines using more than one access point was the first step towards a cooperative system that uses more than one sub-fingerprint prior to estimating a transmitter's position. Not only did collaboration between access points increase positioning accuracies, but also it removed the ambiguity about defining the direction of transmission in cases where junctions are present in underground galleries and tunnels. Localization exploiting R_x spatial diversity is the first chapter of accomplishments and is fully described throughout the publication present in chapter 7 and in the narration of section 12.3.1 p. 144.

Prior to the innovation of collaborative fingerprinting, only one fingerprint was used by only one receiver to extract the distance to a transmitter without knowing the exact direction of transmission. The objective of this chapter is to incorporate more than one fingerprint (i.e., which will be called sub-fingerprint) from spatially distant receivers prior to estimating the final position of transmission. Given the special narrow topology of underground tunnels, two receivers would be enough to cover each tunnel as shown in figure 7.2. The same measurements that were taken from the first receiver R_1 in [31] are used in the opposite direction to simulate the presence of another receiver R_2 as shown in figure 3.1.

Exploiting R_x spatial diversity of two receivers R_1 and R_2 , in the region of

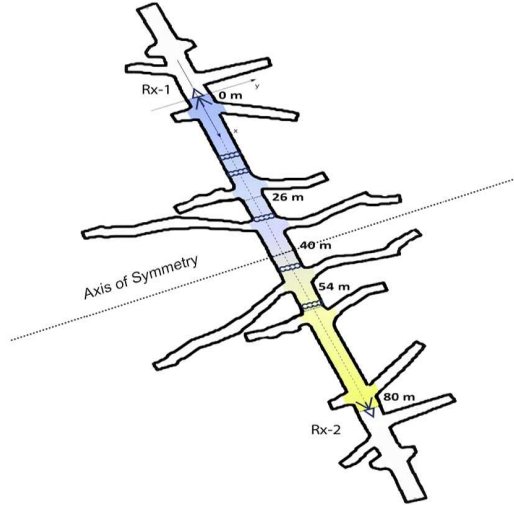


Figure 3.1 – Fingerprinting in the presence of two receivers.

shared coverage, results in two fingerprint sets $S^{R_1} = \{f_1, f_2, f_3, \dots, f_m\}$ and $S^{R_2} = \{f'_1, f'_2, f'_3, \dots, f'_m\}$, respectively. ANNs' output set $D = \{d_1, d_2, d_3, \dots, d_m\}$ represents the distances to one of the receivers which is taken by default to be R_1 's distance to the transmitter. It should also be noted that multiple scenarios are analyzed at receiver separation distances of 60 m, 80 m and 100 m, assuming that signals decay after 64 m as reported in [31] and noticed in the collected measurements. After collecting the measurement sets for each scenario, one can think of two ways to estimate the position of a transmitter using ANNs.

The first design, shown in figure 7.4, allows each receiver to separately localize using its own ANN with seven input parameters corresponding to each respective fingerprint or received signal. By *a priori* knowing the map of the tunnel and the position of each receiver, one can average both distances and estimate the final position of each receiver. The second type is proven to provide better estimation results and is referred to as the cooperative localization technique that uses the sub-fingerprints collected

from both receivers and concatenates them to form spatially diverse fingerprints, which are double the size of the original fingerprint. In other words, concatenating both sets, S^{R_1} and S^{R_2} results in a set of fingerprints represented by:

$$S = \{F_1, F_2, F_3, \dots, F_m\} = \{(f_1, f'_1), (f_2, f'_2), (f_3, f'_3), \dots, (f_m, f'_m)\}. \quad (3.1)$$

As shown in figure 7.5, R_x spatial diversity is exploited using one ANN trained with fingerprints of higher chain lengths. The results of localization using R_x spatial diversity are shown for the training fingerprints in figures 7.6, 7.7 and 7.8 while the testing results are shown in figures 7.9, 7.10 and 7.11, at receiver separation distances of 60 m, 80 m and 100 m, respectively. The final reported estimation accuracies for R_x spatially diverse fingerprinting techniques, after having their ANNs optimized for low fingerprint-acquisition cost as discussed later in section 3.5 p. 32, are summarized in table 4.1 to be 77 cm and 90 cm for 90% of the training and testing data, respectively.

3.2 Localization Exploiting Temporal Diversity

Localization using R_x spatial diversity was effective in regions that are covered by more than one access point. On one hand, the solution lacked an effective technique that could guarantee the same accuracy when losing coverage from the second receiver R_2 . On the other hand, increasing accuracy within the scope of spatial diversity only requires the addition of more than one access point, which is neither feasible nor practical in the confined narrow-shaped tunnels.

A search for a complementary fingerprinting technique, which made use of the limited motion of miners underground, led to the foundation of fingerprint-based localization exploiting temporal diversity. Localization exploiting temporal diversity is the second chapter of accomplishments and it is explained in details throughout the publication

given in chapter 8 and in the proceedings of section 12.3.2 p. 147.

This work introduces a fingerprinting technique that records the signatures (i.e., sets of 7 parameters) up to a certain memory level l . For example, an R_x spatially diverse fingerprint has the same fingerprint length as a temporal fingerprint extracted with memory level $l = 2$. However, the latter is obtained using only one receiver in the presence of memory-recording capability that incorporated the miner's previous sub-fingerprint, at time t_{-1} and concatenated it to another sub-fingerprint at time t_0 . In other words, a temporal fingerprint

$$f_i^j = \left(f_{i_{t_0}}, f_{i_{t_{-1}}}, f_{i_{t_{-2}}}, \dots, f_{i_{t_{-(l-1)}}} \right) \quad (3.2)$$

is the concatenation of sub-fingerprints measured over short time instances while moving towards a destination to be estimated at $d_i^{t_0}$. l being the number of concatenated sub-fingerprints or what we refer to as memory level, defines the length of a temporal fingerprint L_f where:

$$L_f = 7l. \quad (3.3)$$

Localization exploiting temporal diversity only, in the presence of one receiver, is studied for $l = 1, 2, 3, 4$ and 5 (i.e., ANN(1,0), ANN(2,0), ANN(3,0), ANN(4,0) and ANN(5,0)) after which no significant gain is observed.

To further illustrate temporal fingerprint extraction through an example at $l = 2$, consider figure 8.5. For one position at t_0 , five path-fingerprints may be extracted, in the offline phase, and they represent fingerprint chains that combine one previous position's signature extracted from the CIR at t_{-1} as stated in table 8.1. Another example for $l = 3$ is illustrated in details in figure 12.7 where a miner may have up to 25 temporally diverse path-fingerprints for one position only. The number of path-fingerprints j_{max} that may be obtained for a given position is limited by the upper

number of path-fingerprints N_{fp} :

$$j_{max} \leq N_{fp} = 5^{(l-1)}. \quad (3.4)$$

All possible path-fingerprints are collected for all positions of interest while respecting the boundaries of confined tunnels. The total set of temporal fingerprints is denoted by $S = \{S_1, \dots, S_i, \dots, S_m\}$ and it corresponds to all distances $D = \{d_1, \dots, d_i, \dots, d_m\}$. The power of this technique is in its ability to exponentially increase the number of path-fingerprints in the training set, using only one receiver, without the need of extra measurements. However, this comes at the cost of increasing the number of inputs and number of neurons for training ANNs.

The results of localization using temporal diversity are shown for the training fingerprints in figures 8.9 and 8.10 for the training and testing fingerprints, respectively. The final reported estimation accuracies for all temporally diverse fingerprinting techniques showed high accuracy gains with only 50 cm estimation errors for 90% of the fingerprints at $l = 4$ and $l = 5$. Full result overview may be revised in section 8.4.2 p. 75 and in tables 9.1 and 4.1.

3.3 Localization Exploiting Spatio-Temporal Diversity

By comparing R_x spatially and temporally diverse fingerprints, one can conclude that both are unique in their implementation. The former exploits spatial diversity of the collected fingerprints from two distinct receivers while the latter makes use of fingerprint measurements in short time instances. This led to the realization that combining both concepts together in one spatio-temporal fingerprinting technique

would boost location accuracies and add more robustness to the localization system. Indeed, increasing accuracy to near pinpoint precision may not be needed for positioning miners underground but it will be traded off for lower complexity and cost, as later discussed in section 3.5 p. 32. Localization exploiting spatio-temporal diversity is the third chapter of accomplishments and it brought in very accurate and satisfying results which were presented in the publication of chapter 9 and in the proceedings of section 12.3.3 p. 151.

Cooperative memory-assisted localization exploiting spatio-temporal diversity is a result of the collaboration of two receivers when at least one of them is introducing memory (i.e., producing path-fingerprints) [5]. The memory levels of receivers R_1 and R_2 are denoted by l_1 and l_2 , respectively. Fingerprints are extracted for different memory levels and analyzed fully in section 9.3 p. 91. A spatio-temporal fingerprint set S_i , for a given distance d_i , is a concatenation of two subset fingerprints $S_i^{R_1}$ and $S_i^{R_2}$ collected from receivers R_1 and R_2 , respectively, where: $S_i^{R_1} = \{F_i^{R_1,1}, F_i^{R_1,2}, F_i^{R_1,3}, \dots, F_i^{R_1,j_{max}}\}$ and $S_i^{R_2} = \{F_i^{R_2,1}, F_i^{R_2,2}, F_i^{R_2,3}, \dots, F_i^{R_2,j_{max}}\}$. The result is a spatio-temporal fingerprint set, which is concatenated path-wise, and defined for l_1 and l_2 as follows:

$$S_i = \left\{ (F_i^{R_1,1}, F_i^{R_2,1}), (F_i^{R_1,2}, F_i^{R_2,2}), (F_i^{R_1,3}, F_i^{R_2,3}), \dots, (F_i^{R_1,j_{max}}, F_i^{R_2,j_{max}}) \right\}.$$

An example can be drawn when localizing a transmitter at a distance d_i and time instant t_0 with memory levels ($l_1 = 2, l_2 = 1$) which concludes a spatio-temporal fingerprint $F_i = (F_i^{R_1}, F_i^{R_2})$ where

$$F_i^{R_1} = (f_{it_0}^{R_1}, f_{it_{-1}}^{R_1}), \quad (3.5)$$

$$F_i^{R_2} = (f_{it_0}^{R_2}). \quad (3.6)$$

For $(l_1 = 2, l_2 = 1)$, R_2 extracts a fingerprint $F_i^{R_2}$ of length 7 (i.e., memoryless fingerprint) while $F_i^{R_1}$, collected from R_1 , is the concatenation of two sub-fingerprints recorded from two time instances t_0 and t_{-1} (i.e., memory-assisted fingerprint of length 14). As a result, a spatio-temporal fingerprint $F_i = (F_i^{R_1}, F_i^{R_2})$ may be used in a fingerprinting technique that combines 3 CIRs (i.e., 21 parameters) for each position inside the quasi-curvilinear topology of narrow-vein mines. The number of inputs N_{inputs} defines the ANN's design and is identified by the length of the spatio-temporal fingerprint which is dependent on both l_1 and l_2 where:

$$N_{inputs} = 7(l_1 + l_2). \quad (3.7)$$

Testing spatio-temporal fingerprints is done in two steps. At first, R_2 is kept at a memory level $l_2 = 1$ (i.e., without memory) while R_1 's memory level varies (i.e., $l_2 = 2, 3$). Then, in the second step, both memory levels are increased simultaneously. The results of localization using spatio-temporal diversity are shown for the training and testing fingerprints in figures 9.6 and 9.7, respectively. It was proven, in section 9.4 p. 93, that memory-assisted cooperative approaches that combine spatial and temporal diversities to the fingerprints perform better than the solitary techniques even when the length of the fingerprints is the same such as the cases of ANN(3,0) (i.e., exploiting temporal diversity only) and ANN(2,1) (i.e., exploiting spatio-temporal diversity). A glance at the results of all studied spatio-temporal techniques may be reviewed in table 9.1, whereas those resulting from ANNs optimized for low fingerprint-acquisition cost, discussed later in section 3.5 p. 32, are summarized in table 4.1.

3.4 Localization Exploiting R_x and T_x Spatial Diversity

Localization exploiting fingerprints based on dual antenna systems, present in single/multiple input multiple output (SIMO/MIMO) communication systems, is the fourth chapter of accomplishments and it pushes the performance limits of CIR-based localization to a new record. By utilizing the concepts of dual antennas present in SIMO/MIMO-capable communication systems, a new fingerprint-based localization technique is introduced to combine sub-fingerprints extracted from dual transmitter antennas (T_x) and collected at one or more receiver antenna (R_x). The result is a set of spatially diverse fingerprints at both T_x and R_x antennas, which accurately estimate the distance to the transmitter. The foundation of this work is presented in the publication of chapter 11 and in the proceedings of section 12.3.4 p. 153.

In the following, we lay down the groundwork for a new fingerprinting technique that uses SIMO and MIMO-type fingerprints extracted from two transmitter antennas (i.e., T_{x1} and T_{x2}) in the presence of one receiver antenna (i.e., R_{x1}) and two receiver antennas (i.e., R_{x1} and R_{x2}) respectively. Spatial diversity is exploited twice at both the receiver and transmitter where the antenna spacing is $\delta^{T_x} = 1$ m along the x -axis or $\delta^{T_x} = 0.5$ m along the y -axis of the tunnel. From an implementation point of view, antennas may be placed on heavy machinery or built in the miners' suits on the shoulders.

SIMO-type fingerprints (i.e., fingerprints collected at R_1 from two T_x antennas) exploit T_x spatial diversity at the transmitter's end in the presence of one receiver only without the need for memory (cf. chapter 12). A SIMO-type fingerprint is represented as follows:

$$F_i^{SIMO} = (f_i^{T_{x1}}, f_i^{T_{x2}}), \quad (3.8)$$

where $f_i^{T_{x1}}$ and $f_i^{T_{x2}}$ are the fingerprints collected by R_{x1} , at a position i , for T_{x1} and T_{x2} , respectively. On the other hand, MIMO-type fingerprints, which exploit both T_x and R_x spatial diversities, are simulated by considering two receiver antennas R_{x1} and R_{x2} , being those of R_1 and R_2 , respectively. A MIMO-type fingerprint may be expressed as follows:

$$F_i^{MIMO} = \{(f_i^{T_{x1}}, f_i^{T_{x2}}), (f_{i'}^{T_{x1}}, f_{i'}^{T_{x2}})\}. \quad (3.9)$$

$f_i^{T_{x1}}$ and $f_i^{T_{x2}}$ represent the fingerprints collected by R_{x1} , whereas $f_{i'}^{T_{x1}}$ and $f_{i'}^{T_{x2}}$ are the fingerprints collected by R_{x2} , at a position $i' = D - i$, for T_{x1} and T_{x2} , respectively. The final estimation is the distance, along the x -axis, separating R_1 and the midpoint of T_{x1} and T_{x2} . In chapter 11, localization using both R_x and T_x spatial diversities is studied at $\delta_x^{T_x} = 1$ m along the x -axis and at $\delta_y^{T_x} = 1$ or 0.5 m along the y -axis of the tunnel.

Performance results of exploiting T_x and R_x spatial diversities, shown in figure 11.8 and summarized in table 4.1, surpass those of all developed fingerprinting techniques, discussed above, in terms of precision and accuracy. Their accuracies drop below 40 cm for 90% of the testing data. In addition to that, by exploiting the presence of dual antenna systems in fingerprint formation, the localization system's robustness increases and ANNs would, if well designed, interpolate with higher accuracies even in the presence of measurement gaps as later discussed in section 3.5 p. 32.

3.5 Optimization and Cost Reduction Techniques

In the literature, most fingerprint-based techniques are criticized because of their need of expensive measurement campaigns that buildup the training database of ANNs. Reducing the amount of data measurements, on the other hand, may risk

the generalization process that ANNs need in order to interpolate and estimate in measurement gaps not seen throughout the training process. A conclusion drawn after a successful attempt, at the end of chapter 10, is to reap off diversity benefits in exchange for lower fingerprint acquisition cost. However, a more advanced study was performed to challenge all our developed localization techniques that use spatial, temporal, spatio-temporal diversities in the presence of single or dual transmission antennas, and put their respective ANNs to the test of using less data measurements by gradually reducing the training set down to less than one sixth of the grid's measurement points. The obtained number of neurons needed for each technique, which were produced after extensive ANNs simulations, are the clincher of this work and they are fully described in the publication of chapter 11 and in the proceedings of section 12.5 p. 159.

The localization techniques were discussed at sampling step-size $S_x = 1$ m which represents the step size between any two consecutive offline measurement points along the x -axis of the tunnel. This means that ANNs were trained using offline sampling rate S_r of 1 fingerprint-set per meter without consistent gaps in the grid's resolution. In the following, we increase S_x to 2 m, 3 m and up to 6 m (i.e., decrease S_r to a fingerprint set per S_x) resulting in a split of the original grid into 2, 3 and up to 6 sub-grids, respectively, by counting for the transmitter's initial position on the grid.

The challenge of extremely decreasing the number of fingerprints comes in the ability to alternate ANNs' designs by searching for the optimum number of neurons needed for each fingerprint set. Too many neurons would result in deep convergence and overfitting accuracies that would fire back and result in very high estimation errors when localizing in measurement gaps or sub-grids omitted from the training process of ANNs. Similarly, few neurons may cause the system to lose a lot of its performance trying to generalize the solution domain. For that specific reason, an

extensive simulation was performed and over 14,000 ANNs were trained, each with a number of neuron n_n varying between 1 and N_n such that:

$$1 < n_n < N_n = 2N_i + 1, \quad (3.10)$$

where N_i is the number of inputs of the ANN that depends on the used localization technique and memory levels. A successor ANN for each technique is the one that scores the best performance, in terms of accuracy, when tested on its trained sub-grid and on 25% of all the remaining sub-grids at a certain S_x . The number of selected neurons per each localization technique is shown in figure 12.10 and it may be used as a benchmark for future studies.

Surprisingly, the performance results show very accurate records even when ANNs are trained using one sixth of the grid's fingerprints allowing MIMO-type fingerprints to overpass the rest of the localization techniques in terms of robustness to grid's resolution. At $S_x = 6$ m, localization using T_x and R_x spatial diversities attains similar results to the original benchmark in [31] at $S_x = 1$ m. The remaining results of cost optimization for all spatial, temporal and spatio-temporal fingerprinting techniques are presented in the publication of chapter 11 and in the proceedings of section 12.5.1 p. 160 especially in figures 12.13 and 12.14.

Chapter 4

Data Analysis and Findings

The Cumulative Density Function (CDF) is used throughout the dissertation to show and compare the estimation errors of all developed localization techniques focusing on their positioning accuracies in meters versus precision (i.e., percentage of treated fingerprints). The granularity of estimation errors is fully shown in figures [12.8](#), [12.9](#), [12.13](#), [12.14](#) and in table [4.1](#), then performance results are analyzed together in sections [12.4](#) p. [154](#) and [12.5.2](#) p. [162](#). In the following, the developed fingerprint-positioning techniques, which constitute the findings of this work, are compared and analyzed based on important factors such as their accuracy, precision, complexity, robustness and cost.

4.1 Accuracy and Precision

Accuracy is one of the most important performance metrics of any positioning system. In some applications such as in military positioning systems, accuracy is the most important factor and it cannot be traded for complexity and cost, whereas in commercial positioning systems, a tradeoff between accuracy and cost may take place to keep the price within the economical reasonability. On the other hand, the

Table 4.1 – Performance Results with Multiple Resolution

ANN Technique	Grid Resolution Accuracy Results					
	1 m	2 m	3 m	4 m	5 m	6 m
ANN(1,0)	1.42 m	1.44 m	1.81 m	2.04 m	2.12 m	2.83 m
ANN, 2Tx1Rx $\delta_y^{Tx} = 0.5$ m	1.10 m	1.43 m	1.73 m	1.81 m	2.26 m	2.58 m
ANN, 2Tx1Rx $\delta_y^{Tx} = 1$ m	0.85 m	1.36 m	1.53 m	1.66 m	1.94 m	1.97 m
ANN(2,0)	1.15 m	1.35 m	1.58 m	1.92 m	1.97 m	2.07 m
ANN(3,0)	0.53 m	1.36 m	1.58 m	1.78 m	1.94 m	2.02 m
ANN(4,0)	0.48 m	1.30 m	1.46 m	1.72 m	1.91 m	1.93 m
ANN, 2Tx1Rx $\delta_x^{Tx} = 1$ m	1.05 m	1.23 m	1.33 m	1.51 m	1.61 m	2.07 m
ANN(1,1)	0.91 m	1.07 m	1.15 m	1.28 m	1.39 m	1.45 m
ANN, 2Tx2Rx $\delta_y^{Tx} = 1$ m	0.64 m	0.84 m	1.07 m	1.14 m	1.35 m	1.51 m
ANN(2,2)	0.49 m	0.95 m	1.07 m	1.22 m	1.26 m	1.41 m
ANN, 2Tx2Rx $\delta_x^{Tx} = 1$ m	0.43 m	0.93 m	1.10 m	1.14 m	1.19 m	1.32 m
ANN, 2Tx2Rx $\delta_y^{Tx} = 0.5$ m	0.38 m	0.83 m	0.98 m	1.12 m	1.20 m	1.28 m

precision factor defines if a given accuracy is reported frequently throughout multiple measurements. For those reasons, we chose to compare all localization techniques using 90% percentile obtained from the CDFs of each localization technique.

In our localization problem, all the discussed localization techniques may be considered accurate because their positioning errors drop below 1.5 meter. However, for the sake of argument, the most accurate techniques among all is the one that introduces MIMO-type fingerprints pushing the accuracy limits to 38 cm for 90% of the testing data at $S_x = 1$ m. Similar accuracy was reported for spatio-temporal fingerprint positioning with ANN(2,2) with estimation errors dropping as low as 49 cm for the same precision level which are also close to the performance results of temporally-diverse fingerprints with ANN(3,0) and ANN(4,0).

4.2 Complexity

The complexity of the positioning system involves factors such as computation time, memory, hardware and software design, energy consumption and implemen-

tation. When taking into account the system's processing time, fingerprint-based localization techniques may be compared based on the number of neurons used by ANNs in both the input and hidden layers. Training ANNs with fingerprints of high chain lengths is much slower than training ANNs with few input neurons. This would make a memory-assisted technique with ANN(3,0) and accuracy of 53 cm more attractive than ANN(4,0) which reports better accuracy of 48 cm because the latter uses 7 more input neurons. One can also compare both techniques' number of hidden neurons as shown in figure 12.10 to find that they both start off with 40 neurons at $S_x = 1$ m.

On the other hand, from an implementation point of view, adding memory to access points may increase system design's complexity. If complexity is the main concern, fingerprint positioning using T_x and R_x spatial diversities may come at lower complexity than memory-based localization, in terms of fingerprint acquisition and path recognition techniques.

4.3 Robustness

Robustness is the ability to keep the system stable once the received information is corrupted or unknown. For that reason, this work studied the effect of having less data measurements in the training process of ANNs of all techniques. It is shown at $S_x = 6$ m that temporally-diverse fingerprint-positioning techniques failed to maintain their high accuracy results at $S_x = 1$ m, which is tracked to the fact that at higher S_x , sub-fingerprints extracted from previous positions carry less information about the current position of the transmitter. One can observe that spatio-temporal and MIMO-type fingerprints maintained their accuracy trends even when one sixth of the measurements were missing from the training process.

4.4 Cost

The cost of a localization system depends on the complexity of its hardware and software designs; it also depends on the integration factor and time compensation. All fingerprint-based localization techniques have to undergo measurement campaigns that add extra costs to the implementation bill. The more savings a localization technique can bring in, the more attractive it appeals to investors and business owners. Deployment cost is least when using fingerprints that do not introduce memory nor use MIMO-capable devices with dual antennas, but at that low cost comes higher errors and less robustness to sampling resolution. However, it is proven herein that measurement campaigns may be cut in less than half while MIMO-type or spatio-temporal fingerprinting techniques succeed to maintain high performance results.

Chapter 5

Conclusion

To conclude, if spatial, temporal or spatio-temporal diversities are well applied in fingerprint-based localization algorithms, the localization system would gain high precision and pinpoint positioning accuracies. The use of dual antenna fingerprints, on the other hand, is recommended for MIMO-capable devices and is proven to increase the system's performance. In addition to that, reducing the sampling resolution of offline measurements requires careful design of ANNs that succeed to localize in measurement gaps not seen in the training process. Finally, trading off pinpoint accuracy for lower complexity and cost is studied for implantation purposes in an effort to reduce the time needed for fingerprint-acquisition campaigns.

Chapter 6

Future Research

Future studies will analyze the performance of all fingerprint-based localization techniques in different frequency bands such as the milli-meter wave band (i.e., 60 GHz band). The applications of localization at 60 GHz may be useful in the fields of robotics, sensor networks and machine-to-machine communications.

Since the ANN-based localization system is centralized (i.e., location awareness is at the receiver's end), another area of research would be to analyze the capability of broadcasting ANN's weights and biases and allowing users to self-localize themselves in the vicinity of wireless coverage.

Finally, in a best effort to further optimize the localization system, a study may be performed to recommend the optimum number of parameters in each CIR-based fingerprint based on whether localization is exploiting spatial, temporal or spatio-temporal diversities.

Part II

Smart Localization in Underground Mines using Fingerprinting and ANNs: Strategies and Applications

Articles

Chapter 7

Cooperative Localization in Mines Using Fingerprinting and Neural Networks

Authors: Shehadi Dayekh, Nahi Kandil, Sofène Affes and Chahé Nerguizian.

Contribution: The primary author is the main contributor and editor of this work.

Conference: IEEE Wireless Communications and Networking Conference.

Status: Article published on April 21st, 2010.

Abstract

Localizing people in confined and underground areas is one of the topics under research in mining labs and industries. The position of personnel and equipments in areas such as mines is of high importance because it improves industrial safety and security. Due to the special nature of underground environments, signals transmitted in a mine gallery/tunnel suffer from severe multipath effects caused by reflection, refraction, diffraction and collision with humid rough surfaces. In such cases and in cases where the signals are blocked due to the non-line of sight (NLOS) regions, traditional localization techniques based on the RSS, AOA and TOA/TDOA lead to high position estimation errors. One of the proposed solutions to such challenging situations is based on extracting channel impulse response (CIR) fingerprints with reference to one wireless receiver and using an artificial neural network as a matching algorithm to localize. In this article we study this approach in a multiple access network where multiple access points are present. The diversity of the collected fingerprints will allow us to create artificial neural networks that will work separately or cooperatively using the same localization technique. The results will show that using cooperative artificial intelligence in the presence of multiple signatures from different reference points improves significantly the accuracy, precision, scalability and the overall performance of the localization system.

Keywords. Indoor localization, channel impulse response, artificial neural network, fingerprinting technique, multiple access technique.

7.1 Introduction

In the mining industry, knowing the position of miners and/or equipments is an important safety measure that reduces risks and improves the security of that facility. Like any indoor environment, wireless signals transmitted in mines are affected by extreme multipath and non-line of sight (NLOS) conditions. Since mines have their own environment that is made up of connected tunnels, localization using traditional techniques is challenging and fails to provide accurate positioning. Most traditional geo-location systems use the triangulation techniques and are mainly based on the received signal strength (RSS), angle of arrival (AOA), time of arrival (TOA) or the time-difference of arrival (TDOA). Other systems use scene-analysis or fingerprinting techniques, and these include the probabilistic methods, k-nearest neighbours (kNN), support vertex polygon (SMP), support vector machine (SVP), and neural networks. Surveys on wireless indoor positioning techniques [27], [39] provide detailed discussion of each approach. Underground localization using traditional systems would result in an unstable behavior due to the fact that the received signals in an underground environment undergo several reflections, refractions and diffractions that can dramatically change the amplitude, time of arrival and phase at the receiver.

A novel approach to localization has been presented in [31] and it is based on studying the CIR at a specific distance from the transmitter and registering its specifications as a fingerprint to be matched using the neural network technique. The same concept was also used in [42] with less input parameters. The uniqueness of the CIR at each position enhanced the accuracy and precision of localization in indoor facilities. Unlike other approaches [10], [29], [23], [11] which mainly base their fingerprints on the RSS with reference to one or more access points, this approach uses several parameters extracted from one CIR as a fingerprint with reference to one receiver.

One of the drawbacks of using the RSS as a fingerprint is the fact that the signal's strength vary with time at the same position [39], [10], and that the accuracy of localization is mainly enhanced when the number of access points (APs) increases in the same area [9].

In this article we will enrich the localization technique in [31] and open it to a wide range of possibilities where the mobile user is capable of transmitting multiple signals to different access points present in the network. Unlike the approach in [31] which estimates the position based on one receiver, this work will consider the inputs of more than one receiver before giving a position estimate. The received signatures at several references form fingerprints and the position will be estimated using multiple neural network techniques in a cooperative localization concept. In the following section, the fingerprinting technique is discussed, and the neural network is presented as the matching algorithm for localization. In section 7.3, we introduce the localization system and its functionality in the areas containing only one receiver shedding the light on major problems encountered. In section 7.4, several techniques to localization are discussed in the presence of two receivers. The results are compared and analyzed in section 7.5. Finally, the paper is closed by a conclusion in section 7.6.

7.2 Localization Using Fingerprinting and Neural Networks

7.2.1 Fingerprinting technique

The fingerprinting technique is based on collecting information about specific events and then matching the presence or absence of those events based on the pre-acquired data. Fingerprinting techniques can be used in indoor localization approaches in order to identify the channel at different parts of the covered area

[11], [1], [20]. It is similar by analogy to the human fingerprints and it is used here to ensure uniqueness and precision to the indoor channel behavior present in mines. In this paper, the fingerprinting technique is used to identify a position based on the CIR. This technique consists of two phases: the offline phase which is the process of collecting several impulse responses at several distances from the receiver and then storing the information in a database. The second phase of the fingerprinting technique is the real-time phase where in online scenarios the CIR is extracted and then compared to the saved database in order to match a specific position. In the following, the same approach in [31] is discussed along with the different parameters that form the fingerprint of any position. A signature or a fingerprint is a set of seven parameters at a specific distance to the transmitter (discussed below).

Real-time measurement campaigns were carried out 70 meters underground in the CANMET gold mine in Val d'Or city [31], [42]. The measurements in [31] were used in this work and they were recorded at a central frequency of 2.4 GHz in order to have a compatibility with WLAN systems. These measurements consist of 450 measurements along a tunnel as shown in Fig. 7.1. The complex CIR of the wideband measurements was obtained using the frequency channel sounding technique [31]. Once a signal is received, the channel impulse response is extracted and by applying the inverse fast Fourier transform (IFFT), the time impulse response is obtained. Using this impulse response, one can extract several parameters to form a specific signature. Seven parameters for each CIR guarantee uniqueness to the position of the transmitter. The parameters are as follows:

- The mean excess delay ($\bar{\tau}$) that is the first moment of the power delay profile measured at the first detectable signal that arrives at the receiver and is related to the power of that profile. In other words it is related to the amplitudes of

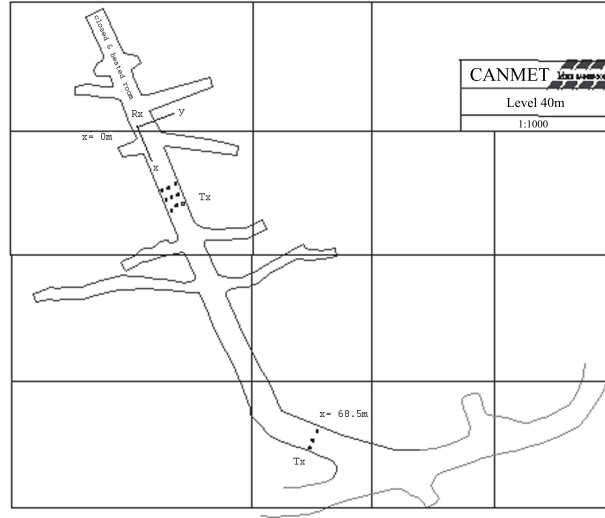


Figure 7.1 – Map of the tunnel.

the multipath components, and it is given by:

$$\bar{\tau} = \frac{\sum_k a_k^2 \tau_k}{\sum_k a_k^2}.$$

- The root mean square (τ_{rms}), and it represents the square root of the second central moment of the power delay profile and it is given by:

$$\sigma = \sqrt{\bar{\tau}^2 - (\bar{\tau})^2},$$

where:

$$\bar{\tau}^2 = \frac{\sum_k a_k^2 \tau_k^2}{\sum_k a_k^2}.$$

- The maximum excess delay (τ_{max}) which is the time at which the signal drops below X dB of the maximum power measured in the power delay profile. It can be seen as the time that a signal stays above a given threshold based on the highest received power in a profile. In the following, the value of 20 dB is taken as a threshold.

- The total power of the received signal (P) measured in dBm.
- The number of multipath components (N) which form the entire received signal measured at a 20 dB floor level.
- The power of the first arrival (P_1) which is the power of the first multipath component.
- The delay of the first path component (τ_1) and it is used along with P_1 in order to distinguish between the LOS and NLOS scenarios.

7.2.2 Artificial neural network

Once the database is ready, the system would need a matching algorithm that can study the spatial variation of the channel with respect to the distance, here comes the importance of neural networks. Artificial neural networks (ANN) are computational models able to perform complex computational operations such as classification, control optimization, and function approximation. The advantage of using a neural network is its ability to find the mathematical relation between the set of signatures and the estimated positions. A trained artificial neural network is suitable for real-time applications because it is capable of matching the set of inputs (sets of signatures) to a set of outputs (distances) forming a mathematical model that can estimate new positions based on new signatures [17].

Several types of neural networks are found and can perform different techniques of computations but the main interest among all is to minimize the error and precisely map the set of inputs to the desired output. In the case of localization problems, function approximation is based on non-linear regression modelling. Thus two types of neural networks can be used which are the Multi-Layer Perceptron (MLP) networks and Radial Basis Function (RBF) networks. Both networks are feed forward

and perform specific learning algorithms. These algorithms have an important role in adjusting the weights and biases and in minimizing the estimation errors. The use of an MLP-type feed forward neural network with a back-propagation learning algorithm has been proven to give better estimation results in underground localization systems [31], [42].

First, the ANN has to be trained on the set of data collected through measurement campaigns. A neural network is mainly made up of input, output, and hidden layers. Each layer contains several neurons that hold weights and biases. In the offline phase, part of the collected data is used to modify the weights and biases leading to a minimum mean square error. However, initializing the network with random weights and biases would lead to different performances [17], and that is why some training iterations are needed before reaching a desirable performance of the neural network. Once a desired performance is reached, the network can be saved and used to estimate trained and untrained data in real-time scenarios.

7.3 Localization Using One Receiver

Traditional techniques of localization mainly require two or more reference points in order to precisely estimate the position of the mobile. Geo-location can also be done in the presence of one receiver only using the fingerprinting and the neural networks techniques, and it can give an accurate distance location of 2 meters for 90% and 80% of the trained and untrained patterns, respectively [31]. The neural network used in this work is a feed forward network with a back propagation learning algorithm. It consists of 7 inputs, one hidden layer, and one output. The inputs correspond to the extracted parameters of the CIR while the output is the distance (d) to the transmitter as shown in Fig. 7.2.

The use of one dimensional position estimation is convenient in mine galleries and

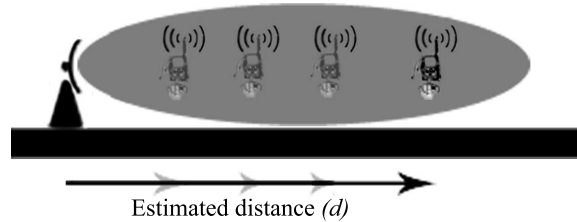


Figure 7.2 – Localization using one fixed receiver. The CIR is extracted at different distances to the transmitter with 1 meter step size.

is later discussed in the following section. The hidden layer consists of 10 neurons and uses a differential tan-sigmoid transfer function unlike the output layer which has a linear type transfer function. The network is trained at several distances away from the transmitter and then the system may estimate the position of the mobile unit (transmitter) based on the received signal. Localization using the CIR in the presence of one receiver is the same technique used in [31] and it is used here as an example of a non-cooperative technique¹. It was shown that position estimation is precise and that the error is less than 1.5 meters for 90% and 80% of trained and untrained data, respectively.

Despite the fact that the results are promising, there are obstacles that prevent using the same technique in underground environments such as mines due to the following reasons:

- The need of a global localization system that can cover all the areas of interest.
- The existence of junctions and connected tunnels, these tunnels may result in misleading information about the exact position of the mobile user or miner.

On the other hand, using cooperative artificial intelligence in a localization technique is encouraging because it would lead to better estimation results. The estimated

¹Unlike the system in [31] which uses both x and y coordinates to estimate the position, the proposed system uses a one-dimension estimation concept (x position) neglecting the small variation of y in mine galleries.

distance to the transmitter in LOS might be precise using one reference point, but the position of the miner can be in different directions depending on how much the tunnels are interconnected. For these reasons, using a cooperative technique where at least two receivers are available will introduce localization as a system applicable in mines and would better estimate the position of the mobile user.

7.4 Cooperative Localization Using Two Receivers or More

The main interest of deploying a wireless transmission system is to insure constant communications between mobile units and base stations, and this can only be possible if the system is able to provide coverage to the whole area of interest. Localization in the area where signals from two access points intersect is the main interest of this work. Unlike the first approach in Sec. 7.3 which used one signature to estimate the distance, the following techniques will use several signatures of more than one receiver (AP) in order to estimate the same distance taking one receiver as a reference point. This concept will enrich the training set of data that will be fed to the neural network. It is more like collecting multiple fingerprints of the same person which is in our case the distance to the transmitter. If one fingerprint caused a wide error, the others will be there to calibrate the location of the transmitter. Cooperative localization in a 2D/3D topology might involve the participation of more than two access points present in the area of interest. However due to the special one-dimensional topology of mines' galleries, two access points should be enough to provide wireless coverage of the whole area in between.

As shown in Fig. 7.3, at each position of the transmitter, the two receivers collect the transmitted signal extracting two different sets of parameters (CIRs). This

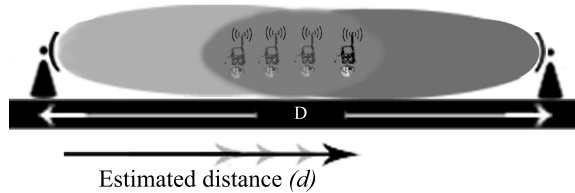


Figure 7.3 – Localization using two signatures of two receivers in the area where two signals intersect.

diversity technique opens a wide range of possibilities and helps the neural network exploit a better position estimation model. A full database is saved containing 14 parameters (2 signatures) for each location which is the distance with respect to one receiver. These sets of fingerprints can be treated by different localization techniques.

7.4.1 Localization based on separate neural networks

This technique uses two of the same neural network exploited in the case of one receiver as in Sec. 7.3. The system receives the signature of receiver 1 and estimates the distance to the transmitter, and uses the signature of receiver 2 to estimate another distance to the transmitter. Two neural networks are needed as shown in Fig. 7.4. In this case, the system has to know the exact location of both receivers on a saved digital map of the connected straight lines (tunnels). The new estimated position would be the midpoint of the two estimated locations; localization here is based on averaging both estimation errors.

7.4.2 Localization based on one neural network

In this approach the system collects the signals from both receivers and forms a set of two CIRs with a total of 14 parameters. The transmitter's position is estimated based on the distance to one of the receivers. As shown in Fig. 7.5, a super neural net-

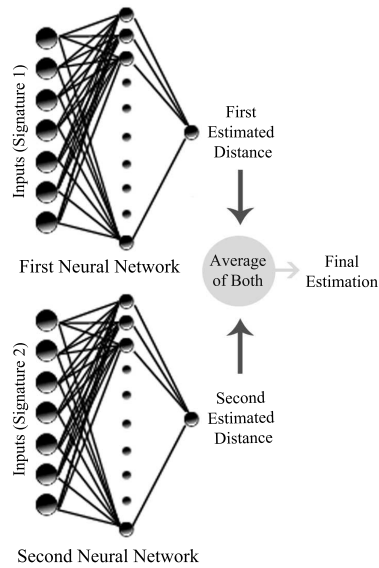


Figure 7.4 – Localization based on two separate estimations.

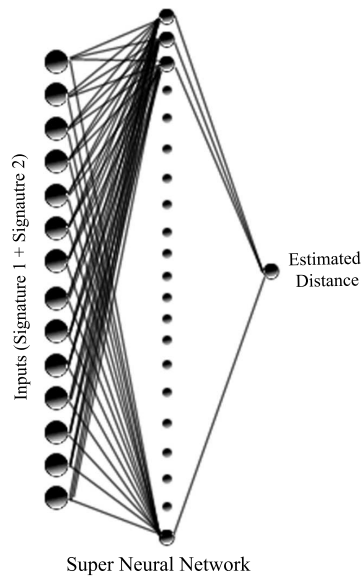


Figure 7.5 – Neural network based on multiple signatures.

work is created and trained to localize a mobile with reference to one of the receivers (fixed points or anchors) based on two different signatures. This network trains 75% of the collected data. Several trainings lead to several performances based on the random initialization of the weights and biases. The best performance was achieved

with 18 neurons in the hidden layer. In order to test the network's performance, the transmitter is simulated to move across the same path then the system uses the -previously trained- neural network to localize the transmitter based on the two received signals. Usually in most network implementations, access points are placed to cover a wide region and the coverage fields intersect in a handoff region. The length of this region varies from one configuration to another which results in a change in the training set of data (inputs and outputs). In each scenario (i.e., separation distance D in Fig. 7.3), a new neural network needs to be trained.

7.5 Results of Different Techniques

The performance of the presented localization techniques will be evaluated using the CDF graph. The first parameter of the CDF is the estimation error which represents the difference between the estimated and the real position measured in meters. The second parameter is the percentage of occurrences for such an estimation error in the collected data. In the following, the coverage of a transmitter is assumed to be 68 meters², the results are shown for several distances separating two receivers. Each CDF graph shows four CDF plots of the position estimation errors using different estimation techniques. The first two plots show the results of the localization technique based on receiver 1 and receiver 2. The third plot represents the position errors when using the super neural network, and the last plot shows the results of using the localization technique based on averaging the two separate estimation errors of both receivers. CDF plots of the trained data for separation distances 60m, 80m and 100m are shown in Figs. 7.6, 7.7 and 7.8, respectively.

In the trained set of data, the position error for one receiver estimation technique

²In real-time measurement scenarios, the transmitted signals fade after this distance resulting in weak signatures.

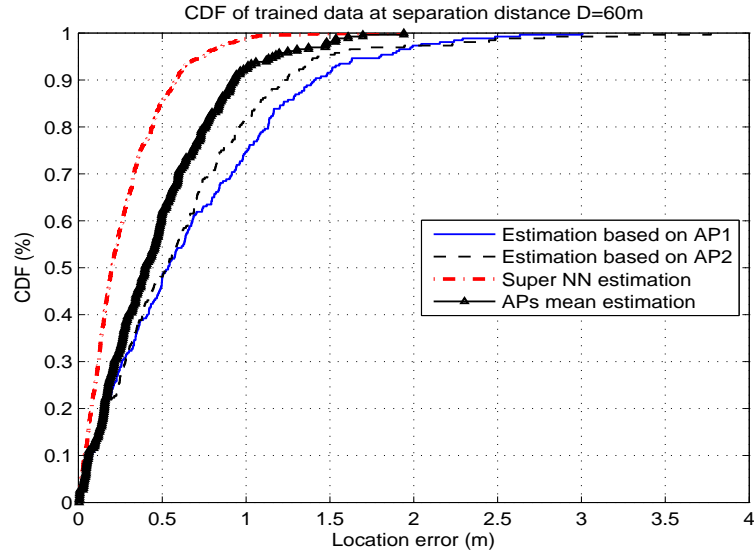


Figure 7.6 – CDF plots of the position estimation errors at a receivers' separation distance $D=60\text{m}$ using several localization techniques.

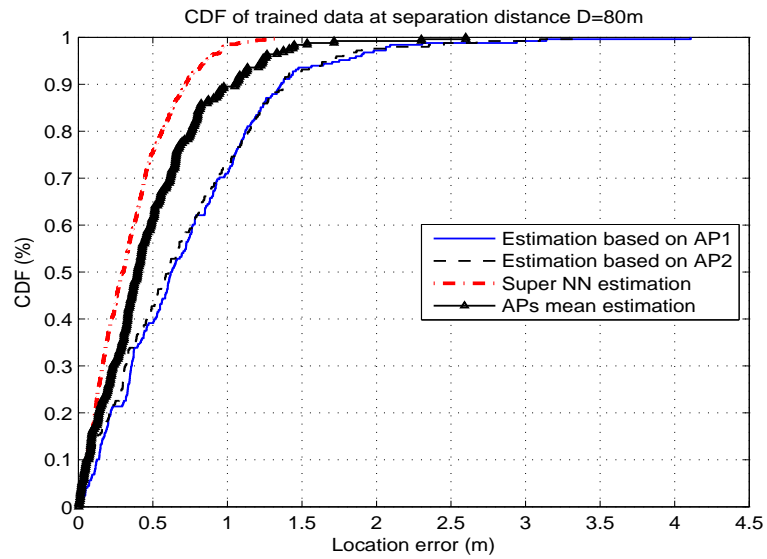


Figure 7.7 – CDF plots of the position estimation errors at a receivers' separation distance $D=80\text{m}$ using several localization techniques.

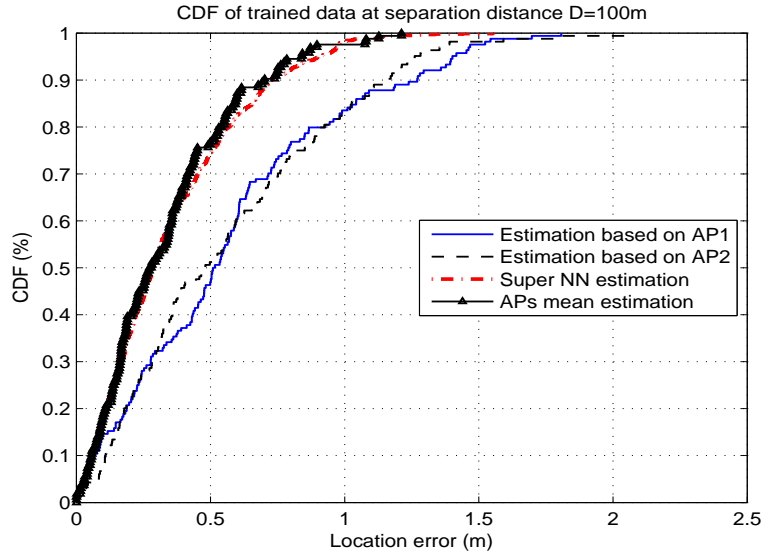


Figure 7.8 – CDF plots of the position estimation errors at a receivers’ separation distance $D=100\text{m}$ using several localization techniques.

ranged between 1.2 and 1.5m for 90% of data. The accuracy of position estimation using receiver 1 is slightly different from that of receiver 2 because for each receiver there is a different neural network that trains the collected corresponding set of data. However, it is obvious from the first two CDF plots that the results of using separate neural networks are almost the same no matter if the estimation is based on receiver 1 or 2. On the other hand, the estimation based on averaging the two position errors showed a better performance and it was recorded to be less than 1m for 90% of data. For the super neural network, the performance was recorded to be less than 60 cm for 90% of trained data at close separation distances. When the separation distance increases, the handoff region becomes narrow resulting in a reduced amount of signatures to be trained. This, in fact, has an effect on the training process of the neural networks because training insufficient data results in finding an inaccurate model for localization. The estimation based on averaging shows better accuracy than that of the super neural network at a separation distance of 100m. The reason is that the separate neural networks are trained using the data acquired throughout the whole

tunnel while the super neural network is trained using the few signatures in the narrow handoff region. However, due to the fact that the input of the super neural network is a combination of two signatures at the same time, it may be noticed that the super neural network manages to be more precise than the two separate neural networks in most scenarios and it can almost provide the same position accuracy even at far separation distances.

CDF plots of the untrained data for separation distances 60m, 80m and 100m are shown in Figs. 7.9, 7.10 and 7.11, respectively. For the untrained set of signatures,

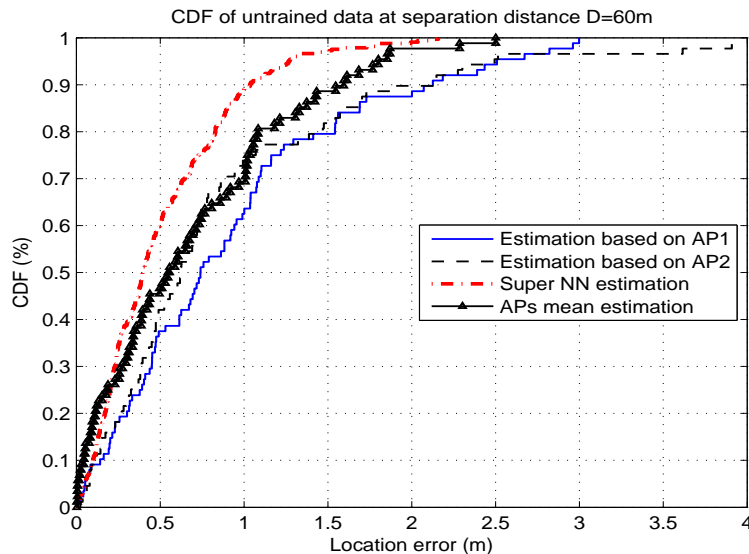


Figure 7.9 – CDF plots of the position estimation errors at a receivers’ separation distance $D=60\text{m}$ using several localization techniques.

it should be noted that data was taken at specific distances between the receivers and that none of the neural networks was trained on the signatures at those distances, i.e. the average was based on two untrained separate estimations. As shown in Figs. 7.9, 7.10 and 7.11, the positioning error of the localization technique based on one receiver varies between 1m and 2m for 90% of the untrained data. For the cooperative localization based on averaging, the performance was again dependent on the accuracy of the two neural networks. As shown in Figs. 7.6 and 7.9, the results of averaging were

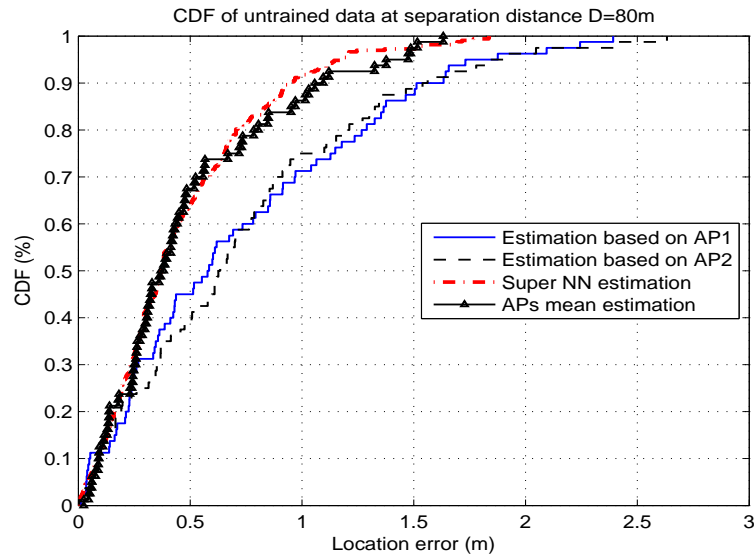


Figure 7.10 – CDF plots of the position estimation errors at a receivers’ separation distance $D=80\text{m}$ using several localization techniques.

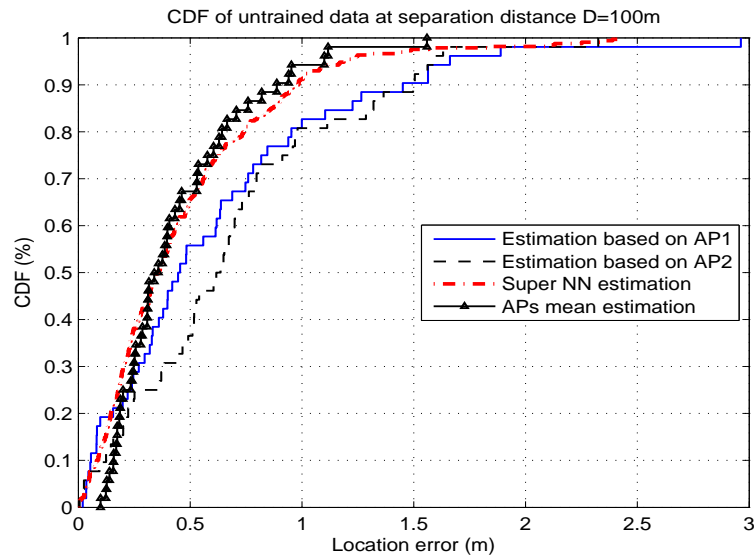


Figure 7.11 – CDF plots of the position estimation errors at a receivers’ separation distance $D=100\text{m}$ using several localization techniques.

precise for the trained data. However, this precision affected the estimation of the untrained data. Using the super neural network, the positioning error was the same for all distances and it gave an error of approximately 1m for 90% of untrained data.

The use of multiple connected neural networks or one super neural network is suitable for indoor localization since both new cooperative localization schemes provide high accuracy, precision and scalability at different separation distances.

7.6 Conclusion

This paper studied the results of using the channel impulse responses as fingerprints for position estimation in the presence of different receivers. While other localization techniques fail to be accurate in environments such as mines, this approach is able to estimate the location of personnel and/or equipment with an error of less than 1m for 90% of trained and untrained data. The use of cooperative neural intelligence not only enriches the set of data to be trained but also improves the overall performance of the system and introduces the cooperative localization concept. The diversity of the captured signatures provides rich training sets for the neural networks leading to a more accurate, precise, scalable and robust positioning system.

This system may be designed for remote or self positioning purposes and may use any of the two techniques introduced in the paper. In the first technique, the user collects several signatures from different receivers and uses separate neural networks to estimate the distances to the transmitter. Then, using a saved map that shows the position of each receiver, the system will be able to average the position of the transmitter. In the second technique, the different signatures are fed into a super neural network to provide one position estimation with significantly increased accuracy. This system may be implemented for other indoor environments such as corridors or arcade type indoors. On the other hand, the system can use different wireless technologies such as UWB, WLAN, or mobile radio.

Chapter 8

Radio-Localization in Underground Narrow-Vein Mines Using Neural Networks with In-built Tracking and Time Diversity

Authors: Shehadi Dayekh, Sofiène Affes, Nahi Kandil and Chahé Nerguizian.

Contribution: The primary author is the main contributor and editor of this work.

Conference: IEEE Wireless Communications and Networking Conference.

Status: Article published on March 31st, 2011.

Abstract

In the mining industry, knowing the position of miners and/or equipments is an important safety measure that reduces risks and improves the security of that facility. Being an indoor environment, wireless transmitted signals in underground narrow-vein mines suffer multiple kinds of distortions due to extreme multipath and non-line of sight (NLOS) conditions. One of the proposed solutions to accurate localization in such challenging environments is based on extracting the channel impulse response (CIR) of the received signal and using the fingerprinting technique combined with cooperative artificial neural networks (ANNs). Such localization systems use the spatial domain where the reference localizing units are implemented at different positions away from the transmitter. In this article, we introduce a localization technique that uses fingerprints successively recorded in time with in-built tracking as an alternative method to localize. Unlike the spatial-domain technique where cooperative localizing units collect memoryless fingerprints from different locations, this technique uses one localizing unit and is capable of estimating the position of a transmitter precisely using its current and previous registered fingerprints in time. Localization using time-domain fingerprinting (i.e., tracking) and ANNs is introduced as a new method that exploits time diversity and improves the accuracy, precision and scalability of the positioning system.

Keywords. Indoor localization, channel impulse response, artificial neural network, fingerprinting technique, cooperative localization, tracking, time diversity.

8.1 Introduction

One of the vast numbers of applications of wireless communication systems is position estimation or localization. Outdoor localization systems such as the Global Positioning System (GPS) are already in the market and are available to anyone providing an important service that can locate the user's position precisely. Different localization techniques base their estimations on one or more extracted parameters out of the received signal such as the received signal strength (RSS), angle of arrival (AOA), time of arrival (TOA) or the time-difference of arrival (TDOA). Other systems use scene-analysis or fingerprinting techniques which include using ANNs as matching algorithms. Once a transmitted signal is received at different locations in space, the variation in the signals' fingerprint, RSS, AOA, TOA, or TDOA is calculated and the position of the transmitter is estimated accordingly. Nevertheless, indoor localization is still a challenging topic due to the fact that the transmitted signals indoor undergo several distortions caused by reflections, refractions, NLOS regions and multipath effects. Unlike outdoor mediums where signals relatively travel almost freely in open spaces, indoor environments such as underground mines stem from more complicated scenarios that need to be modeled in order to estimate how the signal would be received after reacting with the channel. Surveys on wireless indoor positioning techniques [27], [39] provide multiple detailed discussions of different localization approaches.

A new approach to localization in tunnel-shaped underground narrow-vein mines is presented in [31] and is based on extracting the CIRs of the received signal as fingerprints of the transmitter's positions, then using these fingerprints to localize the source of transmission with one receiver or Access Point (AP). Several parameters extracted from the CIR give this approach uniqueness unlike other approaches [10], [29], [23], [11], [9] that mainly base their fingerprints on the RSS only. However,

this technique was not able to cover the whole curve-shaped topology of underground mines until the cooperative localization concept was introduced in [4]. Cooperative localization using the CIR technique benefits from the presence of multiple receivers which collect multiple fingerprints in tunnels before estimating the position of the transmitter. Leading to increased accuracy and precision, the developed technique in [4] uses different cooperative neural network techniques and exploits the spatial diversity of the collected fingerprints. However, in the case where spatial diversity is limited by one localizing unit, the system in [4] fails.

In this article, we will study localization in tunnel-shaped underground narrow-vein mines using the time-domain fingerprint diversity (i.e., tracking) technique combined with ANNs. This technique innovates the idea of integrating tracking within the ANN-based fingerprint matching algorithm for localization. The time-domain fingerprint is made up from a chain of CIRs which are collected for the same transmitter along its path to the position which has to be estimated. ANNs are properly then designed based on different chain length or memory levels then trained on all possible path scenarios. Because of the tunnel-shaped topology of underground narrow-vein mines which is quasi-curvilinear, information about the path that the transmitter is following within the confines of its well-mapped galleries adds valuable input to the ANNs and creates an accurate in-built tracking system. The following section summarizes the concept of cooperative localization using fingerprinting and neural networks in the spatial domain. In section 8.3, localization using tracking is introduced along with the theoretical fingerprinting approach. The results of both the spatial (i.e., cooperation) and time (i.e., tracking) diversity-based localization techniques are compared in section 8.4. In section 8.5, the major complexities/challenges that face the design are highlighted along with their proposed solutions. Finally, conclusions are drawn out in section 8.6.

8.2 Localization using Fingerprinting and Neural Networks

We will briefly describe below as a background reference a localization technique that uses the spatial domain in order to localize a transmitter in a mine tunnel. The system is capable of localizing a transmitter using two receivers that work separately or cooperatively using different neural network techniques. A more detailed discussion of these techniques can be found in [4]. But before doing so, we will study below the underlying fingerprinting technique from which extension using multiple APs was developed in [4].

8.2.1 Localization in the presence of one receiver

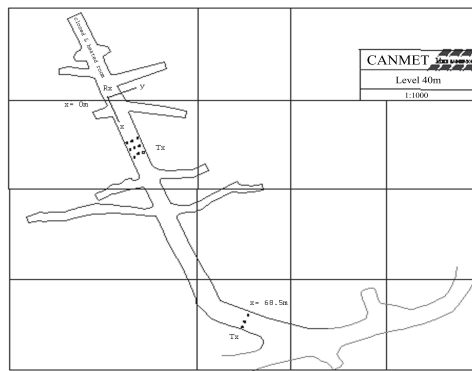


Figure 8.1 – Map of the tunnel.

Due to the special nature of underground narrow-vein mines which are made of quasi-curvilinear connected tunnels as shown in Fig. 8.1, traditional wireless localization systems fail to provide accurate positioning services. This is mainly caused by the distortions of the basic parameters used in localization systems due to the multipath components and NLOS scenarios present in such environments. In such cases, the fingerprinting technique becomes a very promising alternative in that it

confers to each position a specific fingerprint that is then identified by the localizing units using different matching algorithms. In this work, the fingerprinting technique is used to identify a position based on the extracted CIRs at that position.

After conducting a real-time measurement campaign in the CANMET gold mine in Val d’Or city [31], CIRs were collected. For each position across the tunnel in Fig. 8.1, seven parameters were then extracted from the corresponding CIR forming overall a set of fingerprints at different distances (d) away from the receiver as shown in Fig. 8.2. These parameters are the mean excess delay ($\bar{\tau}$), the root mean square

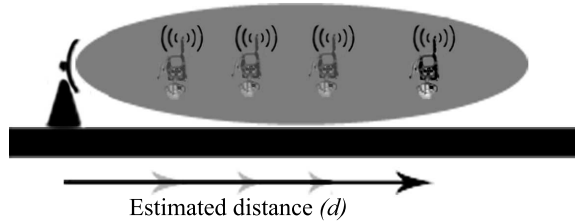


Figure 8.2 – Localization using one fixed receiver.

(τ_{rms}), the maximum excess delay (τ_{max}), the total power of the received signal (P), the number of multipath components (N), the power of the first arrival (P_1) and the delay of the first path component (τ_1). Estimating the position based on the fingerprints is performed using ANNs.

Being able to perform complex computational operations such as classification, control optimization, and function approximation, ANNs proved to be reliable computational models that are widely used for different localization approaches [31], [4], [12], [1], [20]. Every ANN needs to be trained using a set of training data which, in our case, is made up of 75% of the collected fingerprints, leaving 25% of the data for testing. The use of an MLP-type feed forward neural network with a back propagation learning algorithm has been proven to give accurate estimation results in underground localization studies [31], [4]. The simple form of the ANN used in localization in the

presence of one receiver consists of 7 inputs, one hidden layer and one output that is the distance to the transmitter. The hidden layer for this system consists of 10 neurons and it uses a differential tan-sigmoid transfer function, whereas the output layer uses a linear-type transfer function. It was shown that position estimation using one receiver only is precise and that the error is less than 1.5 meters for 90% and 80% of training and non-training data, respectively [4]. Despite the promising accuracy of estimating the distance to the transmitter, this technique cannot by itself guarantee full coverage of the whole tunnel network of an underground mine.

8.2.2 Cooperative localization using two references in space

Precisely, a search for an upgraded technique that can serve as a complete localizing system in underground mines led to the idea of cooperative artificial neural intelligence [4]. The concept of ANN-based cooperative localization using multiple receivers is based on collecting multiple signatures from different receivers forming one fingerprint that corresponds to a transmitter located between the reference endpoints as shown in Fig. 8.3. Because of the quasi-curvilinear topology of tunnels in underground narrow-vein mines, two APs should be enough to provide wireless coverage of the whole area in between in the corresponding tunnel section.

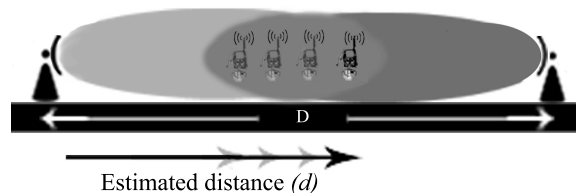


Figure 8.3 – Localization using two signatures of two receivers.

One of the two cooperative localization approaches, discussed in [4], is based on estimating the position of the transmitter by using a single neural network as shown

in Fig. 8.4. Two extracted signatures of the transmitter from two different receivers are fed to this neural network. The latter, which has 14 inputs, is trained to localize a transmitter by estimating the distance to one of the receivers. The separation distance D affects the number of fingerprints that are collected given that each AP (receiver) has a limited wireless coverage. For each separation distance D , a new neural network is created and trained. Unlike the first new cooperative approach in [4] that uses separate neural networks, this approach is based on one position estimation made by one neural network.

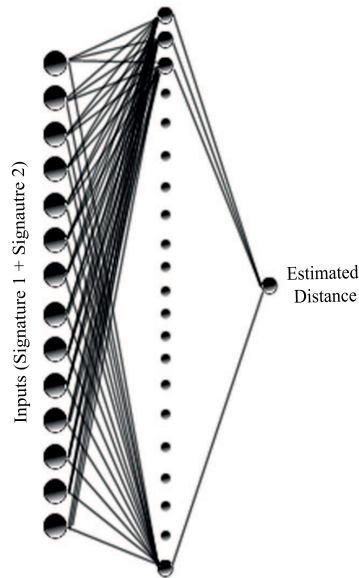


Figure 8.4 – Neural network based on multiple signatures.

8.3 Localization using Tracking in the Time Domain

The major localization systems use the space domain in order to estimate the position of the transmitter. In other words, the reference points or APs that collect the RSS, TOA, AOA, or fingerprints from the transmitted signal at different positions

are fixed in space. In the previous sections, we defined localization using one reference point and a cooperative localization technique using two references in space. Using these systems, the position of the transmitter is estimated regardless of the CIR at its previous positions. Tracking, as studied in the literature, is the algorithm of filtering the trajectory that the mobile unit (i.e., transmitter) follows in order to improve the localization accuracy. Most of these algorithms decrease the positioning error a posteriori by post-processing the estimated results [47], [22], [41]. To the authors' best knowledge, none of the proposed systems integrates a priori tracking within an ANN-based fingerprint matching algorithm for localization. In this section, we will introduce a localization system that properly exploits the time domain where the CIRs of the previous positions play an important role in estimating the new position within the ANN through in-built tracking.

8.3.1 Concept of time domain diversity with tracking

Consider a walking miner who is transmitting wireless signals across the tunnel. One receiver is fixed and set on a time axis in a way that it starts localizing the miner after saving the CIRs from its transmitter up to a certain memory level l . Using one reference in time ($l=1$) is the same as using one reference in space; i.e., one CIR is recorded and the position is estimated for each location separately using the localization technique in sec. 8.2.1 [31] with one receiver only. However, the estimation of the same position would be more accurate if the neural network considers two signatures representing a motion pattern within the limits of the tunnel topology.

In order to estimate the miner's position based on two references in time, a fingerprint should be formed from two CIRs. The first CIR is extracted for the position to be estimated at t_0 while the other CIR is that for the previous position registered in memory at t_{-1} . The speed of motion plays an important role in defining all possible

fingerprints a priori, but it does not vary too much between the two typical stationary and pedestrian speeds in the considered underground mining application. Due to the fact that a miner may come from different directions before reaching a current position, the neural network is trained on chains of all possible fingerprint combinations for each position in a tunnel. Localization using tracking with two memory levels ($l = 2$) exploits temporal diversity in the same way as cooperative localization in [4] does with spatial diversity using two references in space. The accuracy of the neural network (as shown in the following section) increases when increasing the memory level of the system. In this work, we study localization based on tracking using up to five references in time.

Since a miner's movements inside the tunnels of an underground narrow-vein mine are predictable within the confines of its well-mapped galleries due its quasi-curved topology, we are able to add valuable information to our model by creating chains of predictable fingerprint combinations to be fed to the neural network. We assume that a miner may walk to a position from different directions in the tunnel-shaped mine gallery taking into consideration the boundary conditions of the narrow tunnel. Using a time domain motion model, the number of input levels (l) that needs to be considered defines the combinatorial number of possible CIRs from which each fingerprint may be extracted. In the simplest case where $l = 2$, each fingerprint is made up of 14 parameters extracted from two CIRs. The first CIR is that of the position to be estimated at t_0 while the other CIR may be one of the five possible previous positions, as illustrated in Fig. 8.5 and listed in Tab. 8.1. Measurements at either side of a position are included in the generated fingerprint; however, the output of the ANN is selected along the longitude of the tunnel (i.e., the x dimension in Fig. 8.1), the other dimension (i.e., the y dimension in Fig. 8.1) along the narrow tunnel's width being much less significant as a coordinate for localization (but still extremely

useful for its accuracy along the x -axis). The star represents the transmitter at



Figure 8.5 – Possibilities of previous positions for $l = 2$.

t_0 while the filled circles are four possible previous locations at t_{-1} other than the current position (which is also among possible previous positions). For simplicity, motion across diagonals is excluded although our technique can easily take it into account.

Table 8.1 – Fingerprints of each location for $l=2$

Fingerprint	Source of Parameters
1	CIR_{t_0} & CIR_{center}
2	CIR_{t_0} & CIR_{up}
3	CIR_{t_0} & CIR_{down}
4	CIR_{t_0} & CIR_{left}
5	CIR_{t_0} & CIR_{right}

Once l increases, more positions get involved in forming the paths (fingerprints) to the current position of the transmitter. Fig. 8.6 shows the positions that may be considered for creating a path to the current position for $l = 3$. Once again, if the path taken exceeds the boundary conditions of the mine gallery, this path is automatically excluded from being listed as a possible fingerprint. The positions involved in forming the path are highlighted in Fig. 8.6, while the maximum number of fingerprints (N_f) extracted for the miner’s position at level l may be calculated using the following formula:

$$N_f = 5^{(l-1)}.$$

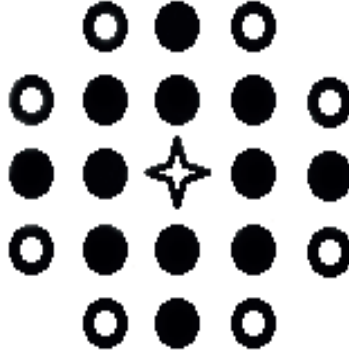


Figure 8.6 – Possibilities of previous positions for $l = 3$.

All possible fingerprints are gathered for all positions in the tunnel after specifying a certain level l ; then the signatures and paths are saved in a database.

8.3.2 ANN structure with time-domain diversity using tracking

The ANN used here is the same feed forward neural network with back propagation learning used in sec. 8.2. The purpose of this choice is to properly compare the results of tracking with the original localization system in [31] and its first extension to spatial diversity (i.e., cooperation) in [4]. Here, the ANN is scalable up to the number of input levels to be used. Since we extract 7 parameters from each CIR signature, adding more signatures in time increases the number of inputs (N_{inputs}) of the neural network such that:

$$N_{inputs} = 7l.$$

The memory level l under study specifies the structure of the neural network used in the positioning system. For $l = 2$, the structure of the ANN is the same as in Fig. 8.4. On the other hand, the number of neurons (N_n) used in the hidden layer is based

on the number of inputs of the neural network:

$$N_n = 2N_{inputs} + 1 = 14l + 1.$$

The output layer contains one neuron which represents the distance in meters to the receiver at time t_0 . The combinatorial number of possible paths increases the combinatorial number of possible chains of CIRs from which the possible fingerprints or input parameters are extracted without necessarily requiring any increase in the number of CIR measurements. As a matter of fact, while keeping the size of measurement data unchanged, the combinatorial exponential increase in the size of the training data (from where stems temporal diversity) overwhelmingly surpasses the linear increase in the number of neurons required to match the corresponding increase in the so-called memory level l . Throughout the training process, 75% of the collected data are classified to train the neural network while 25% are left in order to test the performance of the neural network with data not seen in the training process. Localization using tracking is analyzed up to level 5 (i.e., using as a fingerprint 35 input parameters extracted from 5 CIRs).

8.4 Evaluation Results

The performance of the presented localization techniques is evaluated using the Cumulative Distribution Function (CDF) graph. In CDF graphs, the accuracy of the system is compared to its precision. The x -axis of the CDF is the estimation error which represents the difference between the estimated and the real position measured in meters. The second parameter is the precision or the percentage of occurrences for such an estimation error in the collected data.

8.4.1 Results of cooperative localization in the spatial domain

For the spatial localization approaches, each graph in Fig. 8.7 or 8.8 shows four CDF plots that correspond to the position estimation errors of the different techniques used in sec. 8.2. The first two CDF plots represent the position errors caused by the separate estimations (i.e., cf. sec. 8.2.1) of the first and second receivers, respectively. The third plot represents the result of cooperative localization based on separate estimations (i.e., averaging both estimation errors, cf. sec. 8.2.2). The fourth CDF plot represents the position estimation error of the cooperative neural network technique using one neural network (cf. sec. 8.2.2). At a separation distance (D) of 80 m, the CDF plots of the training and non-training data are shown in Figs. 8.7 and 8.8, respectively. Other plots for different separation distances (D) are

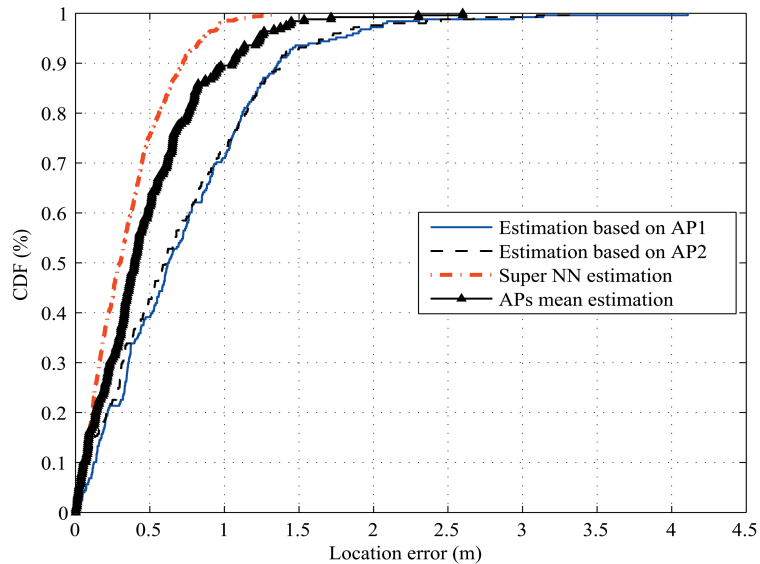


Figure 8.7 – CDF plots of the position estimation errors for the training data at a receivers’ separation distance $D = 80$ m using several localization techniques.

presented in [4]. The accuracy of position estimation using one of the receivers is found to be around 1.2 and 1.5 m for 90% of the training data at different separation

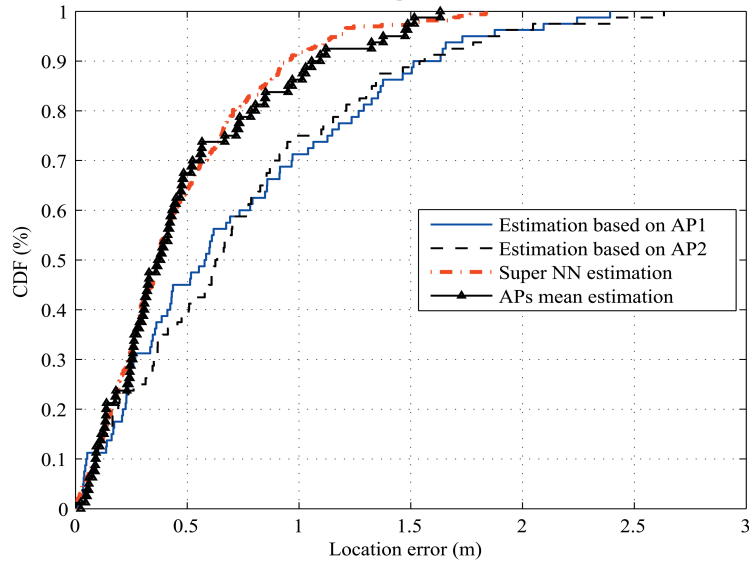


Figure 8.8 – CDF plots of the position estimation errors for the testing data at a receivers’ separation distance $D = 80$ m using several localization techniques.

distances (D). In the non-training set of data, the error varied between 1m and 2 m for 90% of the cases. The accuracy of the cooperative localization method based on averaging the two position errors was recorded to be around 1m and 1.5 m for 90% of the training and testing data, respectively. For the cooperative localization method using one neural network, the position estimation error was recorded to be less than 60 cm and 1m for the training and testing data, respectively.

8.4.2 Results of localization using tracking in the time domain

The CDF plot is used again in order to show the results of localization using tracking at different memory levels. The input level l is the number of signatures a neural network accepts including the fingerprint extracted from the CIR at time t_0 . They are shown for the training and testing data in Figs. 8.9 and 8.10, respectively. For level two, localization using tracking with only one previous CIR shows an estimation error

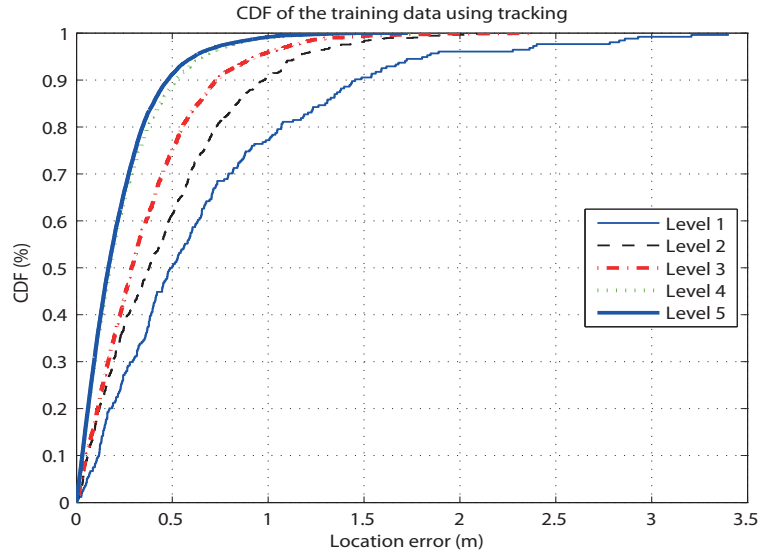


Figure 8.9 – CDF plots for the training data using tracking.

of 1 and 1.25 meters for 90% of training and testing data, respectively. As the input level increases, more paths get involved in the estimation of the current positions. As l increases, the accuracy and precision of the neural network are enhanced forming a better estimation model of the motion principle and the variation of the CIR with respect to distance. At level three, estimation errors of 0.75 and 0.8 meters were recorded for 90% of training and testing samples, respectively. The performance was again improved when adding another previous position to the modeling process, and at level four, the estimation error decreased to 50 cm for 90% of training and testing data. An error of little less than 50 cm was reported at level five clearly suggesting saturation in performance at level 4 beyond which no significant gain is observed. At this level, the input of the neural network is five times larger in size than that of a neural network using one CIR and the number of neurons in the hidden layer is 71.

Both cooperative and tracking localization techniques provide high accuracy of position estimation with high precision. The limitation in space, however, prevents us from decreasing the position estimation errors with more than two APs in a narrow-

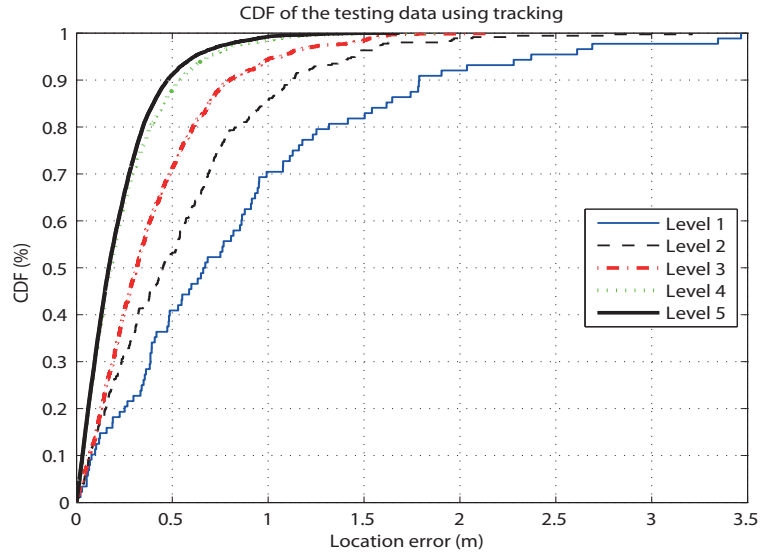


Figure 8.10 – CDF plots for the testing data using tracking.

vein mine tunnel given its quasi-curvilinear topology. On the other hand, due to the flexible scalability of localization using tracking, more inputs are introduced to the neural network resulting in better localization accuracy. At $D = 80$ m, it appears that using cooperative localization has almost the same estimation errors as that of localization using tracking when $l = 3$ and $l = 2$ for the training and testing data, respectively.

8.5 System Design: Complexity vs. Accuracy

The accuracy of the proposed techniques is high compared to simple localization techniques because it uses the CIR as a fingerprint. The major challenge that faces this approach is to extract the CIR at the receivers' end. Being part of a wireless network, each receiver would be capable of transmitting the extracted CIRs to a main server that should handle the process of training the neural network using the separate or cooperative techniques discussed in sections 8.2 and 8.3. The transmitting unit is

supposed to be, in our case, a mini transmitter on the miner’s cap. Since such system works using the fingerprinting technique, collecting multiple fingerprints in different parts of the tunnels is another essential step that builds up the database. Instead of taking measurements manually, collecting the fingerprints in real-time scenarios is easier once the infrastructure is ready i.e. the miners are automatically transmitting signals and the CIRs are collected at a computer server from the receivers.

Since the channel is dynamic, classifying the neural networks based on receivers’ locations and the time of day would be an interesting feature that may lead to better estimation results. The variation of the channel due to human activity may also be adjusted by implementing some fixed transmitters along the galleries for calibration purposes.

Considering a system that uses tracking alone does not create a global localization system in underground mines because it uses one localizing unit as in [31]. The question arises as to whether we are capable of integrating the tracking system in a cooperative neural network technique where two references in space localize using the tracking algorithm and then a final estimation is drawn using one of the two cooperative neural network topologies discussed in sec. 8.2. An ongoing study investigates whether integrating the tracking technique at a given memory level l in a cooperative spatial localizing system (i.e., diversity both in space and time) would lead to higher performances that could match those of tracking alone with higher memory levels l (i.e., only time diversity).

8.6 Conclusion

This article presented a new localization approach that exploits time diversity for radio-localization in tunnel-shaped underground narrow-vein mines. With an in-built tracking algorithm, this technique uses ANNs to localize a transmitter based on

fingerprints extracted from chains of CIRs recorded in time. The proposed system is able to estimate the position of a wireless transmitter in narrow tunnels with high accuracy and precision of 50 cm for 90% of both training and testing data. Compared to cooperative localization in the spatial domain, geo-location using tracking is more accurate and precise with much more flexible scalability. The question of whether this system may be integrated in a cooperative localization technique that exploits spatial diversity is currently under investigation. Although this work was conducted for an underground environment such as mines, localization using tracking may be used in different indoor/outdoor environments. The proposed system may also use different wireless technologies such as UWB, WLAN, or mobile radio.

Chapter 9

Cooperative Geo-location in Underground Mines: A Novel Fingerprint Positioning Technique Exploiting Spatio-Temporal Diversity

Authors: Shehadi Dayekh, Sofène Affes, Nahi Kandil and Chahé Nerguizian.

Contribution: The primary author is the main contributor and editor of this work.

Conference: IEEE Symposium on Personal, Indoor, Mobile and Radio Communications.

Status: Article published on September 14th, 2011.

Abstract

Underground narrow-vein mines result in complex indoor scenarios which require sophisticated localization techniques to maintain basic security measures. While some traditional localization systems use the triangulation techniques for outdoor channels, fingerprint positioning techniques are mostly used in more complex indoor environments like mines. One of the techniques exploited in the quasi-curvilinear topology of underground mines is the Channel Impulse Response (CIR) based fingerprint positioning combined with Artificial Neural Networks (ANNs). This article innovates a CIR-based positioning technique within a cooperative memory-assisted approach that exploits both the temporal (from different time instances) and spatial (from different space positions) diversities of the collected fingerprints. Introducing memory-type signatures in a cooperative localization technique within the spatial confinements of the tunnel-shaped narrow-vein mines significantly increases the accuracy, precision and robustness of the localization system. The cooperative memory-assisted technique is capable of localizing a transmitter with an accuracy of less than 25 cm 90% of the time.

Keywords. Indoor localization, channel impulse response, artificial neural network, fingerprinting technique, cooperative localization, tracking, spatial diversity, temporal diversity.

9.1 Introduction

Chile August 2010, the mine collapsed and many miners were trapped. It took the rescue team 69 days to find the first miner, and 10 weeks to rescue the rest [33]. Localizing miners/equipments in underground and confined areas is not a feature added for luxury, but an essential basis for the well-known principle of the mining industry, "Safety First". However, the special nature of narrow-vein mines' topology which is made of interconnected tunnels challenges any localization system expected to precisely estimate the location of miners underground. Like most wireless localization systems, the distance to the transmitter is estimated based on the received signals' characteristics after being affected by the channel. In underground narrow-vein mines, wireless signals propagate within humid rough surfaces and non-line of sight (NLOS) branching tunnels forming complex multipath components. The received signals' components such as the Received Signal's Strength (RSS), Angle of Arrival (AOA), Time of Arrival (TOA) and Time Difference of Arrival (TDOA) are altered once multipath reception takes place. And since most traditional localization systems use one or more of the mentioned parameters (i.e., RSS, AOA, etc ...) to localize [10] [29] [23] [12] [9], they fail once deployed in underground narrow-vein mines. Another challenge present in narrow-vein mines is the spatial confinement of the interconnected quasi-curvilinear tunnels which prevents a 2D-meshed deployment of localizing units or access points (APs) to further increase the accuracy and precision of underground geo-location.

A search for an alternative led to the innovation of a localization technique that uses artificial neural networks (ANNs) and fingerprints collected from the channel's impulse responses (CIRs) [31]. The system accurately estimates the distance to a transmitter using one receiver only (i.e., solitary localization) with an estimation error of less than 2 meters for 90% of the collected measurements. Since wireless coverage

requires more than one AP in the confinement of narrow-vein mines, the use of another localizing unit introduces geolocation as a cooperative technique that exploits the spatial diversity of the collected fingerprints. The cooperative memoryless localization technique using two receivers later proposed in [4] reduces the location error to less than 1m for 90% of the data making use of two spatially distinct fingerprints to better estimate the user's location. It also introduces two ANN structures that exploit these two fingerprints separately or jointly to better estimate cooperatively the position of the miner in underground narrow-vein mines.

The spatial confinement of the tunnel-shaped topology of narrow-vein mines facilitates the prediction of the patterns of motion. In other words, training ANNs on different motion patterns collected at short time instances enriches the set of fingerprints corresponding to the transmitter's positions. In some localization techniques [47] [22] [41], tracking is a process that follows estimating the position of the users (i.e., post-processing the results). Few are the techniques that implement a priori tracking within an ANN-based localization system. Enhancing the accuracy within this spatial confinement is possible once the system exploits the temporal diversity of the collected fingerprints over short periods of time, a concept proven more recently to be right and promising in [6]. Using one localizing unit, the technique in [6] takes advantage of the limited motion patterns (i.e., spatial confinement) to create a rich database used for fingerprint positioning. The memory-assisted system in [6] targets position accuracies of less than 40 cm for 90% of the collected fingerprints. Yet, the localization system in [6] which exploits the temporal diversity of the collected fingerprints uses one localization unit only, which means that it can be further enhanced once introduced in a cooperative memory-assisted technique that exploits both the spatial and temporal diversities of the signatures.

This article introduces a cooperative memory-assisted localization technique that

exploits both the spatial and temporal diversities of the assembled signatures. The power of a spatio-temporal fingerprint is in its ability to project the signal on two spatially separated receivers with an additional projection in time (i.e., by introducing memory). ANNs are trained to localize all different scenarios of motion in a cooperative localization technique that takes into account the signatures of two APs. The next section highlights different CIR-based fingerprint positioning techniques that use ANNs to localize. The cooperative memoryless (i.e., exploiting the spatial diversity only) [4] and the memory-assisted (i.e., using the temporal diversity only) [6] localization techniques are briefly summarized. In section 9.3, the cooperative memory-assisted localization technique that exploits both the spatial and temporal diversities is introduced. Simulation results are reported and discussed in section 9.4. Conclusions are drawn out in section 9.5.

9.2 Localization in Mines Using CIR-based Fingerprinting and ANNs

The fingerprinting or scene analysis technique is used in scenarios where the channels cannot be easily modeled due to the severe distortion that signals encounter on their way to the receiver. Fingerprint positioning is based on extracting some of the parameters of the received signals (i.e., RSSs, AOAs, etc ...) at different distances and saving them in a database. Different matching algorithms such as probabilistic methods, k-nearest neighbour (kNN), support vector machine (SVM) or ANNs are then used in real-time scenarios to localize [27] [39]. These algorithms try to match the collected fingerprint to the saved measurements in order to estimate the distance to the transmitter. In underground narrow-vein mines, localization based on RSS, AOA, or TDOA is neither accurate nor precise [31] [42] [4]. Increasing the accuracy

of position estimation in confined areas requires deploying more APs to overcome the multipath components and the signals' fluctuation effects. Another approach to accurate positioning innovated in [31] uses seven parameters extracted from the CIR of the received signal to form a fingerprint. The parameters are the mean excess delay ($\bar{\tau}$), the root mean square (τ_{rms}), the maximum excess delay (τ_{max}), the total power of the received signal (P), the number of multipath components (N), the power of the first arrival (P_1) and the delay of the first path component (τ_1). A fingerprint is denoted by $f = (\bar{\tau}, \tau_{rms}, \tau_{max}, P, N, P_1, \tau_1)$ and it corresponds to a distance d . Due to the narrow quasi-curvilinear topology of underground tunnels and for simplicity, the distance to the transmitter d is taken along the x-axis only neglecting the small variation along the tunnels' confined width (i.e., y-axis). It is also a way to ensure that the localization system takes into account the fluctuations of wireless signals for the same position (i.e. more than one fingerprint f may represent the same separation distance d). A measurement campaign at a carrier frequency of 2.4 GHz was carried out in CANMET mine in Val d'Or Canada where the fingerprints were extracted along with their corresponding distances for 480 positions as illustrated in Fig. 9.1. It should be noted that the distance between the consecutive measurement points along the x-axis is one meter. Mapping the set of fingerprints $S = \{f_1, f_2, f_3, \dots, f_n\}$

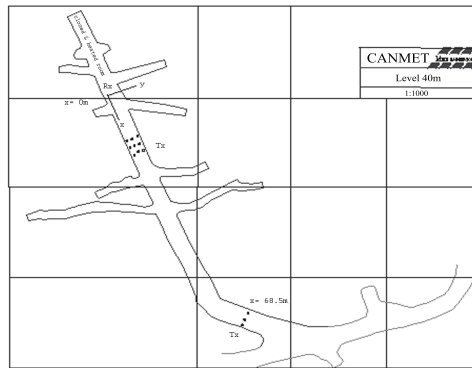


Figure 9.1 – Map of the underground tunnels.

to the corresponding set of distances $D = \{d_1, d_2, d_3, \dots, d_n\}$ is successfully achieved using ANNs. The measurements conducted in [31] for the stationary positions along the tunnel as shown in Fig. 9.1 are used to simulate memory-type fingerprints. For more technical information about the experimental setup, please refer to [31].

ANNs are defined as computational models capable of approximating a function. They are capable of performing non linear regressions which make them suitable for localization in harsh environments [31] [1] [20]. The power of ANNs is that they are relatively simpler than traditional estimation techniques such as Kalman filters especially when modeling a non-linear function which is, in our case, of order 7 (i.e., seven parameters as inputs). An MLP feed-forward ANN with a back-propagation learning algorithm is proven effective for underground geo-positioning [31] [42] [4] [6]. During the learning phase, the neural network is given the training data that corresponds to 75% of the collected measurements. Then, in the testing phase, ANNs are tested using 25% of the fingerprints which are not seen in the training phase.

The solitary memoryless localization system used in [31] estimates the distance to the transmitter instantaneously based on fingerprints extracted from the CIR of the received wireless signals. As shown in Fig. 9.2, this technique accurately localizes

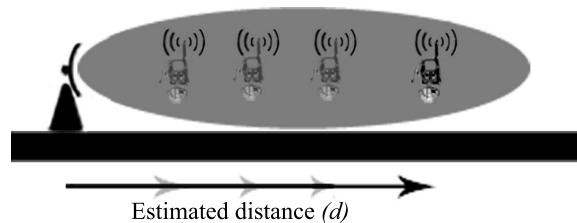


Figure 9.2 – Solitary localization using one receiver.

based on the input of one localizing unit (i.e., one receiver or AP). A simple neural network with 7 input neurons, one hidden layer provides the transmitter’s distance with an approximate accuracy of less than 2 m for 90% and 80% of the training and

testing data, respectively.

9.2.1 Cooperative memoryless localization using spatial diversity

A global localization system requires the participation of multiple APs in estimating the transmitter's location within the quasi-curvilinear topology of underground narrow-vein mines. However, only the two nearest APs found at either end of any given section of a mine tunnel are needed to guarantee its wireless coverage. The cooperative memoryless localization system in [4] exploits spatial diversity taking advantage of the implemented APs to collect different fingerprints. As shown in

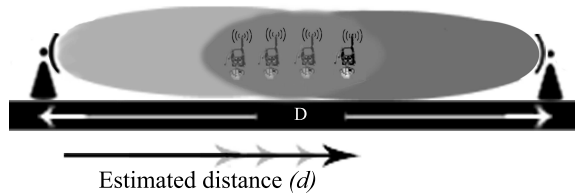


Figure 9.3 – Cooperative localization using two receivers.

Fig. 9.3, the use of two APs within the spatial confinement of the tunnels not only enhances the accuracy of the estimated distance, but also provides correct positioning inside the quasi-curvilinear interconnected tunnels. In the cooperative approach, the sets of fingerprints $S^{R_1} = \{f_1, f_2, f_3, \dots, f_m\}$ and $S^{R_2} = \{f'_1, f'_2, f'_3, \dots, f'_m\}$ are collected from receivers R_1 and R_2 , respectively. Two different ANN architectures are presented in [4] and both accurately estimate the position of the transmitter. One of the ANN designs is shown in Fig. 9.4 where the set of fingerprints $S = \{F_1, F_2, F_3, \dots, F_m\} = \{(f_1, f'_1), (f_2, f'_2), (f_3, f'_3), \dots, (f_m, f'_m)\}$ is the concatena-

tion of both observations, S^{R_1} and S^{R_2} . The output of the ANN is the estimated distance to one of the transmitters $D = \{d_1, d_2, d_3, \dots, d_m\}$. The exploitation of the

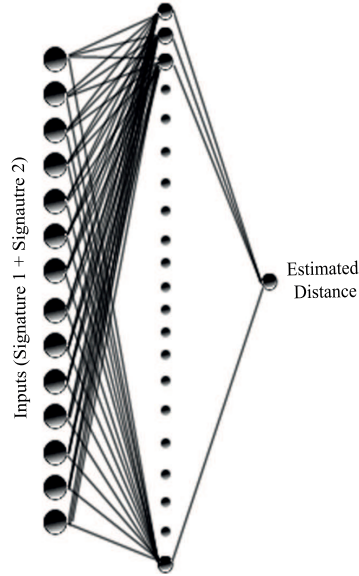


Figure 9.4 – Neural network based on multiple signatures.

spatial diversity of the collected fingerprints introduced a cooperative version of the CIR-based fingerprint positioning technique in [31] for underground geolocation and hence significantly increased its accuracy, precision and reliability.

9.2.2 Solitary memory-assisted localization using temporal diversity

The accuracy of the cooperative memoryless technique discussed in Sec. 9.2.1 may only be enhanced by increasing the number of APs which is not practical given the spatial confinement of narrow-shaped tunnels. However, the narrow curvilinear topology is an advantage because it facilitates the prediction of the user’s motion patterns. The memory-assisted localization technique in [6] utilizes the narrow-shaped topology to introduce an in-built tracking model that exploits the temporal diversity of the recorded fingerprints. The path fingerprint $f_i^j = (f_{i_{t_0}}, f_{i_{t-1}}, f_{i_{t-2}}, \dots, f_{i_{t-(l-1)}})$

represents a concatenation of the fingerprints recorded in time while moving towards a destination to be estimated (i.e., at a distance d_i). More than one path can lead to the same position to be estimated, i.e., more than one path fingerprint f_i^j correspond to the same distance d_i . While l represents the number of concatenated fingerprints or the so called memory level in [6], j is simply an index number that counts the number of possible tracks to a desired destination at a given memory level l . The terms memory level l and time depth are used interchangeably in the article and they represent the number of concatenated memory-type sub-fingerprints that constitute the temporal fingerprint for a given position at distance d_i away from R_1 . The maximum number of path fingerprints j_{max} for a given position is limited by the upper bound N_{f_p} :

$$j_{max} \leq N_{f_p} = 5^{(l-1)}.$$

Since each fingerprint contains 7 parameters, the length of the temporal fingerprint defines the number of inputs of the ANN and it is given by:

$$N_{inputs} = 7l.$$

The design of the ANN depends on l because the number of neurons in the input layer is equal to the length of the path fingerprint N_{inputs} . The number of neurons in the hidden layer is $N_n = 2N_{inputs} + 1$ for all architectures and the output is the distance to the transmitter. Figure 9.5 illustrates a simple fingerprint allocation for



Figure 9.5 – Possibilities of previous positions for $l = 2$.

one position when $l = 2$. The star represents the current position of a transmitter located at a distance d_i to be localized showing the previous possible positions ¹. While respecting the spatial boundary limits of the tunnels, any previous position is selected to create the potential path fingerprints. The length of the combinatorial set of fingerprints for the same position is dependent on l and the geometry of the narrow tunnels. In this example, the combinatorial subset of possible fingerprints collected from a transmitter located at d_i (i.e., star position) within the total set $S = \{S_1, \dots, S_i, \dots, S_m\}$ over all distances D is:

$$S_i = \{F_i^1, F_i^2, F_i^3, F_i^4, F_i^5\}.$$

where,

$$F_i^1 = (f_i, f_i),$$

$$F_i^2 = (f_i, f_{i_{north}}),$$

$$F_i^3 = (f_i, f_{i_{south}}),$$

$$F_i^4 = (f_i, f_{i_{west}}),$$

$$F_i^5 = (f_i, f_{i_{east}}).$$

are all the possible path fingerprints reaching the star position when $l = 2$. The exponential increase in the number of fingerprints N_{fp} due to the linear increase of temporal memorization level l overwhelmingly enriches the information given to ANNs about each position inside the tunnels from the same original set of data measurements.

Speed plays a significant role in defining the sampling time interval that precedes

¹Motion across the diagonals is excluded because it exponentially increases the combinatorial set of path fingerprints without a significant gain.

the collection of the memory-type fingerprints. In order to allow the same trained ANN to accurately localize a transmitter regardless of its limited speed in the confinement of narrow-vein mines, the sampling time at which the sub-fingerprints are collected should be adjusted accordingly. In other words, sampling time is set to allow the extraction of sub-fingerprints measured at any two positions (separated by the distance covered by the transmitter in motion at a velocity below or equal to a given maximum speed) that is shorter than the grid resolution times the memory level or time depth.

Introducing temporal diversity and in-built tracking to the CIR-based fingerprinting technique in [6] outperforms the localization system in [4] in terms of accuracy, precision and scalability within the narrow quasi-curvilinear topology of mine tunnels. However, solitary localization using temporal diversity alone does not benefit from the possible cooperation between multiple localizing units (having each an overlapping radio footprint with their two nearest adjacent neighbors) required anyway for proper coverage of the whole mine galleries and, additionally, it cannot resolve the location ambiguity arising from the presence of tunnel junctions. On the other hand, as shown in the following, the collaboration of memory-assisted localizing units (i.e., spatio-temporal diversity) with lower memory levels allows significant reduction of the complexity encountered when using solitary memory-assisted localization performing at higher time depths while offering better accuracy.

9.3 Cooperative Memory-Assisted Localization Exploiting Spatio-Temporal Diversities

Based on a combination of the two previous solutions, an even more intelligent localizing system integrates the in-built tracking technique at a given memory level l

in a cooperative spatial localizing system (i.e., spatio-temporal diversity). This leads to higher performances that could match those of memory-assisted localization alone at higher memory levels l (i.e., only time diversity). Mixing both spatial and temporal diversities is a technique that further enriches the information given to ANNs resulting in a better mapping of the limited motion patterns in narrow quasi-curvilinear tunnels.

This work innovates a localization system that uses the memory capability (i.e., in-built tracking) cooperatively between two spatially-separated localizing units before estimating the position of the transmitter. Within the spatial confinement of the tunnels and over short periods of time, the signatures recorded at consecutive time instances and collected from two spatially-separated receivers guarantee less-fluctuating spatio-temporal fingerprints. Unlike the system introduced in [6] which exploits the temporal diversity of a solitary receiver, this approach creates chains of path fingerprints from two nodes before training the ANNs. The scalability of the system allows the ANNs to be trained to localize at different separation distances D and memory levels l . The subset of path fingerprints $S_i^{R_1} = \{F_i^{R_1,1}, F_i^{R_1,2}, F_i^{R_1,3}, \dots, F_i^{R_1,j_{max}}\}$ collected from R_1 at a distance d_1 is properly combined path-wise with the other subset $S_i^{R_2} = \{F_i^{R_2,1}, F_i^{R_2,2}, F_i^{R_2,3}, \dots, F_i^{R_2,j_{max}}\}$ gathered from R_2 at a distance $d_2 = D - d_1$ to form the spatio-temporal group of path fingerprints:

$$S_i = \left\{ (F_i^{R_1,1}, F_i^{R_2,1}), (F_i^{R_1,2}, F_i^{R_2,2}), (F_i^{R_1,3}, F_i^{R_2,3}), \dots, (F_i^{R_1,j_{max}}, F_i^{R_2,j_{max}}) \right\}.$$

As discussed earlier in Sec. 9.2.2, the length of the temporal fingerprint is dependent on the memory level l of the solitary receiver where localization is taking place. If we consider two spatially separated APs each collecting fingerprints at different time depths, we may create different scenarios denoted by (l_1, l_2) corresponding to receivers

(R_1, R_2) respectively. For example, localizing a transmitter at a distance d_i and time instant t_0 with memory levels $(l_1 = 2, l_2 = 1)$ is achieved by matching the measured spatio-temporal fingerprint $F_i = (F_i^{R_1}, F_i^{R_2})$ where

$$F_i^{R_1} = (f_{i_{t_0}}^{R_1}, f_{i_{t_{-1}}}^{R_1}),$$

$$F_i^{R_2} = (f_{i_{t_0}}^{R_2}).$$

For $(l_1 = 2, l_2 = 1)$, R_2 provides a fingerprint $F_i^{R_2}$ of length 7 (i.e., memoryless fingerprint) while the fingerprint $F_i^{R_1}$ collected from receiver R_1 is the concatenation of two fingerprints recorded at the time instances t_0 and t_{-1} (i.e., memory-assisted fingerprint of length 14). Concatenating two fingerprints from two spatially separated receivers where at least one is introducing memory creates a spatio-temporal fingerprint for a given position. The length of the spatio-temporal fingerprint defines again the number of inputs N_{inputs} of the ANN and it is dependent on both l_1 and l_2 where:

$$N_{inputs} = 7(l_1 + l_2).$$

9.4 Performance Results

The results of the localization techniques are presented using the Cumulative Density Function (CDF). CDF plots show the accuracy of the positioning technique (i.e., position error in meters) for a given percentage of the treated data. As mentioned earlier and shown in the following graphs, 75% of the collected fingerprints are trained by the ANN whereas 25% are left for testing the generalization of the ANN of any technique. These results are plotted in Figs. 9.6 and 9.7 and summarized in Tab. 9.1.

The performance results of the spatio-temporal fingerprint positioning technique

are compared to the localization technique that uses either spatial or temporal diversity alone. The memory levels of receivers R_1 and R_2 are denoted by l_1 and l_2 , respectively. If one of the receivers is not participating in the localization process (i.e., solitary localization), its memory level is presented as $l = 0$. On the other hand, memoryless localizing units use one fingerprint to localize (i.e., $l = 1$) without the need of fingerprint concatenation. When the memory level is set to $l > 1$, the localizing unit would be concatenating fingerprints in short time instances before feeding them to the ANN. The notation (l_1, l_2) shows the different memory levels at which both receivers are performing their fingerprint allocation. Both observations from R_1 and R_2 are concatenated again and fed to a cooperative ANN that estimates the position of the transmitter.

Merging the temporal path fingerprints of two spatially different receivers and feeding them as one concatenated spatio-temporal fingerprint to one ANN is a breakthrough in the fingerprint positioning techniques (i.e., cooperative memory-assisted technique). The results of spatio-temporal localization are compared to the techniques discussed in 9.2 and presented in Figs. 9.6 and 9.7 for the training and testing data, respectively. These results clearly show the increased accuracy of spatial and temporal combination in the CIR-based localization approach.

Cooperative memory-assisted localization is a result of the collaboration of the receivers when at least one of them is introducing memory (i.e., producing path fingerprints). In the first cooperative memory-assisted approach, R_2 is kept at a memory level $l_2 = 1$ (i.e., without memory) while R_1 's memory level varies (i.e., $l_2 = 2, 3$). In memory-assisted techniques, it is noticed that the cooperative approach that adds spatial diversity to the fingerprints performs better than the solitary technique even when the length of the fingerprints is the same. For example, solo memory-assisted

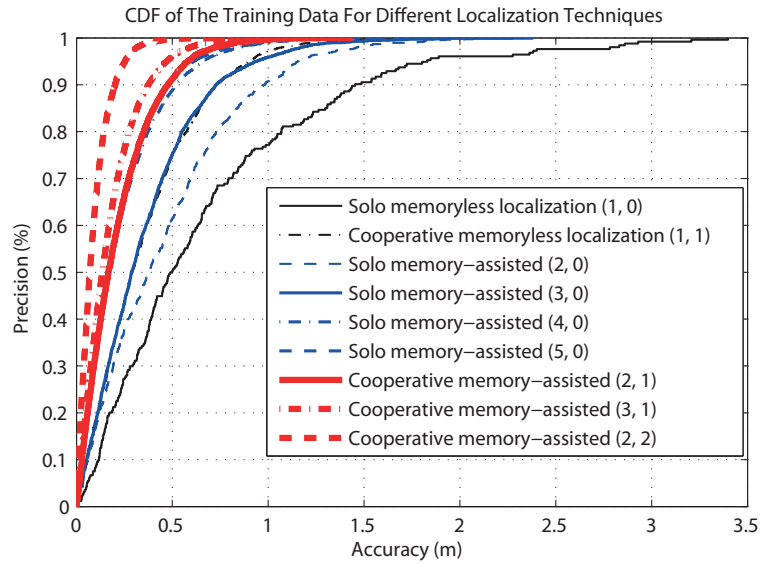


Figure 9.6 – CDF of the training data for different localization techniques at memory levels (l_1, l_2) .

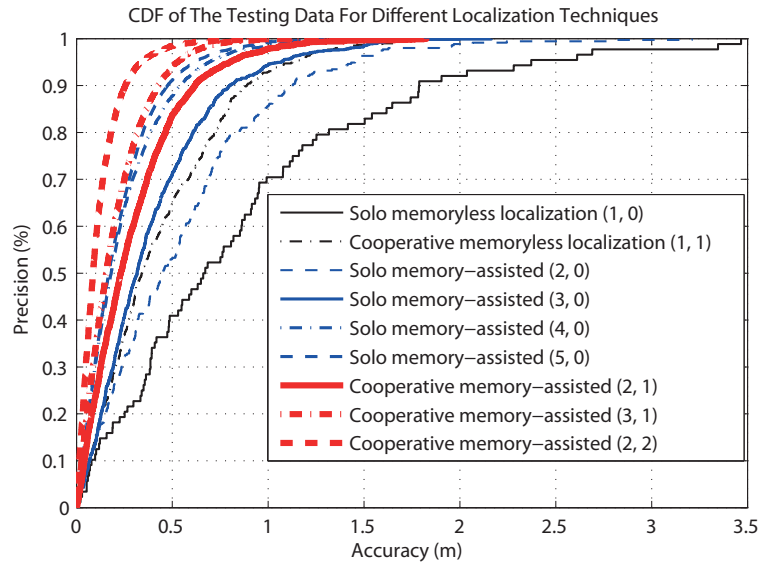


Figure 9.7 – CDF of the testing data for different localization techniques at memory levels (l_1, l_2) .

localization at $(l_1 = 3, l_2 = 0)$ is less accurate than cooperative memory-assisted localization at $(l_1 = 2, l_2 = 1)$ even though both path fingerprints are of length 21. In addition to that, when $(l_1 = 3, l_2 = 1)$, merging spatial and temporal information further increases the location accuracy to values less than 40 cm surpassing the upper limit of solitary memory-assisted localization when $(l_1 = 5, l_2 = 0)$.

In the second cooperative memory-assisted approach, both receivers use in-built tracking or memory to form their fingerprints. Surprisingly, a one step increase in the memory level of R_2 creates uniform spatio-temporal fingerprints where two references in time are taken from two receivers in space. As shown in Figs. 9.6 and 9.7, location accuracy of the last curve drops to 20 cm and 25 cm for 90% of the training and testing data, respectively. It may be seen that the accuracy of a 2-by-2 spatio-temporal localization system [i.e., $(l_1 = 2, l_2 = 2)$] is double the accuracy of a 1-by-1 cooperative spatial system [i.e., $(l_1 = 1, l_2 = 1)$].

Table 9.1 – Estimation errors of different localization techniques

Localization Technique with 90% Precision		<i>Training Errors (m)</i>	<i>Testing Errors (m)</i>
Spatial localization using one receiver [31]		1.5	2
Cooperative spatial localization based on separate ANNs [4]		1	1
Cooperative spatial localization based on one super ANN [4]		0.6	1
Solo memory-assisted localization [6]	$(l_1 = 2, l_2 = 0)$	1	1.25
	$(l_1 = 3, l_2 = 0)$	0.75	0.8
	$(l_1 = 4, l_2 = 0)$	0.5	0.5
	$(l_1 = 5, l_2 = 0)$	<0.5	<0.5
Cooperative memory-assisted localization	$(l_1 = 2, l_2 = 1)$	0.48	0.62
	$(l_1 = 3, l_2 = 1)$	0.38	0.43
	$(l_1 = 2, l_2 = 2)$	0.20	0.25

As shown by the results above, cooperative memory-assisted localization outperforms other memoryless/memory-assisted localization techniques even at lower memory levels or time depths. An optimum solution would uniformly exploit spatial-

temporal (i.e., $l_1 = l_2 > 1$) to overcome the spatial confinement of the environment and significantly utilize the limited motion patterns inside the quasi-curvilinear tunnels. The spatio-temporal localization technique localizes with high accuracy, precision and scalability.

9.5 Conclusion

This article investigated the CIR-based localization techniques and innovated the spatio-temporal fingerprint positioning technique that uses ANNs. The concept of localization using the spatio-temporal diversity in underground narrow-vein mines is satisfied when fingerprints are recorded at short time periods and collected from two spatially separated receivers. This cooperative memory-assisted localization system (i.e., 2-by-2) is able to attain higher accuracies at lower memory levels using ANNs. The estimation error is reduced to 20 cm and 25 cm for 90% of the training and testing fingerprints, respectively. The proposed system is feasible given that its complexity is still affordable, and that it could be integrated into different wireless technologies.

Chapter 10

Smart Spatio-Temporal Fingerprinting for Cooperative ANN-based Wireless Localization in Underground Narrow-Vein Mines

Authors: Shehadi Dayekh, Sofène Affes, Nahi Kandil and Chahé Nerguizian.

Contribution: The primary author is the main contributor and editor of this work.

Conference: 4th International Symposium on Applied Sciences and Biomedical and Communication Technologies.

Status: Invited paper published on October 29th, 2011.

Abstract

One of the main concerns in the mining industry is ensuring the safety and security of miners and their equipment. Being aware of the real-time position of personnel in such harsh environments within a special quasi-curvilinear topology is challenging and requires a sophisticated localization system. While traditional triangulation techniques fail to accurately localize in such indoor scenarios, new approaches that rely on fingerprints extracted from the Channel Impulse Response (CIR) succeed to localize with high accuracy using Artificial Neural Networks (ANNs) for fingerprint-location matching. Signatures collected from different locations in space, at different instances in time, are concatenated to form spatio-temporal fingerprints for improved localization accuracy. In this paper, we overview these novel and very promising localization techniques then investigate the impact of the spatial sampling grid's resolution in fingerprint collection on their accuracy in underground narrow-vein mines. We show by simulations that the significant accuracy gains reaped from the new exploitation of spatio-temporal diversity, if not needed in some applications, can be alternatively traded for remarkable and extremely useful cost reductions in the fingerprint collection step.

Keywords. Indoor localization, channel impulse response, artificial neural network, fingerprinting, cooperative localization, tracking, spatial diversity, temporal diversity.

10.1 Introduction

Wireless localization systems are widespread in the modern world. While some location-based services are used for entertainment, other services such as the Global Positioning System (GPS) are becoming essential necessities for daily life applications. On the other hand, positioning services are demanded by industries for enhanced security measures such as localizing miners underground. The importance of an underground localization system reveals itself in incidents such as the one that happened in Chile in 2010 where miners were trapped more than 69 days underground [33]. A localization system built in the tunnel-shaped topology of the narrow-vein mine definitely simplifies the process of locating the miners and their equipment prior/after any accident. So what makes it hard to deploy?

First, narrow-vein mines are made up of humid rough surfaces that create adverse channel responses to wireless transmitted signals. Indeed, the geological nature of this tough environment causes severe reflections, refractions and non line of sight (NLOS) propagation, thereby making channel modeling and characterization more complex. Therefore, traditional localization techniques fail to accurately estimate the position of transmitters because many of these techniques would rely on conventional channel parameters such as the Received Signal Strength (RSS), Angle of Arrival (AOA), Time of Arrival (TOA) and/or Time Difference of Arrival (TDOA) [10] [29] [9]. Indeed, the tunnels in underground narrow-vein mines constitute a quasi-curvilinear topology which is nearly 1D. Even the y -dimension across the tunnels' width is less significant since it ranges mostly between 1 to 3 meters. In this quasi-curvilinear topology, using the AOA does not reveal the exact direction of arrival because of the numerous reflections that take place in the confinement of the tunnels and their curvatures. For similar reasons, the TOA does not reflect the shortest path to the transmitter [31] [42]. Besides, in cases where junctions exist, estimating the dis-

tance to the transmitter is not enough due to the NLOS propagation which makes cooperative localization techniques more desirable.

The challenges summarized above elevate the complexity level of a localization system expected to perform effectively in the confinement of mine galleries. Introducing ANN-based fingerprint-position matching for wireless localization that is fed by a set of useful parameters extracted from the CIR as an input signature is proven to perform accurately in narrow-vein mines [31] [42]. This novel concept was recently extended to exploit spatial diversity [4], temporal diversity [6], or both [5] for increased accuracy.

In this paper, we overview these novel and very promising localization techniques then investigate the impact of the spatial sampling grid’s resolution for fingerprint collection on their accuracy in underground narrow-vein mines. Simulations suggest that the significant accuracy gains reaped from the new exploitation of spatio-temporal diversity, if not needed in some applications, can be alternatively traded for remarkable and extremely useful cost reductions in the fingerprint collection step. As one example, the cooperative version [4] that exploits a two-branch spatial diversity attains the same accuracy (of 1.5 m at 90% precision) of the original version [31] using for training only 50% of the collected fingerprints stemming from a sampling grid with half the resolution of the original one.

In Sec. 10.2, we briefly describe the original measurement campaign conducted for fingerprint collection [31]. In Sec. 10.3, we overview the novel ANN-based localization techniques and the ways spatial and temporal diversities are exploited in the spatio-temporal fingerprints. In Sec. 10.4, both the solitary [31] and cooperative memoryless [4] localization techniques are, as two representative examples, challenged by lower spatial sampling grid resolutions in the fingerprint collection step to illustrate how accuracy gains can be traded for lower fingerprinting costs. Conclusions are

finally drawn out in Sec. 10.5.

10.2 Measurement Campaign for CIR-BASED Fingerprinting

Measurement campaigns are unavoidable with any fingerprint-based localization technique. Fingerprint-based positioning systems mainly rely on the collected measurements to create the ground rules of the localization algorithms. In other words, localization using the fingerprinting technique is a way of mapping the received wireless signals (i.e., fingerprints) taken at specific locations to the transmitter's position (i.e., distance from the receiver). The grid resolution of the measurement campaign plays an important role in the accuracy of the localization technique. Increasing the grid resolution to improve localization accuracy is time consuming and is not recommended. Therefore, the spatial sampling grid resolution should be optimized to guarantee accuracy without increasing the cost incurred from collecting numerous measurements. We will show here how smart spatio-temporal fingerprinting that exploits both spatial and temporal diversities allows, among numerous benefits, conducting lower-cost measurement campaigns over lower-resolution grids while maintaining accuracy.

A measurement campaign was conducted in CANMET gold mine in Val d'Or Quebec from which a new approach to CIR-based localization was introduced in [31]. A total of 480 measurements were taken in a tunnel as shown in Fig. 10.1. The original grid resolution is set to 1 meter increment per x -position while respecting the boundary conditions of the tunnels. For each position, seven parameters are extracted to form a fingerprint. These parameters are the mean excess delay ($\bar{\tau}$), the root mean square (τ_{rms}), the maximum excess delay (τ_{max}), the total power of the

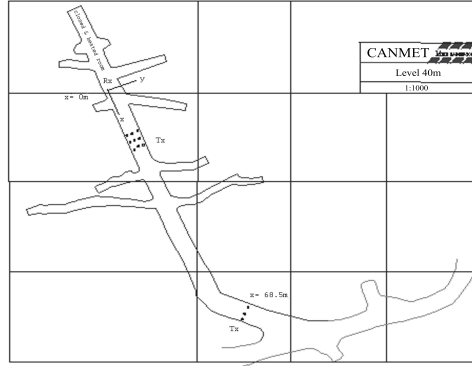


Figure 10.1 – Map of the underground tunnels.

received signal (P), the number of multipath components (N), the power of the first arrival (P_1) and the delay of the first path component (τ_1). Throughout this article, a fingerprint is denoted by $f = (\bar{\tau}, \tau_{rms}, \tau_{max}, P, N, P_1, \tau_1)$ and it corresponds to a transmitter at a distance d away from the localizing unit or receiver R . Given the quasi-curvilinear topology of narrow-vein mines, the variation along the y -position is considered insignificant (i.e., the x -position is taken as the total distance d). However, the fingerprints are taken for all y -positions to simulate the fact that signals fluctuate for the same x -position.

10.3 Overview of ANN-Based Localization Techniques using Fingerprinting

10.3.1 Original technique

Matching the set of fingerprints $S = \{f_1, f_2, f_3, \dots, f_n\}$ to the corresponding set of distances $D = \{d_1, d_2, d_3, \dots, d_n\}$ is performed using Artificial Neural Networks (ANNs). With their ability to perform complex calculations of nonlinear functions,

ANNs are easy to train and operate and they estimate the transmitter’s position instantaneously and accurately. In case where only one receiver is present as shown in Fig. 10.2, the input layer of the ANN is composed of 7 neurons that correspond to the length of each fingerprint in S . The output layer is made of one neuron representing the output distances in D matching the input fingerprints in S .

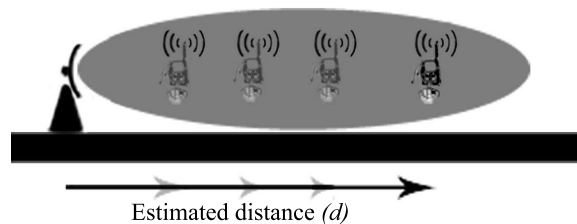


Figure 10.2 – Solitary localization using one receiver.

The ANN is trained to estimate 75% of the collected fingerprints then the remaining 25% of the fingerprints are tested to validate the generalization performance of the trained ANN. The use of MultiLayer Perceptron (MLP) ANN with back propagation learning algorithm gives more accurate and precise results for underground localization [31] [42].

10.3.2 Exploiting spatial diversity

Even though the original technique in [31] was a breakthrough in localization systems for underground and confined areas, recently it was further enhanced in [4] to exploit the spatial diversity of the collected fingerprints. By using the principle of cooperation between multiple Access Points (APs), the cooperative localization technique proved that concatenating more than one fingerprint collected from different locations enriches the information about the exact position of the transmitter. As shown in Fig. 10.3, the transmitter’s position is estimated even in the presence of junctions, interconnected tunnels and NLOS scenarios. Cooperative memoryless

localization in [4] only relies on the spatial diversity of the collected set of fingerprints $S^{R_1} = \{f_1, f_2, f_3, \dots, f_m\}$ and $S^{R_2} = \{f'_1, f'_2, f'_3, \dots, f'_m\}$ measured at receivers R_1 and R_2 , respectively. These receivers may choose to exchange the fingerprints or position estimates collected at an instant t depending on the pre-defined ANN architectures. In case where both receivers feed together their fingerprint measurements, one super ANN shown in Fig. 10.4 concatenates the subset of observations S^{R_1} and S^{R_2} to form the total set $S = \{F_1, F_2, F_3, \dots, F_m\}$ such that:

$$S = \{(f_1, f'_1), (f_2, f'_2), (f_3, f'_3), \dots, (f_m, f'_m)\}.$$

The input layer of the ANN is made of 14 neurons while the output layer is the transmitter's distance in the set $D = \{d_1, d_2, d_3, \dots, d_m\}$ referenced to R_1 .

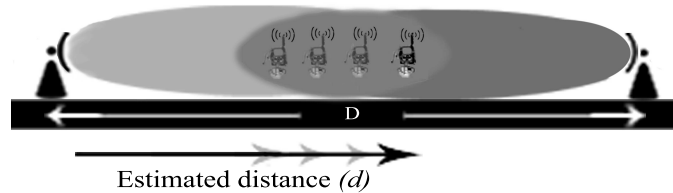


Figure 10.3 – Cooperative localization using two receivers.

10.3.3 Exploiting temporal diversity

In a tunnel-shaped topology, two APs are sufficient to provide wireless coverage for the whole section of the gallery in between. In other words, localization using spatial diversity could be limited to two fingerprints per position. This diminishes, however, its capability of attaining higher accuracies and precisions. A search for better performance led to the development of the memory-assisted localization technique in [6] where temporal diversity is exploited. Using one receiver, solitary memory-assisted

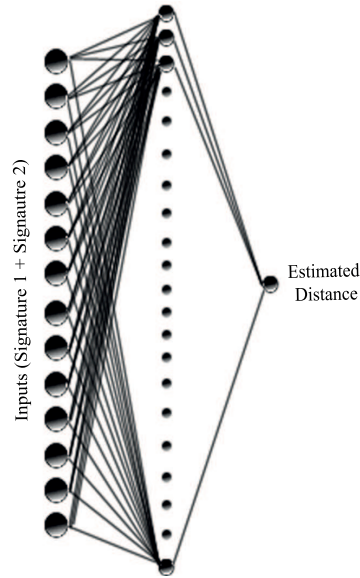


Figure 10.4 – ANN based on multiple signatures.

fingerprinting is illustrated in Fig. 10.5 where the star represents the transmitter’s position to be estimated at time instant t_0 .



Figure 10.5 – Possibilities of previous positions for $l = 2$.

A temporal fingerprint is the concatenation of multiple signatures recorded along the path a transmitter takes reaching a desired position at t_0 , separated by a distance d from the localizing unit. Concatenating only one previous fingerprint at a time instant t_{-1} creates a temporal fingerprint of length $l = 2$ (i.e., 2 fingerprints with a total of 14 parameters). The length of the temporal fingerprint depends on l and corresponds to the number of inputs N_{inputs} fed to the ANN where:

$$N_{inputs} = 7l.$$

In order to generalize the performance of the ANN, all the paths that lead to the star position should be considered as possible temporal fingerprints. This requires collecting all the combinatorial fingerprints surrounding each position while respecting the boundary limits and considering a consistent hop size.¹ It should be noted that a combinatorial set of generated temporal fingerprints exponentially increases from the original set containing 480 measurements. Training ANNs on all possible temporal fingerprints enriches the information given about one location based on fingerprints taken from possible motion patterns, a method that should not be confused with conventional tracking algorithms where the position estimates are enhanced after their estimation takes place [47] [22] [41]. A programmed MATLAB function is responsible for collecting all possible paths and then concatenating their corresponding fingerprints to form chains of temporal fingerprints for all positions in the tunnel based on the pre-defined memory level l . The performance of each ANN is tested for different memory levels up to $l = 5$ (i.e., chains of five concatenated fingerprints per position) after which no significant accuracy gain is reported. The temporal fingerprint is denoted by

$$f_i^j = \left(f_{i_{t_0}}, f_{i_{t-1}}, f_{i_{t-2}}, \dots, f_{i_{t-(l-1)}} \right),$$

and it corresponds to one path that leads to a position at a distance d_i away from R_1 using memory capacity l . Since multiple paths may lead to the same position, the index j is introduced to count the number of temporal fingerprints that point to the same output distance d_i . The maximum number of temporal fingerprints per position j_{max} is affected by the boundary conditions that surround each position and

¹Motion across diagonals is excluded because it exponentially increases the length of temporal fingerprints without significant accuracy gain.

it is proportional to l where:

$$j_{max} \leq 5^{(l-1)}.$$

10.3.4 Exploiting spatio-temporal diversity

Cooperative localization (cf. Sec. 10.3.2) improves positioning accuracy by exploiting the spatial diversity resulting from the chained-topology of the deployed APs but this diversity is practically limited to two branches due to the curvilinear topology of underground narrow-vein mines. An advanced fingerprinting technique is developed in [5] to exploit both spatial and temporal diversities of the collected fingerprints. Cooperative memory-assisted localization is introduced as a technique that creates spatio-temporal fingerprints by concatenating the temporal fingerprints gathered from different localizing units before estimating the transmitter's position. The use of more than one fingerprint saved in time exploits the temporal diversity whereas gathering the fingerprints from multiple localizing units exploits the spatial diversity of wireless signals. The spatio-temporal fingerprint subset denoted by

$$S_i^{R_1} = \{F_i^{R_1,1}, F_i^{R_1,2}, F_i^{R_1,3}, \dots, F_i^{R_1,j_{max}}\}$$

is collected from R_1 which is at a distance d_i and it is concatenated path-wise with the other subset

$$S_i^{R_2} = \{F_i^{R_2,1}, F_i^{R_2,2}, F_i^{R_2,3}, \dots, F_i^{R_2,j_{max}}\}$$

measured at receiver R_2 which is at a distance $d_2 = D - d_i$ to form the group of spatio-temporal fingerprints:

$$S_i = \left\{ (F_i^{R_1,1}, F_i^{R_2,1}), (F_i^{R_1,2}, F_i^{R_2,2}), (F_i^{R_1,3}, F_i^{R_2,3}), \dots, (F_i^{R_1,j_{max}}, F_i^{R_2,j_{max}}) \right\}.$$

The memory levels of receivers R_1 and R_2 are denoted by (l_1, l_2) . The number of parameters that constitute each fingerprint is specified according to the total length of the spatio-temporal fingerprints (i.e., $l = l_1 + l_2$). A 2-by-2 spatio-temporal fingerprint design (i.e., $l_1 = 2, l_2 = 2$) may be achieved by matching the collected spatio-temporal fingerprints $F_i = (F_i^{R_1}, F_i^{R_2})$ where

$$F_i^{R_1} = (f_{i_{t_0}}^{R_1}, f_{i_{t-1}}^{R_1}),$$

$$F_i^{R_2} = (f_{i_{t_0}}^{R_2}, f_{i_{t-1}}^{R_2}).$$

In case where $(l_1 = 2, l_2 = 2)$, the temporal fingerprint collected at a distance d_i from R_1 is equal in length to that collected from R_2 for the same position, but the total concatenated spatio-temporal fingerprint F_i fed to the ANN at the time instance t_0 is of length 28 (i.e., $7l = 7(l_1 + l_2)$).

10.3.5 Overview of performance results

As a background overview, the results of all ANN-based localization techniques that use the fingerprinting approaches discussed above are summarized in Tab. 10.1. Based on the reported performance results, cooperative memoryless localization outperforms the solitary localization technique by exploiting the spatial diversity of the fingerprints providing an accuracy of less than 1 m for 90% of the collected fingerprints. Since cooperative memoryless localization is limited in diversity to two branches due to spatial confinement, memory-type fingerprints are then used to exploit the temporal diversity and achieve better performance results. By concatenating up to 5 temporal fingerprints, the solitary memory-assisted localization technique attains a high accuracy of 50 cm at the same precision. However, smart spatio-temporal fingerprinting achieves even higher accuracy gains by exploiting both the spatial and

temporal diversities. Cooperative memory-assisted localization reduces positioning error to less than 25 cm 90% of the time.

Table 10.1 – Estimation errors of different localization techniques with 90% precision.

Localization Technique		<i>Training vs Testing Errors (m)</i>	
Localization using one receiver [31]		1.5	1.65
Cooperative memoryless based on separate ANNs [4]		1	1
Cooperative memoryless based on one super ANN [4]		0.6	1
Solo memory-assisted [6]	$(l_1 = 2, l_2 = 0)$	1	1.25
	$(l_1 = 3, l_2 = 0)$	0.75	0.8
	$(l_1 = 4, l_2 = 0)$	0.5	0.5
	$(l_1 = 5, l_2 = 0)$	<0.5	<0.5
Cooperative memory-assisted [5]	$(l_1 = 2, l_2 = 1)$	0.48	0.62
	$(l_1 = 3, l_2 = 1)$	0.38	0.43
	$(l_1 = 2, l_2 = 2)$	0.20	0.25

10.4 Impact of Spatial Sampling Grid Resolution

The performance of any localization system is governed by many factors which are not limited to the accuracy and precision of the positioning technique involved. Other factors such as complexity, cost and robustness are also of high importance. An optimized localization system should maintain accuracy, precision, robustness and simplicity at high standards. Because fingerprint positioning techniques require campaign measurements, they are considered of higher complexity or cost compared to conventional localization systems. However, fingerprint-based localization is proven to give much more accurate and precise estimation results in underground narrow-vein mines. A smart fingerprint positioning system would reduce the amount of fingerprints while maintaining the accuracy and robustness of performance results.

In this paper we investigate the effect that grid resolution imposes on the accuracy and precision of the fingerprint positioning system in [31] and [4]. As a rule of thumb, the denser the measurement grid provided to ANNs, the more robust position

estimation is to new testing fingerprints. The ANN-based localization techniques discussed in Sec. 10.3 base their fingerprint positioning on a grid of 1 m/ x -hop. In other words, the ANNs in [31] [4] [6] [5] are trained on sets of spatial and/or temporal fingerprints for positions 1 m apart along the longitude of the tunnel. Here, we investigate the performance of both the solitary [31] and cooperative [4] memoryless localization techniques once the spatial sampling grid’s resolution is reduced to 2 m/ x -hop or 3 m/ x -hop in the fingerprint collection step (cf. Sec. 10.2). This investigation amounts to splitting the original grid into 2 or 3 interleaved sub-grids, respectively. For each tested technique, [31] or [4], its ANN is then trained on 75% of a given sub-grid candidate then tested on the remaining 25% of the same sub-grid (i.e., x -positions seen during training) and on the 25% of each of the other sub-grids (i.e., x -positions never seen during training), thereby resulting into 2 or 3 ANN candidates, respectively. The cumulative distribution function of localization errors collected from the testing of all ANN candidates is plotted at each grid resolution for both the solitary and cooperative versions in Figs. 10.6 and 10.7, respectively. Both

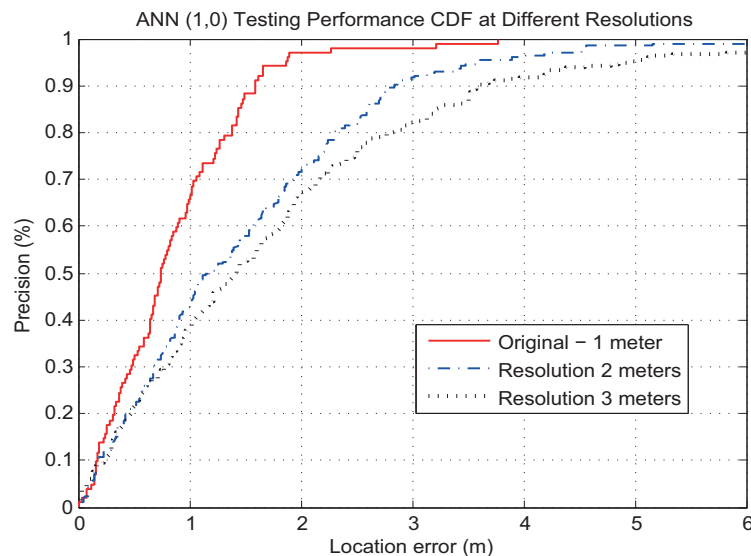


Figure 10.6 – Solitary localization performance.

figures suggest, as expected, the localization accuracy of each technique degrading

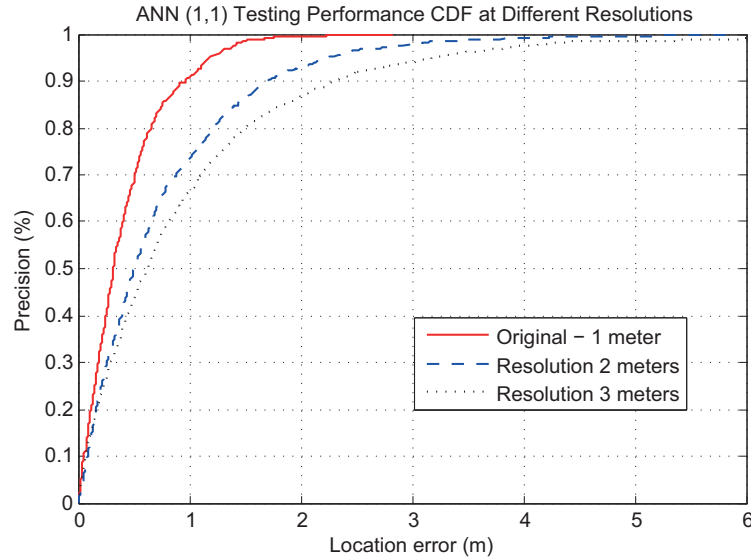


Figure 10.7 – Cooperative localization performance.

with the grid resolution decreasing. Yet at any given grid resolution, the cooperative version [4] always maintains an accuracy gain over the solitary one [31], thereby confirming again the net benefits of exploiting (spatial, but also temporal or spatio-temporal) diversity in fingerprinting for localization even at lower grid resolutions and even when testing positions are never seen during ANN training. Tab. 10.2 reports accuracies obtained at 90% precision in Figs. 10.6 and 10.7. They obviously suggest that the cooperative version [4] offers about the same accuracy (i.e., 1.5 to 1.6 m) of the original solitary version [31] using though for training only 50% of the collected fingerprints. The latter stem from a sampling grid with a resolution (i.e., 2 m) that is half of the original one (i.e., 1 m), thereby speeding up the fingerprinting campaign and reducing its cost by factor 2! Higher speed-up factors could be hence easily expected with the spatio-temporal fingerprinting version [5]. This is the subject of ongoing investigations.

Table 10.2 – Accuracy results at 90% precision for multiple spatial sampling grid resolutions

Localization Technique	Grid Resolution		
	<i>1 m</i>	<i>2 m</i>	<i>3 m</i>
Solo memoryless technique [31]	1.6 m	2.8 m	3.6 m
Cooperative memoryless technique [4]	1 m	1.7 m	2.3 m

10.5 Conclusion

Using spatio-temporal fingerprinting in underground narrow-vein mine increases the performance of ANN-based localization systems in terms of accuracy and precision. Here, we show by simulations that the significant accuracy gains reaped from the new exploitation of spatio-temporal diversity, if not needed in some location applications, can be alternatively traded for remarkable and extremely useful cost reductions in the fingerprint collection step, thereby making the novel ANN-based wireless localization systems even more attractive due to their combined accuracy advantage and relatively reduced cost. These smart fingerprinting techniques could be implemented in different wireless localization services and integrated into any wireless technology.

Chapter 11

Cost-Effective Localization in Underground Mines Using New SIMO/MIMO-Like Fingerprints and Artificial Neural Networks

Authors: Shehadi Dayekh, Sofiène Affes, Nahi Kandil and Chahé Nerguizian.

Contribution: The primary author is the main contributor and editor of this work.

Conference: IEEE International Conference on Communications (ICC)

Status: Manuscript was accepted and should be published on June 14th, 2014.

Abstract

Safety measures have always been a main concern in the mining industry that, despite the modern practices, utilizes old-fashioned surveillance and monitoring systems. Our mission in underground mines stems from the profound need of geo-positioning systems that can accurately localize endangered miners and their heavy machinery in one of Earth's most harsh and rough environments. In underground mines, complex channels' responses to wireless transmitted signals challenge traditional localization techniques, yet they fail to defeat our innovative, cost-effective and accurate fingerprint-based positioning techniques that use artificial neural networks (ANNs) and exploit space-time diversity. Being among the pioneers in underground communications research, we bring forward a more sophisticated and accurate fingerprint-based positioning technique that exploits spatial transmission diversity in the presence of more than one transmitter T_x and/or receiver R_x antenna, such as in the case of single/multiple input multiple output (SIMO/MIMO) communication systems. More importantly, an advanced study is conducted to reduce the cost of fingerprint-acquisition trading off pinpoint accuracy for lower complexity and better ANNs' design. By challenging the localization system using less data measurements, we prove that ANNs, when properly designed, succeed to attain high positioning accuracies even when localizing in measurement gaps that were not seen in the training phase.

Keywords. Indoor localization, underground mines, artificial neural networks, channel impulse response, fingerprinting, time diversity, spatial diversity, SIMO, MIMO, cooperative/collaborative localization.

11.1 Introduction

Indoor localization in complex channels is as yet a topic of research that aims to replicate the success achieved by commercially viable outdoor localization systems. In the mining industry, for example, localizing miners and their heavy machinery is not a luxurious task, but a critical requirement that guarantees basic safety measures and helps avoid potential risks in cases of fire, collapses and other hazardous work activities. In fact, localization techniques that succeed to attain high positioning accuracies in outdoor scenarios fail to maintain similar precision and accuracy in underground mines. In position estimation theories, major parameters extracted from wireless signals, such as the received signal's strength (RSS), time of arrival (ToA), angle of arrival (AoA) and/or time difference of arrival (TDoA), are used to estimate the distance travelled by wireless signals from transmitters to receivers. However, complexity arises when the channel, where wireless transmission takes place, introduces robust distortion, attenuation and/or fading to received signals' characteristics. In complex indoor channels such as the case in the mining environment, *a priori* estimation of complex channel's response to wireless transmission is not yet feasible due to the severe reflections/refractions that signals suffer from due to rough surfaces, water, inter-connected tunnels and heavy machinery in the confinement of underground galleries.

Major research projects at Telebec's Underground Communications Research Laboratory (LRTCS), one of the leading research laboratories in the world for underground communications (cf. surveys [16] and [46]), have revealed new, more accurate indoor localization techniques that use fingerprinting and ANNs in the 2.4 GHz, 5.4 GHz [32], [2], over UltraWide Band (UWB) [34], [42] and recently being investigated in the mmWave/60 GHz bands [26]. Localization using fingerprinting and ANNs is based on extracting parameters from the channel impulse responses (CIRs)

and mapping them to given positions located at different distances away from a given transmitter [31]. In order to overcome some of the challenges, such as the presence of inter-connected tunnels, and to further enhance localization accuracy, more sophisticated fingerprint-based positioning techniques were developed in [4], [6] and [5] by exploiting spatial, temporal and spatio-temporal diversities, respectively.

In this work, we put forward a new fingerprint-based positioning technique that exploits the presence of dual T_x and R_x antennas in nowadays SIMO/MIMO-capable communication equipment. It is shown herein that CIR-based localization exploiting spatial diversity and SIMO/MIMO-type fingerprints significantly increases positioning accuracies and is, so far, the most accurate among all CIR-based fingerprint positioning techniques in underground mines. More importantly, all studied fingerprint-positioning techniques are challenged by lower fingerprint-acquisition rate in the ANNs' training phase. In an effort to reduce measurement campaigns' cost, ANNs are well-designed and trained to attain high positioning accuracies even when they are forced to localize in measurement gaps that, due to the lowered fingerprint-acquisition rate, were never introduced to ANNs' training phases.

In the following section, we review the most recent CIR-based positioning techniques that exploit spatially and/or temporally diverse fingerprints in underground mines. Section 11.3 introduces the novel fingerprint-based localization technique that exploits SIMO/MIMO-type fingerprints. An advanced study is then performed to lower the cost overhead of fingerprint-acquisition in section 11.4 after which performance results are presented in section 11.5. Finally, the paper is closed by a conclusion in section 11.6.

11.2 Localization in Underground Mines Using CIR-based Fingerprinting

The special nature of underground mines shown in Fig. 11.1, which is made of quasi-curvilinear intersecting tunnels, enforces the quest to develop more sophisticated localization techniques seeking better security and safety practices in the mining industry. For more than fourteen years of continuous research, LRTCS and similar research labs have been looking for alternatives to traditional triangulation techniques before the first ANN-based geo-location method was innovated and published in [31]. In the following, we study, as a background exercise, the method in [31] laying the groundwork for discussing more advanced techniques that exploit space-time diversities in [4], [6] and [5].

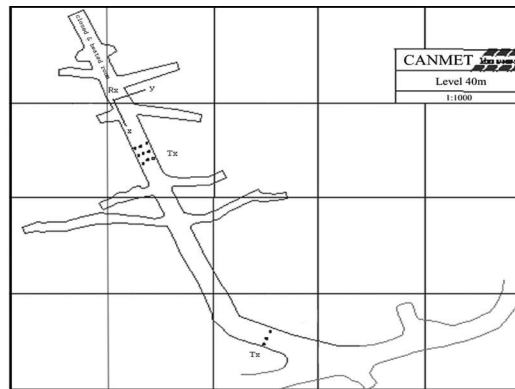


Figure 11.1 – Map of the tunnel.

11.2.1 ANNs and CIR-based fingerprint positioning

Fingerprint positioning techniques rely on mapping wireless signals' parameters to the distance separating the receiver from the transmitter. Due to the special nature of underground propagation channels, some parameters such as the RSS fluctuate for the same position inside the mine and may not be used solely for position estimation

[39]. The same can be said about AoA and ToA, because the former (i.e., AoA) represents the last angle of reflection inside the tunnel while the latter (i.e., ToA) represents the total time travelled after bouncing inside the confined tunnel. In [31], a fingerprint is a combination of seven parameters which are the mean excess delay ($\bar{\tau}$), the root mean square (τ_{rms}), the maximum excess delay (τ_{max}), the total power of the received signal (P), the number of multipath components (N), the power of the first arrival (P_1) and the delay of the first path component (τ_1).

By using Multilayer Perceptron (MLP) ANNs, which are extremely powerful computational models for non-linear problems, a fingerprint $f_i = (\bar{\tau}, \tau_{rms}, \tau_{max}, P, N, P_1, \tau_1)$ is then matched to its corresponding set of distances $D = \{d_1, d_2, d_3, \dots, d_n\}$. For simplicity, the distance is calculated using the x – axis only neglecting minor variations which are of less importance on the y – axis inside the confinement of narrow underground tunnels as shown in Fig. 11.2. The original memoryless technique (i.e., ANN(1,0)), developed in [31] and used as a comparison benchmark, scores an accuracy of 1.3 m and 1.4 m for 90% of the training and testing data, respectively.

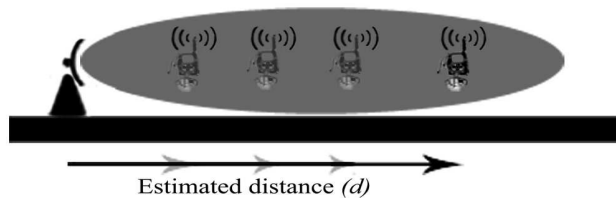


Figure 11.2 – The CIRs are extracted at different distances to the transmitter with 1-meter step-size along the x -axis.

11.2.2 Exploiting R_x spatial, temporal and space-time diversities

At first, the localization technique in [31] was challenged by misleading information about the direction of transmission in case one localizing receiver is placed at junctions of interconnecting tunnels. To overcome such scenarios and to further enhance positioning accuracy, a new fingerprint-based positioning technique was developed in [4] and it exploited R_x spatial diversity at two receivers as shown in Fig. 11.3. A centralized ANN, shown in Fig. 11.4, is then used to collect both signa-

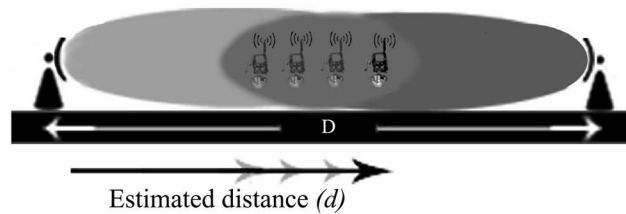


Figure 11.3 – Localization using two signatures of two receivers in the area where two signals intersect.

tures (or sub-fingerprints) from both receivers, R_1 and R_2 separated by a distance $D = 80$ m, forming one fingerprint that contains 14 parameters. The training set S

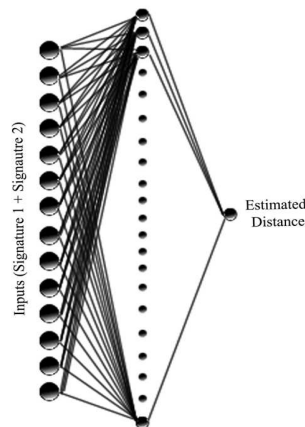


Figure 11.4 – Neural network based on multiple signatures.

that defines the fingerprints' space is a concatenation of two sub-sets, S^{R_1} and S^{R_2} , and is denoted by: $S = \{F_1, F_2, F_3, \dots, F_m\} = \{(f_1, f'_1), (f_2, f'_2), (f_3, f'_3), \dots, (f_m, f'_m)\}$, where f_i and f'_i represent the sub-fingerprints collected, for a position i , at R_1 and R_2 , respectively. By using one ANN with two sub-fingerprints from R_1 and R_2 , localization accuracy significantly increases to prove the effectiveness of exploiting R_x spatial diversity and errors slip to 77 cm and 90 cm for the training and testing data, respectively.

Increasing the accuracy and robustness using R_x spatial diversity only may require increasing the number of access points which is not an option in the limited space of underground mine tunnels. However, the use of temporal diversity increases the system's accuracy when more than one fingerprint is concatenated in time slots prior to estimating the transmitter's final position at $d_i^{t_0}$ [6]. A temporal fingerprint is represented by:

$$f_i^j = \left(f_{i_{t_0}}, f_{i_{t_{-1}}}, f_{i_{t_{-2}}} \dots, f_{i_{t_{-(l-1)}}} \right),$$

where l is the memory level or the number of concatenated fingerprints. The length of a temporal fingerprint L_f depends on the memory depth where:

$$L_f = 7l.$$

An example of a temporal fingerprint is demonstrated for $l = 3$ in Fig. 11.5. The maximum number of path fingerprints j_{max} that may be obtained for a given distance is upper bounded by N_{f_p} where:

$$j_{max} \leq N_{f_p} = 5^{(l-1)}.$$

All possible sub-fingerprint, for $l = 3$, at t_{-1} and t_{-2} are concatenated to the sub-fingerprint at t_0 forming 25 temporal fingerprints (or path fingerprints) each of length

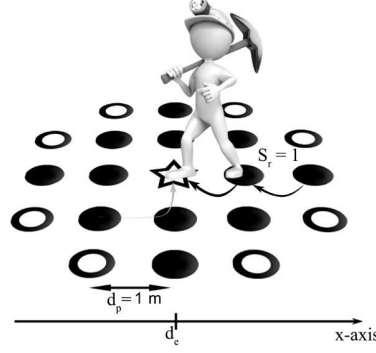


Figure 11.5 – Possibilities of previous positions for $l = 3$.

$L_f = 21$. For each memory length l , there exists one ANN that is trained to count for all possible path-fingerprints leading to a given distance d along the x -axis of the tunnel. With a step-size of $d_p = 1$ m along the x -axis of the tunnel, the miner's possible path fingerprints may be extracted from the CIRs at the filled-circled positions in Fig. 11.5. For simplicity, motion across diagonals is excluded. Multiple scenarios were tested for different memory levels (i.e., $l = 1, 2, 3, 4$) and their position estimation errors start at 89 cm and 1.14 m, at $l = 2$, and drop down to 48 cm, at $l = 4$, for 90% the training and testing data, respectively.

After maximizing accuracy gains of temporally diverse fingerprints, a new fingerprinting technique was developed in [5] and it uses both R_x spatial and temporal diversities of the collected fingerprints. By exploiting R_x spatial diversity from both collaborative receivers and combining memory-type fingerprints, the developed localization system topped the accuracy benchmark, surpassing those achieved by previous fingerprint-based techniques in [31], [4] and [6]. The fingerprint subset $S_i^{R_1}$, collected at a distance d_i away from R_1 , is concatenated path-wise with the second fingerprint subset $S_i^{R_2}$ collected at R_2 , where: $S_i^{R_1} = \{F_i^{R_1,1}, F_i^{R_1,2}, F_i^{R_1,3}, \dots, F_i^{R_1,j_{max}}\}$, $S_i^{R_2} = \{F_i^{R_2,1}, F_i^{R_2,2}, F_i^{R_2,3}, \dots, F_i^{R_2,j_{max}}\}$. The spatio-temporal fingerprint subset S_i

extracted for one specific distance d_i is designed as follows:

$$S_i = \left\{ (F_i^{R_1,1}, F_i^{R_2,1}), (F_i^{R_1,2}, F_i^{R_2,2}), (F_i^{R_1,3}, F_i^{R_2,3}), \dots, \right. \\ \left. (F_i^{R_1,j_{max}}, F_i^{R_2,j_{max}}) \right\}.$$

The dynamic design of spatio-temporal fingerprints allows variable memory depths ranging between $l = 1$ (no memory) and $l = 5$ (beyond which no increased performance is noticed) reproducing multiple spatio-temporal fingerprint scenarios that we denote by (l_1, l_2) . Each receiver, R_1 or R_2 , can be set to introduce any memory depth, l_1 or l_2 , respectively. At lower complexity, a spatio-temporal ANN performing at $(l_1 = 2, l_2 = 2)$ is capable of achieving performance accuracies of less than 50 cm, at $S_x = 1$ m, which matches the results obtained by a complex memory-assisted ANN performing at $l = 4$ in the presence of one receiver only. It will be shown later in Sec. 11.5.2 that at higher S_x , long chains of memory-type fingerprints become less significant while spatio-temporal techniques maintain a better posture at lower fingerprint sampling rate. Results of other scenarios involving different memory allocations (i.e., ANN(2,1), ANN(3,1), etc ...) at each receiver may be reviewed in [5].

11.3 Exploiting T_x and R_x Spatial Diversities: SIMO/MIMO-type Fingerprint Positioning

So far, we discussed R_x spatial diversity (i.e., at two receivers R_1 and R_2) and temporal diversity (i.e., using memory) showing how they are both used to design new fingerprint-based positioning techniques. Although their performance results, as shown later in Sec. 11.5, are outstanding in terms of positioning accuracy and precision, we push their performance limits forward and introduce a more advanced

fingerprint positioning technique that exploits the presence of dual T_x antennas ¹. In addition to that, the novel technique simultaneously uses R_x spatial diversity which significantly increases localization performance. SIMO-type fingerprints are formed from sub-fingerprints of two adjacent T_x antennas in the presence of one receiver or R_x . A SIMO-type fingerprint is denoted by:

$$F_i^{SIMO} = (f_i^{Tx_1}, f_i^{Tx_2}),$$

Where $f_i^{Tx_1}$ and $f_i^{Tx_2}$ are fingerprints collected, at a position i , by R_{x_1} for T_{x_1} and T_{x_2} , respectively. On the other hand, MIMO-type fingerprints are concatenated by extracting two T_x sub-fingerprints at both receivers R_{x_1} and R_{x_2} . A MIMO-type fingerprint is represented as:

$$F_i^{MIMO} = \{(f_i^{Tx_1}, f_i^{Tx_2}), (f_{i'}^{Tx_1}, f_{i'}^{Tx_2})\},$$

where $f_i^{Tx_1}$ and $f_i^{Tx_2}$ represent sub-fingerprints collected at R_{x_1} , whereas $f_{i'}^{Tx_1}$ and $f_{i'}^{Tx_2}$ are sub-fingerprints extracted by R_{x_2} , at a position $i' = D - i$, for T_{x_1} and T_{x_2} , respectively.

The use of SIMO/MIMO-type fingerprints is so far the most robust CIR-based localization technique with accuracies that drop below 50 cm as shown later in Sec. 11.5. By comparing both SIMO/MIMO-like fingerprints and spatio-temporal fingerprints, many conclusions may be drawn. First, T_x spatial diversity comes as an alternative to memory-type sub-fingerprints that result from exploiting temporal diversity, leading to lower system complexity and better design efficiency in the scenarios where transmitters are equipped with two T_x antennas. Second, as we discuss further in the following section, temporal diversity fingerprints prove to produce lower performance

¹Real measurements taken every 0.5 m and 1 m along the y -axis and x -axis simulate dual antenna spacing of $\delta_y^{Tx} = 0.5$ m and $\delta_x^{Tx} = 1$ m, respectively.

when measurement gaps are introduced in an effort to reduce the cost of measurement campaigns. However, localization using T_x and R_x diversities maintains low position estimation errors even when the resolution of fingerprint-acquisition is reduced.

11.4 Complexity and Cost Reduction

Fingerprinting techniques are mainly criticized because they require extensive measurement campaigns that are costly and time consuming. What if the measurement campaigns' cost can be cut down to less than one quarters of its original value? Would localization techniques, which based their fingerprints on CIRs exploiting space and/or time diversities, hold as accurate and cost-effective positioning techniques for underground mines? A study was conducted to answer the reasonable questions in an effort to tune pinpoint accuracies and trade it for lower fingerprint-acquisition cost. By introducing measurement gaps or sub-grids that are not fed to the ANNs in the training phases, we challenge all CIR-based localization techniques and test their positioning accuracies and precision at higher sampling step-size S_x ². ANNs are carefully designed to interpolate measurement gaps by running trial and error simulations that aim to optimize the number of neurons needed for each S_x . For each localization technique and S_x , a trial is run three times while varying the number of neurons n as follows:

$$1 < n_n < N_n = 2N_i + 1,$$

where N_i is the number of inputs fed to the ANNs which varies depending on the spatial, temporal or spatio-temporal fingerprints' chain length. As shown in Fig. 11.6, the number of neurons drops with the decrease in the number of fingerprints for

² S_x , ranging from 1 m to 6 m, represents the step-size between consecutive offline measurement positions along the x -axis of the tunnel.

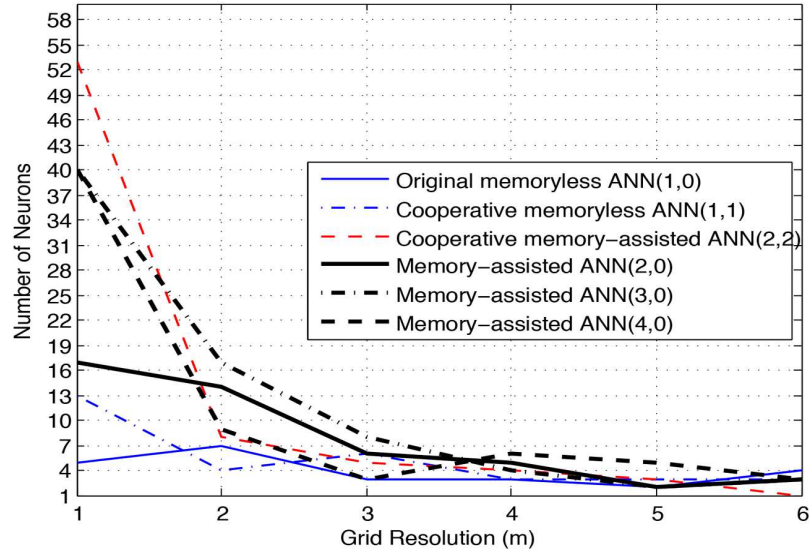


Figure 11.6 – Optimum number of neurons for different ANNs.

each training set which comes as a result of cutting down the cost (i.e., reducing the measurement campaign’s acquisition rate).

11.5 Performance Results

The performance results of CIR-based localization techniques are presented using the cumulative density function (CDF) that shows, on one axis, the accuracy of position estimations in meters, and on another, the precision accomplished by a given localization technique. It should be noted that all ANNs are trained on 75% of the collected fingerprints while leaving 25% for the testing phase at $S_x = 1$ m. In the case where $S_x \geq 2$ m, training results represent 75% of the sampled sub-grid then ANNs are tested using 25% of every sub-grid not seen in the training phase. All spatial, temporal and spatio-temporal positioning techniques are analyzed at $S_x = 1$ m first, after which they are compared, at 90% precision, using different sampling grid’s resolution in Figs. 11.7, 11.8 and Tab. 11.1.

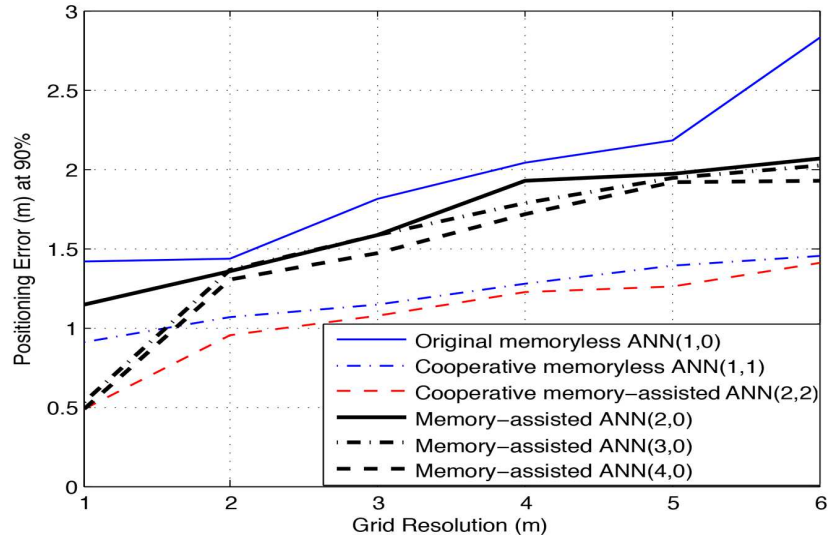


Figure 11.7 – Positioning errors from CDFs of testing data at 90% precision.

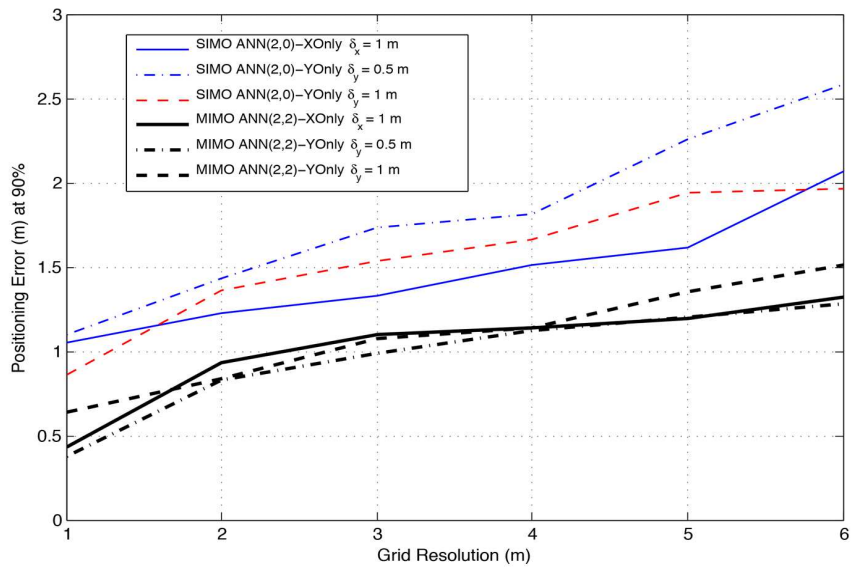


Figure 11.8 – Positioning errors from CDFs of SIMO/MIMO-type testing data at 90% precision.

11.5.1 Results of SIMO/MIMO-type fingerprinting using T_x and R_x spatial diversities

SIMO/MIMO-type fingerprints, discussed in Sec. 11.3, constitute the groundwork for a new, more sophisticated and less complicated type of a CIR-based fingerprint positioning technique. They bring in the advantages of exploiting spatial diversity at both the receiver and transmitter, without introducing memory, raising positioning-accuracy levels to a new record in underground mines. Since we have one T_x -antenna separation distances at the x -axis and two at the y -axis, we shall report them separately using the notations $\delta_x^{Tx} = 1$ m, $\delta_y^{Tx} = 1$ m and $\delta_y^{Tx} = 0.5$ m, respectively. SIMO-type fingerprints are denoted by $2Tx-1Rx$ whereas MIMO-type fingerprints use the $2Tx-2Rx$ notation and their performance results are reported in Fig. 11.8 and Tab. 11.1.

If we compare, at $S_x = 1$ m, SIMO-type techniques to ANN(2,0) that uses the same fingerprint length of $L_f = 14$, we notice that SIMO-type fingerprints localize more accurately with a an estimation error of 85 cm as compared to 1.15 m using memory-assisted techniques with ANN(2,0). Another example can be drawn from comparing spatio-temporal diversity, such as ANN(2,2), to the accuracy of MIMO-type fingerprints using $2Tx-2Rx$ ANN. While the first uses temporal diversity to boost accuracy results to 49 cm, the latter (i.e, using MIMO-like fingerprints) succeeds to score accuracies of 43 cm and 38 cm at $\delta_x^{Tx} = 1$ m, $\delta_y^{Tx} = 0.5$ m, respectively. The use of SIMO/MIMO-like fingerprints surpasses the performance limits achieved by temporally diverse fingerprints and provides a less complex fingerprinting technique that does not include memory when localizing transmitters in underground mines. It is also beneficial to state the importance of having R_x and T_x diversities at the same time when localizing at lower sampling resolution or higher S_x as discussed in the following section.

11.5.2 Results of low fingerprint-acquisition rate on accuracy

The pinpoint accuracies obtained from fingerprint localization exploiting R_x and/or T_x spatial, temporal and spatio-temporal diversities, reported above, may be controlled and traded off for lower fingerprint-acquisition cost. Location accuracies at $S_x \geq 2$ m provide less fingerprints in the training phases of ANNs and reduces the time needed for offline fingerprint-acquisition. More than 14k ANNs were tested in this simulation in the best effort to optimize the number of neurons used for each CIR-based localization technique and the significant results are shown in Fig. 11.6. In the following, we shall judge each localization technique based on its ability to sustain the benchmark obtained by the original technique ANN(1,0) developed in [31] which, at $S_x = 1$ m, which has an estimation error of 1.42 m 90% of the time (circled in Tab. 11.1). After selecting the most effective number of neurons based on S_x from Fig.

Table 11.1 – Performance Results with Multiple Resolution

ANN Technique	Grid Resolution Accuracy Results					
	1 m	2 m	3 m	4 m	5 m	6 m
ANN(1,0)	1.42 m	1.44 m	1.81 m	2.04 m	2.12 m	2.83 m
ANN, 2Tx1Rx $\delta_y^{T_x} = 0.5$ m	1.10 m	1.43 m	1.73 m	1.81 m	2.26 m	2.58 m
ANN, 2Tx1Rx $\delta_y^{T_x} = 1$ m	0.85 m	1.36 m	1.53 m	1.66 m	1.94 m	1.97 m
ANN(2,0)	1.15 m	1.35 m	1.58 m	1.92 m	1.97 m	2.07 m
ANN(3,0)	0.53 m	1.36 m	1.58 m	1.78 m	1.94 m	2.02 m
ANN(4,0)	0.48 m	1.30 m	1.46 m	1.72 m	1.91 m	1.93 m
ANN, 2Tx1Rx $\delta_x^{T_x} = 1$ m	1.05 m	1.23 m	1.33 m	1.51 m	1.61 m	2.07 m
ANN(1,1)	0.91 m	1.07 m	1.15 m	1.28 m	1.39 m	1.45 m
ANN, 2Tx2Rx $\delta_y^{T_x} = 1$ m	0.64 m	0.84 m	1.07 m	1.14 m	1.35 m	1.51 m
ANN(2,2)	0.49 m	0.95 m	1.07 m	1.22 m	1.26 m	1.41 m
ANN, 2Tx2Rx $\delta_x^{T_x} = 1$ m	0.43 m	0.93 m	1.10 m	1.14 m	1.19 m	1.32 m
ANN, 2Tx2Rx $\delta_y^{T_x} = 0.5$ m	0.38 m	0.83 m	0.98 m	1.12 m	1.20 m	1.28 m

11.6, we show the performance accuracies of all localization techniques using higher step-sizes of $S_x = 3$ m and $S_x = 6$ m in Figs. 11.9 and 11.10. The rest of step-size scenarios are shown for 90% precision in Figs. 11.7 and 11.8 then summarized in Tab.

11.1 to show the granularity of positioning accuracies for different T_x antenna spacing or δ^{T_x} . The performance of temporal fingerprints was expected to degrade at lower

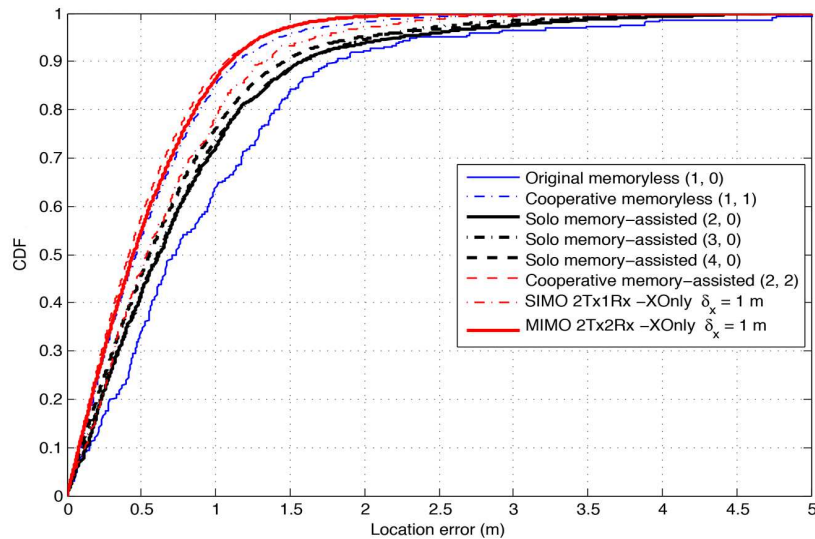


Figure 11.9 – Localization performance at $S_x = 3$ m.

sampling resolution (i.e., higher S_x) because temporal sub-fingerprints, collected at positions separated by higher step-sizes, carry less information about the position to be estimated. An example can be drawn from the performance of ANN(4,0) which fails to sustain the 1.42 m accuracy beyond $S_x = 2$ m.

However, taking a closer look at the results of memory-assisted localization techniques that only exploit R_x spatial diversity reveals an outstanding performance for ANN(2,2) which achieves, at $S_x = 6$ m, an accuracy matching the benchmark of 1.42 m obtained by ANN(1,0) at $S_x = 1$ m! The same can be said about ANN(1,1) which can maintain the benchmark using only one fifth of the measurement campaign’s data (i.e., at $S_x = 5$ m).

The new positioning techniques that use SIMO/MIMO-like fingerprints reveal the power of combining R_x and T_x diversities in the realm of fingerprint positioning using ANNs in underground mines. The use of SIMO-type fingerprints exploiting spatial

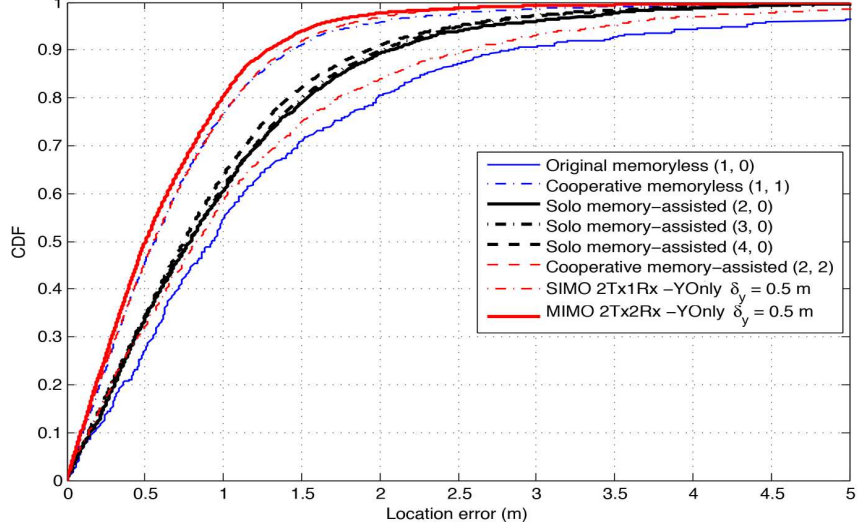


Figure 11.10 – Localization performance at $S_x = 6$ m.

diversity at T_x only is not the best candidate for localization because it reports lower accuracy performance compared to ANN(1,1) which uses R_x spatial diversity only. However, the performance limits of MIMO-like fingerprints exploiting both T_x and R_x diversities surpass those of the original techniques, especially at $\delta_y^{T_x} = 0.5$ m highlighted in Tab. 11.1, to achieve location accuracies of 38 cm and 1.28 m for the testing data at $S_x = 1$ m and $S_x = 6$ m, respectively. One can cut down the cost of data measurements to half by using $S_x = 2$ m and still obtain positioning accuracies of 83 cm 90% of the time! Localization using MIMO-like fingerprints in the presence of well-designed ANNs proves to be an accurate, robust and cost-effective technique in underground mines.

11.6 Conclusion

The focus of this study stems from years of research for an accurate, cost-effective positioning techniques that can improve safety practices in underground mines. The

new fingerprint positioning technique, presented here, uses MIMO-like signatures that combine R_x and T_x spatial diversities and brings forward new positioning accuracies of less than 50 cm, at sampling step-size $S_x = 1$ m, while achieving high accuracy records of 1.28 m when ANNs are challenged, in the training phases, using only one sixth of the measurement campaign's fingerprints (i.e., at $S_x = 6$ m). When correctly applying the discussed ANNs' design strategies, localizing using MIMO-type fingerprints turns out to be, as yet, the most accurate and cost-effective CIR-based positioning technique and it may be implemented using different wireless technologies in underground mines.

Chapter 12

Neural-Networks and Fingerprint-Based Localization in Underground Mines with Novel Use of Collaboration and Space-Time Diversity

Authors: Shehadi Dayekh, Nahi Kandil, Sofène Affes and Chahé Nerguizian.

Contribution: The primary author is the main contributor and editor of this work.

Conference: IEEE Transactions on Vehicular Technology.

Status: Journal submitted on April 30th, 2014.

Abstract

Miners' positioning inside Earth's intricate entrails made of harsh and hazard-prone tunnels in underground mines is one of the most challenging indoor localization. Yet it is of outmost importance to the mining industry that is criticized for its lagging-behind safety practices. Reviewing the most recent localization techniques in narrow quasi-curvilinear tunnels reveals the effective accuracy and precision results of the original concept of indoor localization using Artificial Neural Networks (ANNs) fed by judiciously-defined fingerprints extracted from the channel impulse responses (CIRs). To our best knowledge of being the first to introduce the concepts of collaboration and diversity in the realm of ANN-based localization, we put forward a new, more accurate fingerprint-positioning technique based on single/multiple input multiple output (MISO/MIMO) signatures that combine spatially and/or temporally diverse fingerprints. More importantly, the localization system is optimized to use small fingerprint sets trading off pinpoint accuracy for lower design complexity and fingerprint-acquisition cost. The novel exploitation of collaboration and space-time diversity boosts positioning accuracies even when ANNs are challenged to interpolate and estimate positions in measurement gaps that, due to the lowered fingerprint-acquisition rate, are never seen by ANNs in the training phases. **Keywords.** Indoor localization, underground mines, artificial neural networks, channel impulse response, fingerprinting, time diversity, spatial diversity, MISO, MIMO, cooperative/collaborative localization.

12.1 Introduction

Localization of mobile users in different parts of the globe is one of the modern technology applications most used. The concept is simple; once the localizing unit receives a signal, the transmitter's location is estimated by analyzing the received signals' parameters that are altered by the channel where transmission takes place. Different approaches to localization have been presented in the literature [27], [39]. While some stay in the theoretical realm, others are implemented and used in multiple commercial applications such as the global positioning system (GPS). Geo-location very often attempts to relate the transmitter's position to the effect of the channel on some of the transmitted signals' characteristics such as the received signal's strength (RSS), the time of arrival (TOA), time difference of arrival (TDOA) and angle of arrival (AOA).

Localization techniques which operate accurately in outdoor scenarios face major challenges in indoor environments, more so in harsh underground environments such as mines [16], [46]. In underground mines, estimating a transmitter's position using mathematical models requires complex estimation of the channel's response to transmitted signals. Neither RSS, AOA, nor TOA alone would consistently succeed to estimate a given position in underground mines, a conclusion drawn from about fifteen years of research at Telebec's Underground Communications Research Laboratory (LRTCS), a pioneering lab among very few in the world with research focus on underground mine communications (cf. surveys [16] and [46]). Looking for alternatives, based on LRTCS' pioneering works on wireless channel characterization and modeling in underground mines at 2.4 GHz and 5.8 GHz [32], [2], then over Ultra-wideband (UWB) [34], and more recently with mmWave/60 GHz transmission technologies [26], led to the foundation of a totally novel localization paradigm that combined for the first time CIR-based fingerprinting and ANNs-based position

matching [31], that has been since a reference benchmark. Introduced originally in the 2.4 and 5.8 GHz bands, this new localization paradigm was later applied successfully using UWB-based transmission technologies [42]. Beyond broadening the range of its applicability to different radio access technologies (current efforts investigate the mmWave band) over the past years, this work discloses the new findings of simultaneous intense research efforts devoted to revamping its core concept. Owing to novel exploitations for the very first time of the principles of collaboration [4] (or cooperation) and diversity (in space and/or time) [6], [5] - that we borrow from the field of wireless communications - in the context of localization, we push the performance limits of the new indoor positioning paradigm [31] far beyond its original accuracy marks while significantly reducing its implementation cost.

As mentioned earlier, one of the new principles worth exploiting to boost performance is collaboration and diversity in space and/or time. In wireless sensor networks (WSNs), for example, cooperation between nodes helps them determine their locations with respect to their anchors [37], [35]. After each node uses a self-localization technique, location is shared among other nodes in an effort to refine positioning accuracies. Another application of cooperative localization is in cognitive radio networks (CRN) [21], [28]. In the latter, location awareness is an important factor that supports various spectrum allocation techniques. As a result of implementing cooperative localization, CRNs localize Primary Users (PUs) more accurately allowing dynamic spectrum allocation for Secondary Users (SUs). Cooperative localization techniques discussed in the literature that rely on Bayesian's estimation to track transmitters using motion models given the posteriori distribution of the noise process [45]. While most cooperative localization techniques rely on nodes that can self-localize themselves, few are the localization techniques that gather signal parameters from different positions prior to estimating the final location of the transmitter

in a centralized manner. One of this paper's goals is to show how cooperation between Access Points (APs) is innovated using ANNs prior to estimating a transmitter's final location. What is more important lies within the diverse fingerprinting techniques that exploit spatial, temporal and spatio-temporal diversities of the collected signatures paving the way for a new positioning technique that uses MISO/MIMO-type fingerprints collected from equidistant Tx antennas and studied for one or two Rx antennas, respectively. Furthermore, another focus of this work is to investigate the effect of the sampling grid's resolution at which CIRs and fingerprints are measured and collected, respectively, in the training phase on the new proposed localization schemes. Reducing the cost and time of measurement campaigns by lowering the sampling grid's resolution (i.e., increasing the sampling step-size) generates less fingerprints for the training of ANNs. A dynamic ANN design is needed in order to maintain high positioning accuracies while using less training fingerprints and, at the same time, challenging the system to localize in the whole grid. The variable number of spatial, temporal or spatio-temporal fingerprints collected for each sampling rate requires a dynamic allocation of the number of neurons utilized in each of the developed ANNs' architectures.

This paper is organized as follows. In section 12.2, we draw attention to the special nature of mines and the challenges localization techniques face in underground environments highlighting some of the most recent published work for underground localization. Cooperative localization in the presence of multiple ANNs exploiting spatial diversity [4] and exploiting the temporal/spatio-temporal diversity of fingerprints [6] [5] are discussed in section 12.3. The composition of spatio-temporal fingerprints lays the groundwork for a new, sophisticated approach that uses MISO/MIMO-like fingerprints from different locations and feeds them to a collaborative localization system. The results outlined in section 12.4 show the performance results of the new

MISO/MIMO localization technique and compares them to the previously-developed spatial, temporal and spatio-temporal localization techniques. In section 12.5, an advanced study is conducted to reduce the set's size of training fingerprints and challenge the developed positioning systems with lower grid resolution while carefully designing ANNs for each sampling step-size and localization technique. Finally, the paper is closed by a conclusion in section 12.6.

12.2 Related Work

Localization in underground and confined areas has been a research topic for several years. One of the pioneers in this domain is the LRTCS which, in the framework of major collaborative research projects, continues to investigate underground localization using different transmission technologies at 2.4 GHz and 5.8 GHz [32], [2], then over UWB [34], [42], and currently with mmWave/60 GHz [26]. This work stems from the proven results of [31] that use fingerprinting combined with ANNs providing very accurate estimation results in underground mines.

12.2.1 Localization challenges in underground mines

Underground mines are known for their special nature which is made up of interconnected tunnels such as that shown in Fig. 12.1. The curve-shaped topology of tunnels prevents using triangulation techniques to estimate the position of the user. On the other hand, the presence of rough humid surfaces along with NLOS regions generates multipath components of the transmitted signals that severely affect the signals' extracted parameters at the receiver's end. For example, estimating the transmitter's position using the AOA technique is almost impossible due to multiple reflections/refractions that signals encounter on their way to the receiver. Similarly, a

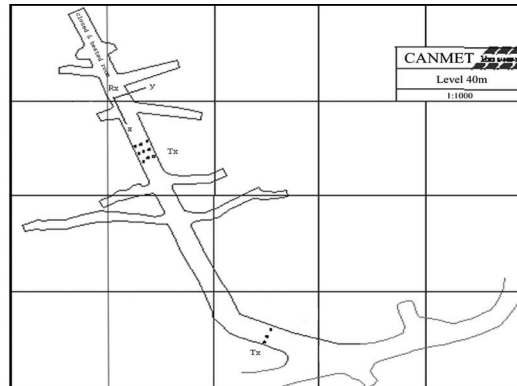


Figure 12.1 – Map of the tunnel.

received signal with the lowest TOA represents the shortest path of reflections inside the tunnel and does not represent the shortest direct distance [42]. Likewise, using the RSS alone is not sufficient to provide accurate positioning because it fluctuates for the same position in underground mines [39], [10]. For the mentioned reasons, many work groups are in continuous research for alternative techniques leading to the development of a reliable and accurate underground localization system that properly monitors miners' positions in an effort to enhance their work environment's safety measures. CIR-based fingerprint positioning, which is summarized here for background overview, provides accurate position estimation by exploiting spatio-temporal diversities and uses CIR-based fingerprinting technique combined with cooperative ANNs. Then, the cooperative localization system that exploits both Tx and Rx spatial diversities is introduced in Sec. 12.3.4 as a better localization system at lower sampling grid's resolution.

12.2.2 Localization using wireless sensor networks

Solving the localization problem in underground mines has got considerable attention in the field of WSNs. RSS-based localization using WSNs is studied in [30] and the results show that RSS alone may not contribute in high positioning accuracies

unless the number of implemented sensors is increased. On another hand, a feasibility study was conducted in [3] to use of UWB technology for positioning purposes with the help WSNs focusing on UWB channel characterization, fingerprint-based positioning and a two step TOA estimation algorithm. Other approaches such as [13] used RSS measurements from Wireless Fidelity (WiFi) radios and combined them with TOA from UWB radios to localize. An interesting Zibgee-based localization method in [38] localizes using Radio Frequency Time-of-Fly (RF-TOF) producing relatively high accuracies. In [40], simultaneous sensor localization using TOA measurements is studied with a focus on sensors' positions refinement and target tracking. Likewise, vehicle tracking in long wall mines, in the absence of NLOS scenarios, is investigated in [18]. In [24], software and hardware designs are proposed for WSN implementation in underground tunnels. Similarly, an RSSI-based system is designed in [25] to use mobile, reference and gateway nodes for localization in underground tunnels.

Despite the latest advancements in WSN-based positioning techniques, localization using WSNs requires the implementation of several nodes in the tunnels that is costly and hard to maintain in harsh environments such as mines. The deployment of WSNs in multi-level mines made of inter-connected tunnels and the ability to provide continuous power supply to all sensors may not appeal as an optimum solution for investors.

12.2.3 Localization using fingerprinting and ANNs

Fingerprinting is a method used to allocate a signature for each position in the area of interest. In [10], [29], a fingerprint is formed of the RSS measured at different distances from the receiver. Another example is [42], where the signature is a combination of the RSS, TOA and the direction of the transmitter. Similarly,

multiple techniques use different fingerprints and ANNs to define the position of the user [12], [1], [20]. A novel approach to localization was presented in [31], and it uses the CIR from which the fingerprints are extracted. For the benefit of this study, we shall draw attention to the fingerprinting technique in [31] that constitutes the starting point for the new solutions we develop in Sec 12.3. For a detailed discussion of this technique, refer to [31].

CIR-based fingerprinting is based on parameters extracted from the CIR for the positions to be estimated. From the CIR, seven parameters are extracted to ensure the uniqueness of the position inside the narrow-shaped tunnels. These parameters are the mean excess delay ($\bar{\tau}$), the root mean square (τ_{rms}), the maximum excess delay (τ_{max}), the total power of the received signal (P), the number of multipath components (N), the power of the first arrival (P_1) and the delay of the first path component (τ_1). A fingerprint extracted from the CIR at a distance d_i away from the receiver is denoted by $f_i = (\bar{\tau}, \tau_{rms}, \tau_{max}, P, N, P_1, \tau_1)$. A measurement campaign was conducted in the CANMET mine in Val d'Or, Quebec, and the CIRs were extracted for 480 positions inside a tunnel as shown in Fig. 12.1 from which the fingerprints were obtained. The collected set of fingerprints $S = \{f_1, f_2, f_3, \dots, f_n\}$ is then successfully matched to the corresponding set of distances $D = \{d_1, d_2, d_3, \dots, d_n\}$ using an ANN. It should be noted that for simplicity, the distance to the transmitter d_i is taken along the x -axis only neglecting the small variation on the y -axis which is less significant inside the confinement of the narrow tunnels. On the other hand, this approach ensures that the fluctuation of wireless signals for the same position is taken into account (i.e., more than one measurement is recorded along the y -axis for the same x -position or d_i). ANNs are computational models able to perform complex calculations, function optimizations and model estimations. Being referred to as intelligent matching algorithms, ANNs derive meanings from complex relation-

ships between sets of inputs and outputs by performing different error optimization techniques, which makes them suitable for indoor CIR-based localization problems. ANNs are made of multiple layers, which are the input, output and hidden layers. In our tunnel-shaped quasi-curvilinear localization problem, a fingerprint (i.e., 7 inputs) is matched to a distance to the transmitter (i.e., 1 output) using one hidden layer.

The hidden layer contains the weights and biases which are adjusted in the training process using different learning algorithms. In our case, the mathematical relationship between the set of inputs and the distance to the transmitter requires a non-linear matching technique. ANNs performing non-linear computations are of two types, Multi-Layer Perceptron (MLP) and Radial Basis Function (RBF) neural networks. The use of feed forward MLP ANNs with back-propagation learning algorithm is proven to give accurate estimation results in underground narrow-vein mines [31], [42], [4]. After training an ANN, the values of the weights and biases

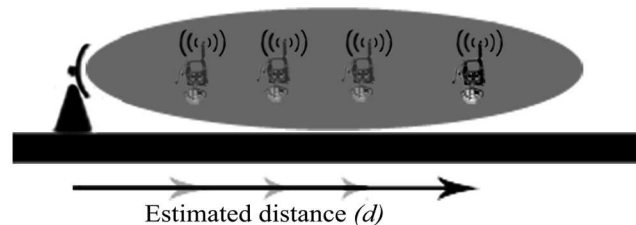


Figure 12.2 – The CIRs are extracted at different distances to the transmitter with 1-meter step size along the x -axis.

are saved and the model would be ready to estimate any new position based on the extracted fingerprints. In order to ensure that the model is not exclusive to the collected fingerprints, ANNs are trained to estimate the position of transmission using 75% of the collected fingerprints while keeping 25% of the data for testing purposes. CIR-based fingerprint positioning in the presence of one receiver only is shown in Fig. 12.2. After extracting the CIR from the received signal, a fingerprint is obtained

and the position of the miner is estimated instantaneously using a trained ANN. The novel CIR-based fingerprinting approach introduced in [31] localizes accurately with 2 meters estimation error for 90% and 80% of the trained and untrained patterns, respectively.

As we demonstrate later in Sec. 12.3, a fingerprint's length (L_f) depends on the localization technique put in practice which also defines the number of inputs fed to a given ANN where:

$$N_{inputs} = L_f.$$

The output of the ANNs is the distance to the transmitter with respect to R_1 . In [4], [6] and [5], N_{inputs} is used to calculate the number of neurons n_n that define the hidden layer of ANNs as follows:

$$n_n = 2N_{inputs} + 1 = 14l + 1.$$

In this paper, we further enhance the design of ANNs by searching for the optimum number of neurons needed for each localization technique and fingerprinting set. Dynamic allocation of n_n is proven to be very useful in the case of different sampling resolution and will be discussed in more details in Sec. 12.5.

12.3 Cooperative Localization Using Spatial and Temporal Diversities

The high accuracy of the CIR-based fingerprint-positioning system in the presence of one receiver and the need for a global localization system that covers the whole underground tunnel-shaped topology of mines led to the innovation of a new cooperative CIR-based fingerprint-positioning system in [4]. The introduction of cooperation

between different APs or localizing units prior to estimating a mobile's position is the first step to globalize the underground localization system. The cooperative approach in [4] not only enhances the positioning accuracy by exploiting Rx spatial diversity of different fingerprints in underground mines, but also removes the ambiguity that surrounds the mobile's exact position in the presence of junctions by using data measurements collected from more than one receiver. Yet, the system in [4] is challenged by the spatial confinement of narrow-shaped quasi-curvilinear tunnels on one hand and the fluctuation of fingerprints for the same position on the other. Memory-type fingerprints are introduced in [6] to empower the basic cooperative solution and enrich the fingerprints by using the temporal diversity of the limited motion patterns within the confinement of narrow-shaped tunnels. By exploiting Rx spatial diversity on one side and the temporal diversity on another, a cooperative memory-assisted technique is finalized in [5] as an accurate wireless localization system for underground narrow-vein mines. In the following discussion, we explain the fundamentals of each technique separately then we introduce a new MISO/MIMO-type fingerprinting technique that exploits both Tx and Rx spatial diversities. In addition to that, we further enhance the systems in [4], [6] and [5] by finding the optimum number of neurons needed for each localization technique and sampling grid's resolution using a trial and error mechanism. For simplicity, all developed techniques are explained at sampling step-size $S_x = 1 \text{ m}$ ¹ then they are fully analyzed at different S_x in Sec.12.5.

12.3.1 Exploiting Rx -spatial diversity

In underground narrow-vein mines, two receivers separated by a spatial distance D are able to cover the narrow-shaped topology of a tunnel as shown in Fig. 12.3. Exploiting the spatial diversity of both receivers to localize a transmitter in between

¹ S_x , measured in meters, is the step size between consecutive offline fingerprint measurement points along the x -axis of the tunnel.

efficiently increases the accuracy and precision of the CIR-based localization technique. In addition to that, estimating the distance from more than one receiver distributed in the tunnel-shaped topology removes the ambiguity surrounding the exact mobile's location in the presence of junctions. Cooperation is the key behind deploying a complete wireless localization system in underground narrow-vein mines. When the signal arriving from a transmitter fades, it may lead to faulty position estimation. However, when exploiting the spatial diversity of two receivers, a signal fading at receiver R_1 may still hold significant information about the transmitter's position once the signature is added to the fingerprint collected from R_2 being present at better Radio Frequency (RF) conditions.

Cooperation may be addressed in different techniques. The first technique gives each receiver the privilege of estimating the distance based on the collected fingerprint, then an average of both estimation errors is taken as a final result by a central system containing the map of the mine and the exact positions of the deployed localizing units or APs. Another technique which succeeds to provide better results in [4] concatenates the two signatures (i.e., sub-fingerprints) forming one fingerprint which is double the size of the conventional CIR-based fingerprint in [31] (i.e., 14 parameters, 7 from each AP). The length of the fingerprint defines the number of inputs of the ANN, hence, each of the designs requires a different ANN architecture. As

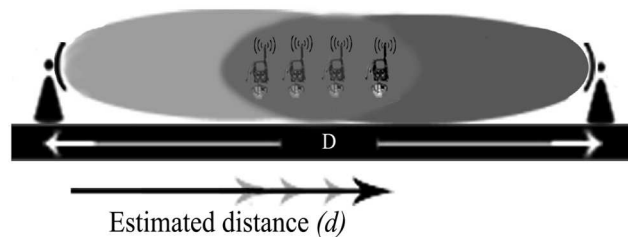


Figure 12.3 – Localization using two signatures of two receivers in the area where two signals intersect.

the transmitter moves inside the tunnel, the transmitted signals are collected from receivers R_1 and R_2 forming two sets of fingerprints $S^{R_1} = \{f_1, f_2, f_3, \dots, f_m\}$ and $S^{R_2} = \{f'_1, f'_2, f'_3, \dots, f'_m\}$. Using S^{R_1} and S^{R_2} we may create two different ANN designs depending on whether we want to process the fingerprints separately or jointly. The output of this ANN is $D = \{d_1, d_2, d_3, \dots, d_m\}$ which represents the estimated distances to R_1 . It should be noted that the distance to the transmitter is taken along the longitude of the tunnel (i.e., x positions) while neglecting the y -dimension across its width because it is less significant.

Localization using separate neural networks

Using this technique, the sets of fingerprints S^{R_1} and S^{R_2} are fed to ANN_1 and ANN_2 , respectively. The structure of the neural network is shown in Fig. 12.4. The estimated mobile's position d_i^* is obtained with respect to R_1 by averaging both approximations produced by ANN_1 and ANN_2 . The positioning error reported in [4] for this technique is 1 m for 90% of the training and testing data.

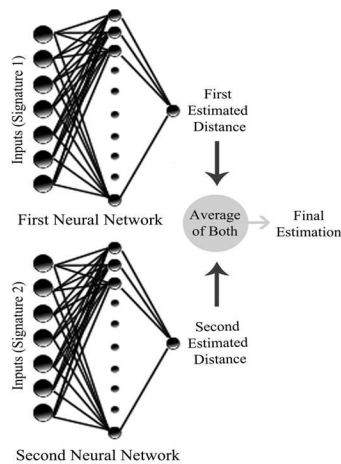


Figure 12.4 – Localization based on two separate estimations.

Localization using one neural network

In this technique, one neural network collects the extracted parameters from both receivers forming one fingerprint that contains 14 parameters (7 from each receiver). By concatenating both sets, S^{R_1} and S^{R_2} , the final set of fingerprints is represented by:

$$S = \{F_1, F_2, F_3, \dots, F_m\} = \{(f_1, f'_1), (f_2, f'_2), (f_3, f'_3), \dots, (f_m, f'_m)\}.$$

As shown in Fig. 12.5, Rx spatial diversity is exploited using one neural network that is trained based on fingerprints of higher chain lengths. The localization accuracies shown in Sec. 12.4.1 for this technique are 77 cm and 90 cm for 90% of the training and testing data, respectively.

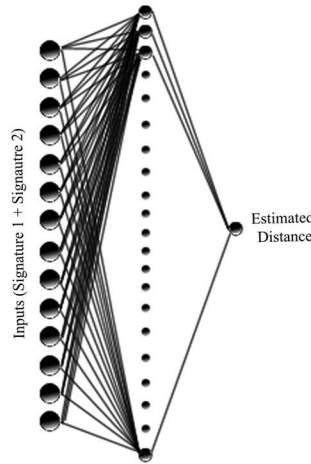


Figure 12.5 – Neural network based on multiple signatures.

12.3.2 Exploiting temporal diversity

Up to this point, the fingerprints extracted from the CIRs represent the signatures of instantaneous measurements without introducing memory. Any further enhancement of the spatial technique requires implementing more APs, which is neither reasonable nor cost effective in the confinement of the narrow-shaped tunnels. When

exploiting spatial diversity only, the previous positions of the transmitter do not affect the estimation of its current location. This work introduces a fingerprinting technique that records the signatures (i.e., sets of 7 parameters) up to a certain memory level l . The chain length of the fingerprint increases as l increases. A fingerprint that is extracted from two distinct receivers as in Sec. 12.3.1 has the same chain length as a fingerprint extracted with memory level $l = 2$. However, the latter is obtained using one receiver only exploiting temporal diversity whereas the memoryless fingerprint generated from two receivers in Sec. 12.3.1 exploits spatial diversity.

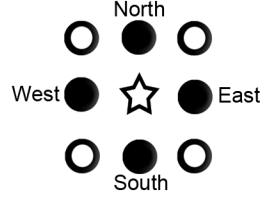
Making use of the quasi-curvilinear topology of narrow-vein mines, a scalable ANN is trained on the possible combinatorial paths (i.e., possible temporal fingerprints) that may lead to potential mobile positions inside the tunnels at time t_0 . The path fingerprint

$$f_i^j = \left(f_{i_{t_0}}, f_{i_{t_{-1}}}, f_{i_{t_{-2}}}, \dots, f_{i_{t_{-(l-1)}}} \right).$$

is the concatenation of the fingerprints measured over short time instances while moving towards a destination to be estimated at $d_i^{t_0}$. l is the memory level or the number of concatenated fingerprints and it defines the length of a temporal fingerprint L_f where:

$$L_f = 7l.$$

Since the fingerprints of all positions in the mine are known, temporal fingerprints with given chain lengths are obtained while taking into account all the possibilities to reach a given position. Because of the tunnel-shaped topology of the narrow-vein mines, motion inside the tunnels is predictable and the temporal fingerprints are organized in chains representing all possible motion patterns inside a tunnel. A simple example is illustrated for $l = 2$ in Fig. 12.6 where the star represents the miner's position at time t_0 . Assume that the previous possible positions at t_{-1} are the highlighted circles in addition to the current position (i.e. stationary). The CIR-


 Figure 12.6 – Possibilities of previous positions for $l = 2$.

based temporal fingerprints for the case where $l = 2$ are listed in Tab. 12.1 where the possible temporal concatenations reaching the star position are:

 Table 12.1 – Fingerprints of each location for $l = 2$

Fingerprint	Source of Parameters
1	CIR_{t_0} & CIR_{center}
2	CIR_{t_0} & CIR_{north}
3	CIR_{t_0} & CIR_{south}
4	CIR_{t_0} & CIR_{west}
5	CIR_{t_0} & CIR_{east}

$$F_i^1 = (f_i, f_i), F_i^2 = (f_i, f_{inorth}), F_i^3 = (f_i, f_{isouth}), F_i^4 = (f_i, f_{iwest}), F_i^5 = (f_i, f_{ieast}).$$

Five path fingerprints are obtained for the same position located at d_i (i.e., star position) forming a combinatorial subset $S_i = \{F_i^1, F_i^2, F_i^3, F_i^4, F_i^5\}$. Moving the star character like a pointer for all positions inside the tunnel, we collect all possibilities for all positions of interest while respecting the boundary conditions of confined tunnels. The total set of temporal fingerprints is denoted by $S = \{S_1, \dots, S_i, \dots, S_m\}$ and it corresponds to all distances $D = \{d_1, \dots, d_i, \dots, d_m\}$. As l increases, more paths may be drawn from previous possible positions as shown in Fig. 12.7 where $l = 3$. Temporal sub-fingerprints are recorded and concatenated as the miner heads to a position to be estimated (i.e., at the star position). For each position, all path fingerprints (i.e., concatenated sub-fingerprints) are combined in the offline phase forming the training set of the ANNs. The maximum number of path fingerprints

j_{max} that may be obtained for a given position is limited by the upper bound N_{f_p} :

$$j_{max} \leq N_{f_p} = 5^{(l-1)}.$$

When increasing the memory level l , the combinatorial number of possible finger-

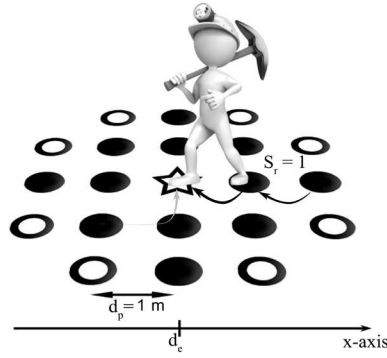


Figure 12.7 – Possibilities of previous positions for $l = 3$.

prints increases the size of training data exponentially (without the need of additional data measurements), while it linearly increases the number of neurons n_n . This satisfies the rule of thumb for generalization where N_{inputs} must be four times greater than n_n [17].

A localization technique that exploits temporal diversity only (i.e., in the presence of one receiver) is investigated and the results are shown in Sec 12.4. The ANN is scalable according to L_f but it follows the design presented in Sec. 12.3.1 and shown in Fig. 12.5. For each time depth l , a new ANN is trained using 75% of the generated fingerprints. Memory-assisted localization using temporal diversity in the presence of one receiver only is analyzed up to $l = 4$ after which no significant performance is achieved.

12.3.3 Exploiting both Rx -spatial and temporal diversities

By comparing temporal diversity fingerprinting techniques in Sec. 12.3.2 to the cooperative techniques used in Sec. 12.3.1, some conclusions may be drawn. First, the path fingerprinting technique exploits time diversity whereas the cooperative technique uses Rx spatial diversity to enhance the accuracy and precision of the estimated results. Second, the accuracy of geo-location using the temporal technique may be increased by increasing the memory level (l) without the need of implementing more access points in mine tunnels. Although the temporal diversity at high memory levels outperforms the use of cooperative memoryless localization in Sec. 12.3.1 in terms of accuracy and precision, using one receiver alone may result in misleading information about the exact position (i.e., direction) of the mobile user or miner in the presence of junctions and interconnected tunnels. A more intelligent localizing system integrates the in-built path fingerprinting technique at a given memory level l in a cooperative spatial localizing system (i.e., diversity in both space and time). This would lead to higher performances that could match those of memory-assisted localization alone at higher time depth l (i.e., only time diversity).

Consider the two receivers as shown in Fig. 12.3 with memory capabilities. In a cooperative memory-assisted localization technique that exploits the spatio-temporal diversity, the subset of path fingerprints $S_i^{R_1} = \{F_i^{R_1,1}, F_i^{R_1,2}, F_i^{R_1,3}, \dots, F_i^{R_1,j_{max}}\}$ measured at a distance d_i away from R_1 is properly combined path-wise with another subset $S_i^{R_2} = \{F_i^{R_2,1}, F_i^{R_2,2}, F_i^{R_2,3}, \dots, F_i^{R_2,j_{max}}\}$ collected at a distance $d_2 = D - d_1$ away from R_2 forming the spatio-temporal fingerprint set:

$$S_i = \left\{ (F_i^{R_1,1}, F_i^{R_2,1}), (F_i^{R_1,2}, F_i^{R_2,2}), (F_i^{R_1,3}, F_i^{R_2,3}), \dots, (F_i^{R_1,j_{max}}, F_i^{R_2,j_{max}}) \right\}.$$

By letting R_1 and R_2 extract fingerprints with time depth l_1 and l_2 respectively, different cooperative memory-assisted localization scenarios may be obtained and they are denoted by (l_1, l_2) . For example, a transmitter located a distance d_i and time t_0 may be localized using the cooperative memory-assisted technique $(l_1 = 2, l_2 = 1)$ based on the concatenated spatio-temporal fingerprint $F_i = (F_i^{R_1}, F_i^{R_2})$ where

$$F_i^{R_1} = (f_{i_{t_0}}^{R_1}, f_{i_{t_{-1}}}^{R_1}),$$

$$F_i^{R_2} = (f_{i_{t_0}}^{R_2})$$

are fingerprints collected from R_1 and R_2 , respectively. The spatio-temporal fingerprint F_i used in memory-assisted localization for $(l_1 = 2, l_2 = 1)$ is formed from 3 CIRs (i.e., 21 parameters) for each position inside the quasi-curvilinear topology of narrow-vein mines. In other words, for this specific example, R_1 's fingerprint is the concatenation of two fingerprints recorded at time instances t_{-1} and t_0 (memory-assisted fingerprinting with $L_f^{R_1} = 14$), whereas R_2 's fingerprint is recorded at t_0 only (memoryless fingerprinting with $L_f^{R_2} = 7$). Thus, the number of inputs N_{inputs} of the ANN is defined by the length of the spatio-temporal fingerprint which is dependent on both l_1 and l_2 where:

$$N_{inputs} = 7(l_1 + l_2).$$

Several test cases were conducted while increasing the memory levels l_1 and l_2 of R_1 and R_2 , respectively, and may be fully reviewed in [5].

The temporal sampling rate S_r increases at higher V_t providing the ANN with the same spatio-temporal fingerprint that may be collected at a lower V_t and lower S_r . The relationship may be demonstrated as follows:

$$V_t \leq d_p / \tau_s \leq d_p S_r,$$

where V_t is transmitter's speed, d_p is the distance separating consecutive fingerprint measurement positions, τ_s is the sampling time and S_r is the sampling rate. In our case $d_p = 1$ m which concludes that the sampling rate S_r at which the fingerprints are extracted is lower bounded by the transmitter's speed V_t :

$$S_r \geq V_t.$$

12.3.4 Exploiting both Tx and Rx spatial diversities

In Sec.12.3.1, Rx spatial diversity is exploited by collecting two fingerprints from two distinct receiver antennas at Rx_1 and Rx_2 using one transmitter antenna Tx_1 . In the following, we introduce a new SIMIO/MIMO-type fingerprinting technique that exploits the spatial diversities of more than one Tx being at a close antenna spacing of $\delta^{Tx} = 1$ m or less. From an implementation's point of view, antennas with $\delta^{Tx} = 1$ m or $\delta^{Tx} = 0.5$ m may be placed on heavy machinery or built in the miners' suits on the shoulders. For MISO-like fingerprints (i.e., fingerprints collected at R_1 from two Tx antennas), Tx spatial diversity is exploited at the transmitter's end in the presence of one receiver only without the need of memory. A MISO-type fingerprint is denoted by:

$$F_i^{MISO} = (f_i^{Tx_1}, f_i^{Tx_2}),$$

Where $f_i^{Tx_1}$ and $f_i^{Tx_2}$ are the fingerprints collected by Rx_1 , at a position i , for Tx_1 and Tx_2 , respectively. MIMO-type fingerprints exploit both Tx and Rx spatial diversities. They are simulated by considering two receiver antennas Rx_1 and Rx_2 of R_1 and R_2 , respectively. A MIMO-type fingerprint is denoted by:

$$F_i^{MIMO} = \{(f_i^{Tx_1}, f_i^{Tx_2}), (f_{i'}^{Tx_1}, f_{i'}^{Tx_2})\}.$$

While $f_i^{Tx_1}$ and $f_i^{Tx_2}$ represent the fingerprints collected by Rx_1 , $f_{i'}^{Tx_1}$ and $f_{i'}^{Tx_2}$ are the fingerprints collected by Rx_2 , at a position $i' = D - i$, for Tx_1 and Tx_2 , respectively. The estimated distance of the transmitter is always taken along the x -axis and it represents the distance separating R_1 and the midpoint of Tx_1 and Tx_2 . MISO/MIMO-type fingerprints are studied at $\delta_x^{Tx} = 1$ m along the x -axis and at $\delta_y^{Tx} = 1$ or 0.5 m along the y -axis.

12.4 Experimental Results

The Cumulative Density Function (CDF) is used to show the precision (i.e., percentage of treated measurements) of each localization technique compared to its positioning accuracy (i.e., localization error in meters). First, localization results are analyzed for both the training and testing data when cooperative Rx spatial diversity is introduced. Then the results of exploiting temporal and spatio-temporal diversities are presented. In Sec. 12.4.4, positioning accuracies using Tx spatial diversity and MISO/MIMO-type testing fingerprints are discussed then compared to all developed localization techniques. It is important to add that every localization approach undergoes an extensive search for the optimum number of neurons to be used in the hidden layer of its respective ANN design. The search for the optimum number of neurons is favored to increase the positioning accuracy of the testing fingerprints while maintaining accurate positioning for the training data. As a result, localization robustness is increased producing unbiased positioning results that can be compared for the same techniques at lower sampling resolution later in Sec. 12.5. Moreover, all fingerprints used below are collected at $S_x = 1$ m and divided into training data (i.e., 75% of the total number of fingerprints) and testing data (i.e., 25% of the total number of fingerprints).

12.4.1 Results of memoryless localization techniques using Rx spatial diversity

The localization techniques that exploit Rx spatial diversity are discussed in Sec. 12.3.1 and their results are plotted in Figs. 12.8 and 12.9 for the training and testing data, respectively. CDF plots shown in each figure correspond to the estimation error of different spatial, temporal and spatio-temporal localization techniques. Compared to the original memoryless (1,0) technique developed in [31], the positioning errors that result from exploiting Rx spatial diversity are marked as the cooperative memoryless (1,1) localization technique. It should be noted that the results shown here

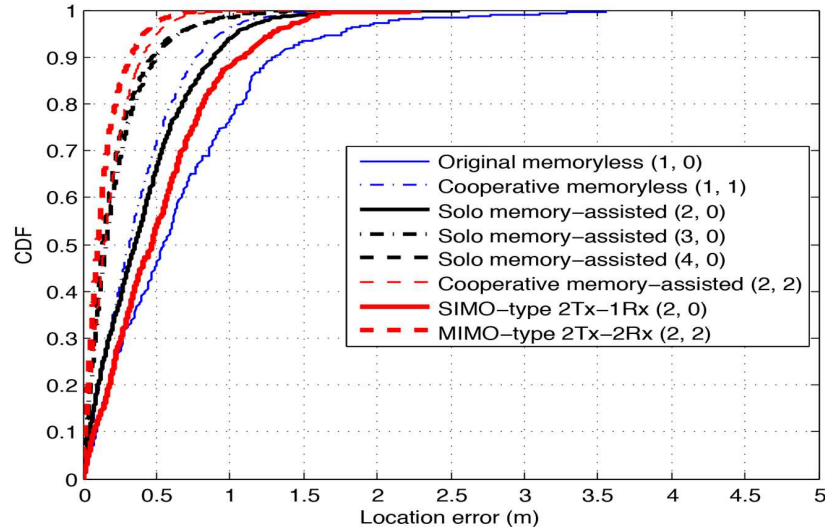


Figure 12.8 – CDF of the training data for different localization techniques at memory levels (l_1, l_2) .

are analyzed for a separation distance $D = 80$ m where other scenarios may be reviewed in [4]. The estimation errors of localization based on one receiver only were reported to be 1.3 m and 1.4 m for 90% of the training and testing data, respectively. Performance results show close similarity from both ends (i.e., R_1 and R_2) although two different ANNs were trained at both ends. For consistency, only results of R_1

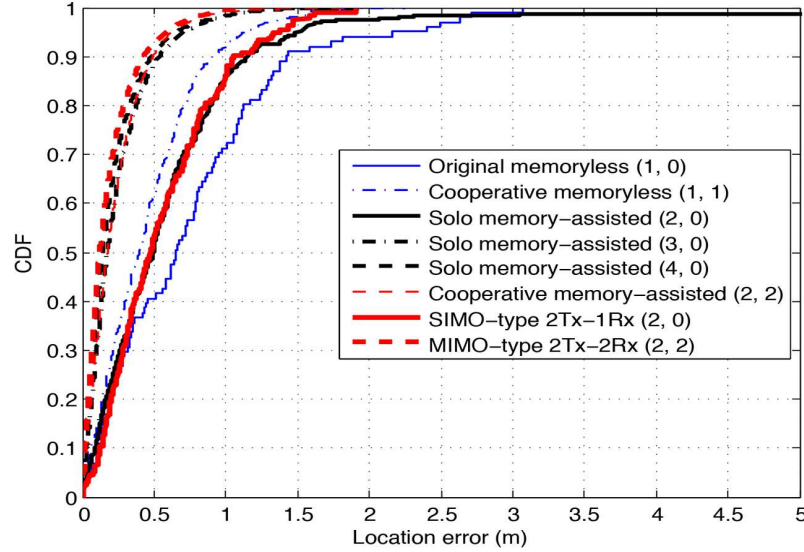


Figure 12.9 – CDF of the testing data for different localization techniques at memory levels (l_1, l_2) .

are reported. This accuracy is enhanced for the training data after the cooperative localization technique was introduced in [4]. Using the cooperative technique based on separate ANNs discussed in Sec. 12.3.1, the estimation error drops to 1 m for 90% of both the training and testing data [4]. Again, the spatial cooperative technique that uses one neural network with 14 inputs resulted in estimation errors of 77 cm and 90 cm for the training and testing data, respectively.

12.4.2 Results of solo memory-assisted localization techniques

The results of solo localization (i.e., in the presence of one receiver) using in-built path fingerprinting discussed in Sec. 12.3.2 are optimized for different memory levels up to $l = 4$. The results of the training and testing fingerprints using solitary memory-assisted localization ($l_1 = 2, 3, 4, l_2 = 0$) are shown and compared to the developed techniques in Figs. 12.8 and 12.9, respectively. For each l , a new ANN is created and trained on 75% of the generated fingerprints. For $l = 2$, estimation

errors are reported to be 89 cm and 1.14 m for 90% of the training and testing data, respectively. For the same precision of 90% at $l = 3$, localization errors are found to be 50 cm and 53 cm for the training and testing data, respectively. The estimation error keeps on decreasing with the increase of the fingerprints' chain length (i.e., time depth) and it reaches 48 cm for $l = 4$ for both the training and testing data. At $l = 5$, the error maintains a similar accuracy to the one attained at $l = 4$ but no significant gain is obtained [5].

12.4.3 Results of cooperative memory-assisted localization using spatio-temporal diversity

As discussed earlier in Sec. 12.4.2, cooperative memory-assisted localization techniques exploit both temporal and Rx spatial diversities of CIR-based fingerprints. The results of the training and testing fingerprints are shown and compared to the previous techniques in Figs. 12.8 and 12.9, respectively. Performance results are plotted according to the memory levels (l_1, l_2) of receivers (R_1, R_2) , respectively. The best performance among spatio-temporal localization techniques is achieved once both receivers cooperate and introduce memory. In the case where $(l_1 = 2, l_2 = 2)$, the error drops below 50 cm for 90% of the training and testing data, respectively.

It is worth stating at this point that cooperative spatio-temporal localization technique performs better than the previously discussed techniques in Secs. 12.3.1 and 12.3.2. To illustrate this point we compare the performance of all developed techniques based on the length of the fingerprint L_f that defines the design of their respective ANNs. For example, at $L_f = 14$, cooperative memoryless localization (i.e., exploiting spatial diversity only) outperforms solo memory-assisted localization (i.e., exploiting temporal diversity only) when $l = 2$ and surprisingly provides a close performance to solo memory-assisted localization technique with $L_f = 21$ (i.e., $l = 3$).

This result shows the importance of cooperation between two spatially separated receivers prior to position estimation and clearly highlights the gain achieved by Rx spatial diversity. When comparing at $L_f = 28$, the best performance is achieved by the new 2-by-2 memory assisted localization technique ($l_1 = 2, l_2 = 2$) introduced in [5]. The one-step increase in the memory levels at both receivers significantly increases the accuracy and precision surpassing the previously discussed scenarios with much lower complexity as compared to the temporal approach that performs at $l = 4$. Location errors for 90% of the testing fingerprints of the different localization techniques are listed for $S_x = 1$ m in Tab. 12.2.

12.4.4 Results of MISO/MIMO-type fingerprinting using Tx and Rx spatial diversities

As discussed in Sec. 12.3.4, Tx spatial diversity is added to increase the robustness and performance of CIR-based fingerprint-positioning techniques. By concatenating a new Tx sub-fingerprint, we increase the length of the fingerprint fed to the ANN taking advantage of the information it brings about the position of the transmitter. MISO-type fingerprints are denoted by $2Tx-1Rx$ and they use an ANN design of 14 inputs taken from two Tx antennas separated by a given distance δ^{Tx} along either the x or y axis. Similarly, MIMO-type fingerprinting techniques are denoted by $2Tx-2Rx$ techniques. At this point, we draw attention to localization results at $S_x = 1$ m shown in Fig. 12.14 and Tab. 12.2 for both MISO-type and MIMO-type fingerprint positioning at $\delta_x^{Tx} = 1$ m, $\delta_y^{Tx} = 1$ m and $\delta_y^{Tx} = 0.5$ m. When compared at the same L_f with $S_x = 1$ m and $\delta_y^{Tx} = 1$ m, localization errors of using $2Tx-1Rx$ fingerprints drop to 85 cm compared to 1.15 m when using memory-type fingerprinting with ANN(2,0). When comparing Tx and Rx spatial diversity fingerprint-positioning techniques, we notice that Rx spatial diversity of ANN(1,1) that use $1Tx-2Rx$ finger-

prints outperform that of Tx spatial diversity using $2Tx-1Rx$ MISO-like fingerprints, however, increased performance is noticed by the addition of a second Tx fingerprint when compared to the original technique of ANN(1,0) which uses $1Tx-1Rx$ fingerprints. It is important at this point to mention that exploiting Rx spatial diversity is more beneficial than temporal diversity. One can compare the localization accuracy of ANN(1,1) (i.e., $1Tx-2Rx$ ANN) to ANN(2,0) and draw the conclusion that, for the same L_f , exploiting Rx spatial diversity only (i.e., using ANN(1,1)) results in positioning errors of 91 cm, 90% of the times, for the testing fingerprints as compared to errors of 1.15 m using ANN(2,0). The same conclusion holds when comparing training spatio-temporal fingerprints of ANN(2,2) to memory-type fingerprints of ANN(4,0) with localization errors of 40 cm and 47 cm, respectively.

Exploiting both Tx and Rx spatial diversities within the same localization techniques increases localization robustness and reduces the complexity of introducing memory-type fingerprints. For $\delta_y^{Tx} = 1$ m, Tx and Rx spatial diversities may show a slight degradation in accuracy once compared to ANN(2,2), however, the use of MISO/MIMO-type fingerprints proves to sustain positioning precision for all the remaining antenna spacing scenarios (i.e., $\delta_x^{Tx} = 1$ m and $\delta_y^{Tx} = 0.5$ m) and paves the road for a solid localization technique that performs accurately even at lower grid resolution as discussed in the following section.

12.5 Reaping Diversity Benefits to Simplify Measurement Campaigns

Cutting down the cost of measurement campaigns while, at the same time, maintaining high performance is one of the challenges that confront any fingerprinting approach. By reducing the amount of collected measurements, fingerprinting tech-

niques risk losing information that ANNs need in order to interpolate the relationship between the CIR-based fingerprints and transmitter's distances. A smart localization system would maintain high positioning accuracy while using less fingerprint measurements [7]. Earlier in Sec.12.4.2, the performance results were conducted using the original grid's resolution where offline fingerprints were collected at $S_x = 1$ m. In the following, we study the effect of sampling resolution on the proposed localization techniques in [31], [4], [6], [5] and the new developed localization technique that exploits Tx spatial diversity of MISO/MIMO-type fingerprints. The spatial sampling resolution is reduced by increasing S_x to 2 m, 3 m and up to 6 m resulting in a split of the original grid into 2, 3 and up to 6 sub-grids, respectively, by counting for the transmitter's initial position on the grid.

12.5.1 Designing ANNs at higher S_x : Interpolation versus accuracy

The objective of this experiment is to analyze the effect of grid resolution (i.e. reducing training data measurements by increasing S_x) on the positioning accuracy of each spatial and/or temporal ANN technique. The challenge that ANNs face with less data measurements and different grid resolution lies in their ability to map the fingerprints of one sub-grid resolution to its respective output distances on one hand. On the other hand, the ANN trained on one sub-grid should effectively generalize the solution space, interpolate and localize fingerprints collected from the remaining sub-grids within the same resolution while maintaining reasonable accuracy and precision. A simple example would be two ANNs trained on fingerprints measured at odd and even distances, respectively. With S_x increased to 2 m, both ANNs are tested on their own sub-grid (i.e., odd or even) and then challenged by the supplementary sub-grid fingerprints within the same spatial sampling resolution [7]. By doing so, not only

do we reduce the cost of data measurement collection but we also identify the most accurate ANN-based positioning techniques discussed in the literature for different sampling resolution.

In order to come up with an adequate ANN design, a search for the optimum number of neurons for each ANN technique becomes very essential. While ANNs of each sub-grid are trained on 75% of the same sub-grid measurements, they are then tested on 25% of the remaining x -position patterns that may be seen during training plus 25% of the other sub-grid candidates within the same spatial sampling resolution set (i.e., 25% of x -positions of sub-grids never seen in the training phase). The variable size of training data sets that result from splitting the grid's resolution requires a dynamic allocation of the number of neurons to be used. Too many neurons would produce a very accurate ANN design for the specific sub-grid while causing high error rates for the remaining sub-grids. Similarly, few neurons would not bring accurate positioning results. Optimizing the number of neurons based on the number of fingerprints of each ANN is done by trial and error. A massive simulation was performed in order to find the successor ANN designs for each technique and for each resolution sub-grid.

A successor ANN is the one that can most accurately localize its own sub-grid and 25% of the remaining sub-grids in each sampling resolution setup. The reported accuracy of each sampling grid's resolution, for a given ANN technique, is based on the joint accuracy results of the successor sub-grid ANNs. The simulation was conducted using MATLAB to train multiple sub-grid ANNs while varying the number of neurons n_n between 1 and N_n such that:

$$1 < n_n < N_n = 2N_i + 1,$$

where N_i is the number of inputs of the ANN that depends on the used localization technique and memory levels as discussed in Sec. 12.3.2. The same experiment is done for all the remaining sub-grids within the same S_x . After running three consecutive trials for each n_n , a successor ANN design is selected for the given sampling resolution. Performance results combine all sub-grid ANNs' positioning errors performing on a given number of neurons and a certain S_x . It should be noted that this experiment is also repeated for each localization approach as the number of inputs varies between spatial and spatio-temporal fingerprint-positioning techniques and so does the maximum number of neurons in the experimental range.

12.5.2 Experimental results

Running a simulation of more than 14,000 ANNs including all possible design scenarios, the optimum number of neurons required for each sampling step-size S_x and localization technique were identified and were used as a benchmark for further ANN designs as shown in Fig.12.10. The localization accuracy of 1.41 m (circled in Tab. 12.2) obtained at $S_x = 1$ m using the elemental localization technique ANN(1,0) in [31] will be used as a benchmark to be compared with the performance of the evolved spatio-temporal techniques at different S_x . The efficiency of each technique lies in its ability to sustain the 1.41 m target at higher sampling step-size S_x (i.e., lower sampling grid's resolution) bearing in mind the number of neurons needed to do so. It can be noticed that localization techniques exploiting temporal diversity (i.e., ANN(2,0), ANN(3,0) and ANN(4,0)) require higher number of neurons compared to spatial localization techniques (i.e., ANN(1,0) and ANN(1,1)).

On the other hand, and for the same number of inputs or memory level, a spatio-temporal technique such as ANN(2,2) starts off with a higher number of neurons at $S_x = 1$ m when compared to ANN(4,0). The increased complexity that comes with

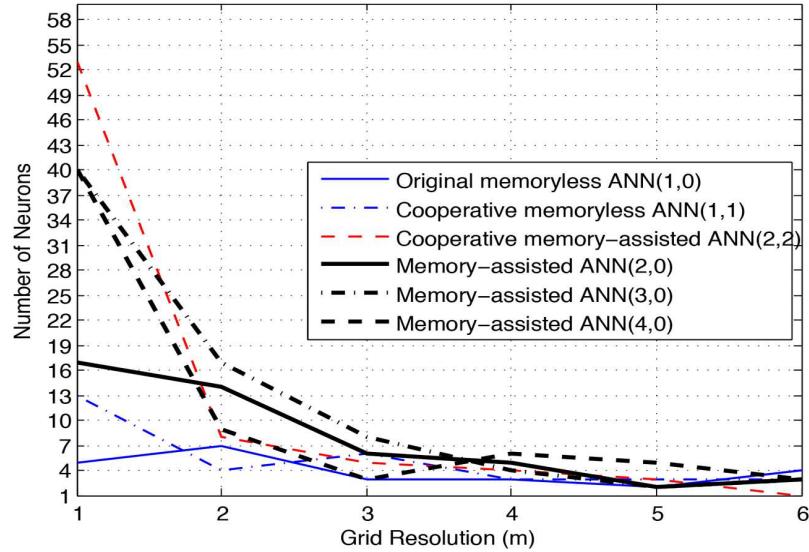


Figure 12.10 – Optimum number of neurons for different ANNs.

increasing the number of neurons is traded off for a better accuracy and precision. An interesting theory shows that the number of neurons also decreases with the decrease in sampling resolution until they all settle below 7 neurons. After selecting the optimum number of neurons, we compare the accuracy and precision of each technique for different sampling resolutions. Sample CDF plots in Figs. 12.11 and 12.12 were selected to show the cumulative testing localization errors of all localization techniques at $S_x = 3$ m and $S_x = 6$ m, respectively. The remaining grid resolution results, at 90% precision, are divided between Figs. 12.13 and 12.14 to better visualize the performance of each of the developed localization techniques for different δ^{Tx} and S_x .

As expected, the localization accuracy decreases at lower grid resolutions. Furthermore, when excluding Tx spatial diversity from the equation, the spatio-temporal localization technique ANN(2,2) holds as the most accurate technique even with lower sampling resolution. In fact, ANN(2,2) surprisingly achieves the same accuracy of 1.4 m at $S_x = 6$ m when compared to the benchmark technique using ANN(1,0) at

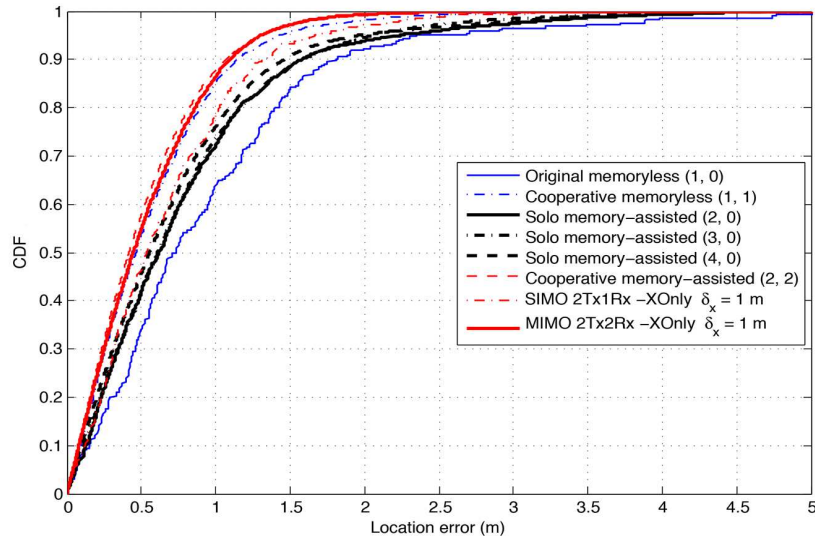


Figure 12.11 – Localization performance at $S_x = 3$ m.

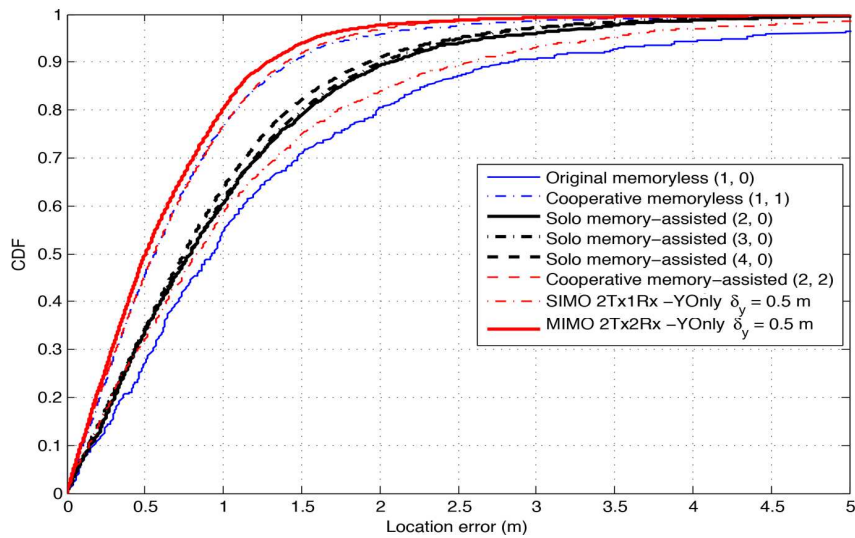


Figure 12.12 – Localization performance at $S_x = 6$ m.

$S_x = 1$ m. It can also be noticed that ANN(1,1) performs better than the remaining temporal techniques at lower grid resolution and may achieve the 1.4 m benchmark at $S_x = 5$ m. Temporal fingerprints, which are chains of consecutive sub-fingerprints, carry lower information about the current position at lower sampling resolution (i.e., higher S_x) because the correlation between sub-fingerprints decreases when they are spatially apart. With accuracies of around 2 m for 90% of the testing data at $S_x = 6$ m, memory-assisted fingerprinting techniques cannot be considered as the best candidates for localization at lower grid resolution. If cost is the main concern in the absence of Tx spatial diversity, ANN(1,1) proves to maintain close accuracies compared to ANN(2,2) at 90% precision level and it may be selected as a localization technique for lower grid resolution being less complex than ANN(2,2) in terms of fingerprint concatenation and ANN design.

By introducing Tx spatial diversity and analyzing the 90% performance results

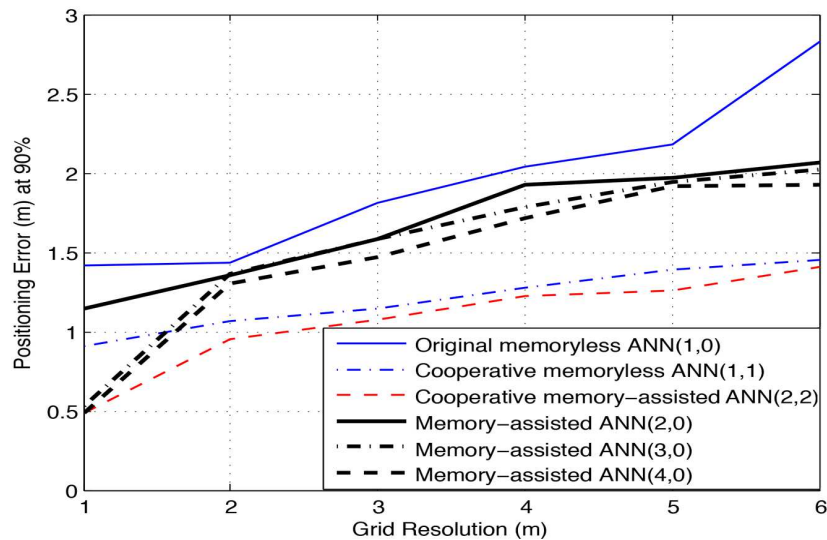


Figure 12.13 – Positioning errors from CDFs of testing data at 90% precision.

of MISO/MIMO-type fingerprints shown in Fig. 12.14 and Tab. 12.2, many conclusions may be drawn. First, by increasing S_x to 2 m, the measurement campaign's cost

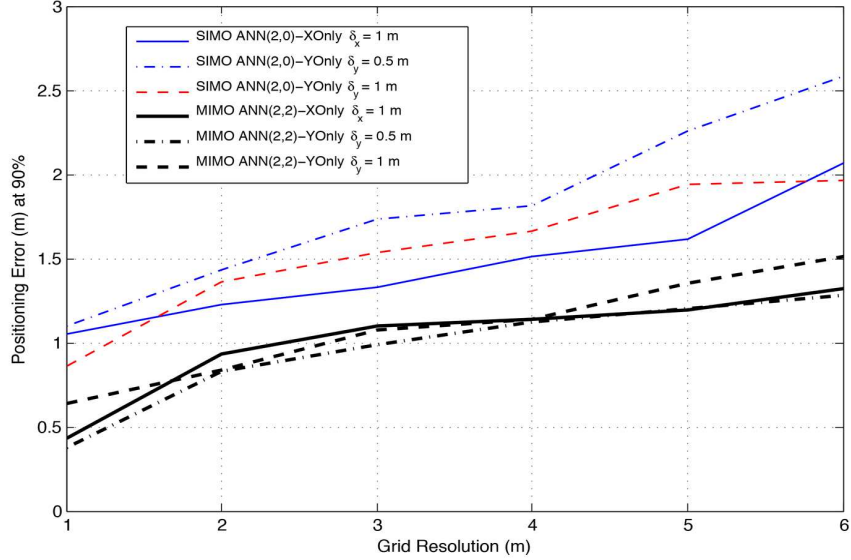


Figure 12.14 – Positioning errors from CDFs of MISO/MIMO-type testing data at 90% precision.

is cut down to half while maintaining accurate localization using MISO/MIMO-type fingerprints with positioning errors as low as 83 cm 90% of the time! Secondly, although MISO-type fingerprints using $2T_x1R_x$ succeed to show high accuracy results, MIMO-type fingerprints, being the best candidates for low grid resolution localization, prove to maintain very accurate positioning results of 38 cm and 1.28 m for the testing data at $S_x = 1$ m and $S_x = 6$ m, respectively. The outstanding performance of MIMO-type fingerprints at $\delta_y^{Tx} = 0.5$ m (highlighted in dotted lines in Tab. 12.2) surpasses the benchmark of the original localization technique using ANN(1,0) even when performing at $S_x = 6$ m. Localization using MIMO-type fingerprints and ANNs is, as yet, the most accurate and cost-efficient solution that attains 1.28 m positioning error, 90% of the time, using only one sixth of the data measurements.

Table 12.2 – Performance results with multiple resolution

ANN Technique	Grid Resolution Accuracy Results					
	1 m	2 m	3 m	4 m	5 m	6 m
ANN(1,0)	1.42 m	1.44 m	1.81 m	2.04 m	2.12 m	2.83 m
ANN, 2Tx1Rx $\delta_y^{Tx} = 0.5$ m	1.10 m	1.43 m	1.73 m	1.81 m	2.26 m	2.58 m
ANN, 2Tx1Rx $\delta_y^{Tx} = 1$ m	0.85 m	1.36 m	1.53 m	1.66 m	1.94 m	1.97 m
ANN(2,0)	1.15 m	1.35 m	1.58 m	1.92 m	1.97 m	2.07 m
ANN(3,0)	0.53 m	1.36 m	1.58 m	1.78 m	1.94 m	2.02 m
ANN(4,0)	0.48 m	1.30 m	1.46 m	1.72 m	1.91 m	1.93 m
ANN, 2Tx1Rx $\delta_x^{Tx} = 1$ m	1.05 m	1.23 m	1.33 m	1.51 m	1.61 m	2.07 m
ANN(1,1)	0.91 m	1.07 m	1.15 m	1.28 m	1.39 m	1.45 m
ANN, 2Tx2Rx $\delta_y^{Tx} = 1$ m	0.64 m	0.84 m	1.07 m	1.14 m	1.35 m	1.51 m
ANN(2,2)	0.49 m	0.95 m	1.07 m	1.22 m	1.26 m	1.41 m
ANN, 2Tx2Rx $\delta_x^{Tx} = 1$ m	0.43 m	0.93 m	1.10 m	1.14 m	1.19 m	1.32 m
ANN, 2Tx2Rx $\delta_y^{Tx} = 0.5$ m	0.38 m	0.83 m	0.98 m	1.12 m	1.20 m	1.28 m

12.6 Conclusion

This work pushes the performance limits of indoor positioning in the harshly-conditioned galleries and tunnels in underground mines by reducing fingerprint acquisition complexity and, at the same time, boosting accuracy gains of CIR-based localization. In addition to that, the fundamentals of collaboration and ANNs’ design, which stem from years of research in underground positioning techniques, are laid down prior to revealing the new, more accurate MISO/MIMO-type fingerprint-positioning model. When both Tx and Rx spatial diversities are exploited, position estimation errors drop to 50 cm and 1.28 m for 90% of the testing fingerprints at $S_x = 1$ m and $S_x = 6$ m, respectively. The presented CIR-based localization techniques, currently being tested in the mmWave/60GHz band, may be implemented in different wireless technologies and are highly cost-effective when the discussed sampling and ANNs’ design strategies are applied.

Bibliography

- [1] P. Bahl and V.N. Padmanabhan. Radar: an in-building rf-based user location and tracking system. *Industrial Electronics and Applications, IEEE Conference ICIEA*, 2008.
- [2] M. Boutin, A. Benzakour, C.L. Despins, and S. Affes. Radio wave characterization and modeling in underground mine tunnels. *IEEE Trans. Antennas Propagat.*, 56(2):540–549, Feb 2008.
- [3] A. Chehri, P. Fortier, and P. M. Tardif. Uwb-based sensor networks for localization in mining environments. *Ad Hoc Networks*, September 2009.
- [4] S. Dayekh, S. Affes, N. Kandil, and C. Nerguizian. Cooperative localization in mines using fingerprinting and neural networks. *IEEE Conference, WCNC*, 2010.
- [5] S. Dayekh, S. Affes, N. Kandil, and C. Nerguizian. Cooperative geo-location in underground mines: A novel fingerprint positioning technique exploiting spatio-temporal diversity. *IEEE Conference, PIMRC*, 2011.
- [6] S. Dayekh, S. Affes, N. Kandil, and C. Nerguizian. Radio-localization in underground narrow-vein mines using neural networks with in-built tracking and time diversity. *IEEE Conference, WCNC*, 2011.

-
- [7] S. Dayekh, S. Affes, N. Kandil, and C. Nerguizian. Smart spatio-temporal fingerprinting for cooperative ann-based wireless localization in underground narrow-vein mines. *ACM Conference, ISABEL*, 2011.
- [8] H. Demuth and M. Beale. *Neural Network toolbox for use with Matlab (User's Guide)*. The MathWorks Inc., 2002.
- [9] K. Derr and M. Manic. Wireless based object tracking based on neural networks. *Industrial Electronics and Applications, IEEE Conference, ICIEA*, 2008.
- [10] X. Ding, H. Li, F. Li, and J. Wu. A novel infrastructure wlan locating method based on neural network. *Tsinghua University and Department of Computer Science and Technology, China*, November 2008.
- [11] E. Elnahrawy, X. Li, and R.P. Martin. Using area based presentations and metrics for localization systems in wireless lans. *The 4th IEEE Workshop on Wireless Local Networks (WLAN), Tampa, FL*, November 2004.
- [12] E. Elnahrawy, X. Li, and R.P. Martin. Using area based presentations and metrics for localization systems in wireless lans. *IEEE: Annual International Conference on Local Computer Networks*, pages 650–657, November 2004.
- [13] A. T. Eskildsen, T. F. Pedersen, M. Gidlund, J. Sjoberg, and B. H. Fleury. Positioning system for underground mines based on wireless signals. *Masters Thesis, Department of Electronic Systems, Aalborg University*, 2013.
- [14] A. E. Forooshani. Positioning system for underground mines based on wireless signals. *Ph.D. thesis submitted to the University of British Columbia*, 2013.
- [15] A. E. Forooshani, S. Bashir, D. G. Michelson, and S. Noghianian. A survey of wireless communications and propagation modeling in underground mines. *IEEE Communcations Surveys & Tutorials*, 15(4), Fourth Quarter 2013.

-
- [16] S. Gezici. A survey on wireless position estimation. *Wireless Personal Communications*, 44(3):263–282, Feb 2008.
- [17] S. Haykin. *Neural Networks: A Comprehensive Foundation*. Prentice-Hall In., 2 edition, 1999.
- [18] M. Hedley and I. Gipps. Accurate wireless tracking for underground mining. *IEEE International Conference on Communications*, June 2013.
- [19] R. A. Scholtz J.-Y. Lee. Ranging in a dense multipath environment using an uwrb radio link. *IEEE Journal of Selected Areas Communications*, 20(9):1677–1683, 2002.
- [20] K. Kaemarungsi and P. Krishnamurthy. Modeling of indoor positioning systems based on location fingerprinting. *IEEE: Twenty Third Annual Joint Conference of the IEEE Computer and Communications Societies*, 2:1012–1022, March 2004.
- [21] S. Kandeepan, S. Reisenfeld, T. C. Aysal, D. Lowe, and R. Piesiewicz. Bayesian tracking in cooperative localization for cognitive radio networks. *Vehicular Technology Conference, VTC IEEE 69th*, Spring 2009.
- [22] S. Kandeepan, S. Reisenfeld, T.C. Aysal, D. Lowe, and R. Piesiewicz. Bayesian tracking in cooperative localization for cognitive radio networks. *IEEE 69th Vehicular Technology Conference*, Spring 2009.
- [23] P. Krishnan, A. Krishnakumar, W. Ju, C. Mallows, and S. Ganu. A system for lease: Location estimation assisted by stationary emitters for indoor rf wireless networks. *IEEE INFOCOM*, 2004.
- [24] Z. Liu, C. Li, Q. Ding, and D. Wu. A coal mine personnel global positioning system. *World Congress on Intelligent Control and Automation*, July 2010.

-
- [25] Z. Liu, C. Li, D. Wu, W. Dai, S. Geng, and Q. Ding. A wireless sensor network based personnel positioning scheme in coal mines with blind areas. *Sensors MDPI*, pages 9891 – 9918, November 2010.
- [26] C. Lounis, N. Hakem, and G.Y. Delisle. Characterization of the 60 ghz channel in underground mining environment. *IEEE Antennas and Propagation Society International Symposium*, 2012.
- [27] H. Lui, H. Darabi, P. Banerjee, and J. Lui. Survey of wireless indoor positioning techniques and systems. *IEEE Transactions on Systems, Man, and Cybernetics-Part C: Applications and Reviews*, 37(6), Nov 2007.
- [28] P. Mankar, S. S. Pathak, and R. V. Rajakumar. A cooperative secondary user localization based primary user localization method for cognitive radio networks. *National Conference on Communications (NCC)*, February 2012.
- [29] E. A. Martinez, R. Curz, and J. Fevela. Estimating user location in a wlan using backpropagation neural networks. *Asian Conference On Internet Engineering*, pages 47–55, 2008.
- [30] M. Ndoh and G. Y. Delisle. Geolocation in underground mines using wireless sensor networks. *Antennas and Propagation Society International Symposium*, 3B:229 – 232, July 2005.
- [31] C. Nerguizian, C. Despins, and S. Affes. Geolocation in mines with an impulse response fingerprinting technique and neural networks. *IEEE Transactions on Wireless Communications*, 5(3), March 2006.
- [32] C. Nerguizian, C. L. Despins, S. Affes, and M. Djadel. Radio-channel characterization of an underground mine at 2.4 gh. *IEEE Trans. Wireless Commun.*, 4(5):2441–2453, Sept 2005.

- [33] BBC News. Chile Miners' 69 Days Trapped Underground. <http://www.bbc.co.uk/news/world-latin-america-11528912>, October 2010. [Online].
- [34] B. Nkakanou, G. Y. Delisle, and N. Hakem. Experimental characterization of ultra-wideband channel parameter measurements in an underground mine. *Journal of Computer Networks and Communications*, 11, 2011.
- [35] P. Oguz-Ekim, J. Gomes, and P. Oliveira. Rss based cooperative sensor network localization with unknown transmit power. *Signal Processing and Communications Applications Conference*, April 2013.
- [36] IEEE P802.15.4a/D4. Part 15.4: Wireless medium access control (mac) and physical layer (phy) specifications for low-rate wireless personal area networks (lrwpan). *Amendment of IEEE Std 802.15.4*, July 2006.
- [37] N. Patwari, J. N. Ash, S. Kyperountas, A. O. Hero, R. L. Moses, and N. S. Correal. Locating the nodes: Cooperative localization in wireless sensor networks. *Signal Processing Magazine, IEEE*, 22:54 – 69, July 2005.
- [38] Y. Qin, F. Wang, C. Zhou, and S-H. Wang. A distributed newton iteration based localization scheme in underground tunnels. *UKACC International Conference on Control*, September 2012.
- [39] A. Roxin, J. Gaber, M. Wack, and A. Nait-Sidi-Moh. Survey of wireless geolocation techniques. *Globecom Workshops, IEEE*, 2007.
- [40] V. Savic, H. Wymeersch, and E. G. Larsson. Simultaneous sensor localization and target tracking in mine tunnels. *IEEE Proc. of International Conference on Information Fusion*, July 2013.

-
- [41] C. Takenga and K. Tao Peng Kyamakya. Post-processing of fingerprint localization using kalman filter and map-matching techniques. *The 9th International Conference on Advanced Communication Technology*, Feb 2007.
- [42] A. Taok, N. Kandil, and S. Affes. Neural networks for fingerprinting-based indoor localization using ultra-wideband. *Journal of Communications*, 4(4), May 2009.
- [43] D. Torrieri. Statistical theory of passive location systems. *IEEE Trans. Aerosp. Electron. Syst.*, 20(2):183–197, March 1984.
- [44] M. K. Simon W. C Lindsey. Phase and doppler measurements in two-way phase-coherent tracking systems. *New York: Dover*, 1991.
- [45] H. Wymessrsch, J. Lien, and M. Z. Win. Cooperative localization in wireless networks. *Proceedings of the IEEE*, 97(2), February 2009.
- [46] S. Yarkan, S. Guzelgoz, H. Arslan, and R.R. Murphy. Underground mine communications: A survey. *IEEE Communications Surveys & Tutorials*, 11(3):125–142, Aug 2009.
- [47] V. Zhang, A. Wong, and Kam Tim Woo. Hybrid toa/aoa-based mobile localization with and without tracking in cdma cellular networks. *IEEE Conference, WCNC*, 2010.

Appendix A

Copyright Permission Letter

Dear Profs. Affes, Kandil and Nerguizian,

I am writing/editing/contributing to an academic work under the provisional title "Smart Localization in Underground Mines using Fingerprinting and ANNs: Strategies and Applications", to be published by the *Institut National de la Recherche Scientifique- Énergie Matériaux Télécommunications* (INRS-EMT), and my dissertation is submitted in partial fulfillment of the requirements for the degree of Doctor of Philosophy. I hereby request your permission to include the following material in this work:

- S. Dayekh, S. Affes, N. Kandil, and C. Nerguizian. Cooperative Localization in Mines Using Fingerprinting and Neural Networks. IEEE Wireless Communications & Networking Conference (WCNC), Sydney Australia, April 2010.
- S. Dayekh, S. Affes, N. Kandil, and C. Nerguizian. Cooperative Geo-location in Underground Mines: A Novel Fingerprint Positioning Technique Exploiting Spatio-Temporal Diversity. IEEE Personal Indoor and Mobile Radio Communications (PIMRC), Toronto Canada, Sep. 2011.
- S. Dayekh, S. Affes, N. Kandil, and C. Nerguizian. Radio-Localization in Underground Narrow-Vein Mines using Neural Networks with In-built Tracking and Time Diversity. IEEE

Wireless Communications & Networking Conference (WCNC), Cancun Mexico, March 2011.

- S. Dayekh, S. Affes, N. Kandil, and C. Nerguizian. Smart Spatio-Temporal Fingerprinting For Cooperative ANN-Based Wireless Localization In Underground Narrow-Vein Mines. ACM Conference, ISABEL, Barcelona Spain, Oct. 2011.
- S. Dayekh, S. Affes, N. Kandil, and C. Nerguizian. Neural-Networks and Fingerprint-Based Localization in Underground Mines with Novel Use of Collaboration and Space-Time Diversity, IEEE Transactions on Vehicular Technology, journal submitted in April, 2014.
- S. Dayekh, S. Affes, N. Kandil, and C. Nerguizian. Cost-Effective Localization in Underground Mines Using New SIMO/MIMO-Like Fingerprints and Artificial Neural Networks, IEEE International Conference on Communications (ICC), Sydney Australia, accepted on Feb 21st, 2014.

Please indicate your agreement to this request by signing this letter. By your countersignature, you warrant that you control these rights and are authorised to grant this permission.

Yours sincerely,
Shehadi Dayekh

By signing hereby, I/we grant the permission detailed above.

Sofiène Affes: _____

Nahi Kandil: _____

Chahé Nerguizian: _____